Modelling and Simulation of a Pressure Swing Reactor

Submitted in partial fulfilment of a Master's Degree in Chemical Engineering at the University of Cape Town,

August 2001

Cayle Sharrock

B.Sc. Chem Eng Hons UCT

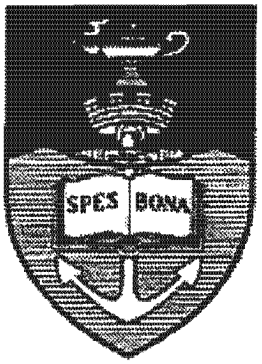

Acknowledgements

First and foremost, I must thank my supervisor, Dr. **Klaus Möller**. He gave this entire project impetus, was a constant source of ideas and was unfailingly supportive throughout the process.

I must also mention the following people who are especially deserving of my thanks:

Dr. **Warwick Duncan** for introducing me to Linux and making my life immeasurably easier. I am fantastically grateful for the impromptu LaTeX, gnuplot and bash tutorials which he willingly provided.

Craig Balfour and **Bill Randall** for dealing with all of my computing and networking foibles.

To **SASOL** for providing the financial assistance that allowed me to complete my degree in Cape Town, the finest city in the world.

Finally, I'd like to acknowledge all my friends and family, who can finally stop asking me how my thesis is going.

Synopsis

A Pressure Swing Reactor is a unit designed to incorporate simultaneous reaction and separation into one unit operation. The concept expands on the well-established method of Pressure Swing Adsorption, with the addition of catalyst to allow reaction to take place.

The PSR is operated with a four step cycle, according to the Skarstrøm process.

This thesis uses a combination of analytical and numerical analyses on a mathematical model of the PSR to characterise the units general behaviour under various conditions. The model was based on the isomerisation reaction $A \leftrightharpoons B$.

The steady-state solutions for the adsorption step provide a benchmark for performance. This was found analytically in a closed form for the isothermal case.

The Langmuir isotherm model predicts that separation performance is better at low partial pressures of the key components. This suggests the use of low total pressures or the introduction of an inert species into the reactor. The multi-component Langmuir isotherm predicts lower separation performance than linear isotherms.

First-order reversible kinetics yield simple linear mathematical expressions. As a result the dependence of the reaction rate on the pressure drop between the adsorption and desorption step is linear. This means that relatively speaking, the reaction rate remains constant, irrespective of the pressure. Thus, the low pressure steps do not slow the reaction rate sufficiently to improve separation.

Two parameters, the Reynolds number and the Euler number produced massive numerical instability in the Navier-Stokes equation. This was overcome by using small values for these parameters. Another approach may be to use the zeroth-order expansions of the perturbed equations for the PSR which were developed. Although no closed form analytical solution for these equations is possible, they may be amenable to numerical simulation.

The numerical analysis of the Pressure Swing Reactor system produced a large array of

results. Simulations were carried out until cyclic steady state was reached. Performance was characterised in two ways, using purity and yield indices.

The adiabatic model indicated that temperature effects are significant in the simulations insofar as increasing the amount of time needed to reach cyclic steady state. To facilitate more in-depth analysis of the operating parameters, the isothermal model was used instead.

Two approaches to PSR operation were studied. Only one approach gave any success. This involves using an adsorbent selective to the feed component only. Using this approach, product purities in excess of 99% were obtained, corresponding to overall yields of 62%.

The isotherm gradient or Henry's constant of adsorption emerged as the most important parameter to successful PSR operation. Larger values for the Henry's constant resulted in better performance.

An optimum reaction rate was found with respect to product purity. Performance also underwent a maximum when the adsorption capacity was varied.

Mass transfer limitations were found to be unimportant in the range investigated.

Longer adsorption steps tended to improve performance. Shorter purge steps tended to improve performance but also increased the time necessary to reach cyclic steady state.

Many negative results were obtained for PSR and hence not all reactions can be considered for Pressure Swing reaction. However, some combinations of parameters clearly indicate the potential of PSR to reduce overall capital and operation costs in future chemical processes.

Table of Contents

List of Tables

List of Figures

Nomenclature

ΔG_{rxn}	Gibb's free energy of reaction,	kJ/mol
ΔH_{ads}	heat of adsorption,	J/mol
ΔH_{rxn}	heat of reaction,	J/mol
μ	viscosity,	Pa.s
ρ	density,	kg/m^3
A	cross-sectional Area,	m^2
A_0	maximum reaction rate,	$m^3/kg.s$
B	Henry's constant for adsorption,	m^3/mol
C	concentration,	mol/m^3
C_p	heat capacity,	J/kg.K
D_e	effective diffusivity,	m^2/s
D_z	diffusion coefficient,	m^2/s
E_a	activation energy,	kJ/mol
k	adsorption rate constant,	s^-1
k_z	conductivity,	W/m.k
k_{rxn}	reaction rate constant,	$m^3/kg.s$
L	length of reactor,	m

M_r	Average molar mass,	kg/mol
P	pressure,	Pa
P_H	adsorption pressure,	Pa
P_L	desorption pressure,	Pa
q	concentration in adsorbed phase,	mol/kg
q^*	equilibrium adsorbed phase concentration,	mol/kg
$\overline{q}$	average adsorbed phase concentration,	mol/kg
R	universal gas constant,	W/mol.K
r	reaction rate,	mol/kg.s
T	temperature,	K
t	time,	s
v	interstitial velocity,	m/s
v_0	inlet velocity,	m/s
z	position along reactor,	m

Dimensionless Quantities

Cr	Heat capacity ratio
Ea0	reference reaction number
Eu	Euler number
Ha	dimensionless heat of adsorption
Hr	dimensionless heat of reaction
Ke	equilibrium constant
Ke0	reference equilibrium number

Pe	Peclet number
Pe_m	Peclet number for mass-transfer
P_{iL}	dimensionless desorption pressure
Qa	adsorption number
Re	Reynolds number
Rn	reaction number
u	dimensionless velocity
x	dimensionless position
y	mole fraction
β	dimensionless Henry's constant for adsorption
χ	adsorbed partial pressure, see (3.25)
κ	dimensionless adsorption rate constant
ϕ	dimensionless adsorbed phase concentration
Π	dimensionless pressure
σ	dimensionless reaction rate
τ	dimensionless time
θ	dimensionless temperature
θ	surface coverage
ϵ	bed voidage
ϵ	small parameter
φ	dimensionless concentration
ω	wavenumber

Subscripts

0	inlet, or reference condition
A	species A
B	species B
i	species parameter
s	solid, either adsorbent or catalyst

Chapter 1

Literature Review

The idea of incorporating reaction and separation in one operational unit has been around for some time. The first occurrences of a separating reactor appear in the literature in the 30's as Chromatographic reactors. The first real commercial reactor/separator units appeared in the early 80's with the advent of catalytic distillation but it was not until the late eighties that the idea of putting catalyst inside a Pressure Swing Adsorber came about.

The unit was termed a Periodic Sorption reactor, although it has also been referred to as a Pressure Swing Adsorber Reactor (PSAR), Sorption-enhanced Reaction Process (SERP) and perhaps the most appropriately, Pressure Swing Reactor (PSR).

In the last 14 years little progress has been made in PSR progress, due in part to lack of interest by the academic community and partly because of the difficulties in the mathematical complexities of the system.

This review presents some of the significant developments that lay the theoretical foundation for the PSR. It also examines the past work on the subject, with a strong emphasis being placed on the mathematical models that have been developed to date.

1.1 Separation Processes

Separation is driven by differences in the physical properties of mixtures. Distillation takes advantage of differences in boiling points. In adsorption, separation takes place based on the relative affinities for the adsorbent. Other separation processes make use of density (hydrocyclones), particle sizes (filtration), electronic characteristics (ion exchange) and so on. In this review, special attention is paid to adsorption. The fundamentals of adsorption, adsorption bed operation and in particular, Pressure Swing Adsorption are discussed below.

1.1.1 Adsorption

The adsorptive process is achieved primarily by the gross structural discontinuity that results at the surface of a solid. Forces present in the solid are not balanced by completely surrounding molecules at the surface. This results in an attractive force that causes other molecules to become attached (Yang, 1987). The solid surface molecules can be regarded as being unsaturated, and thus gas molecules readily and strongly affix to this surface.

As this is a surface process, the surface area of the solid plays a large role in the amount of gas adsorbed. The larger the surface area, the more molecules adsorb, and thus the more effective the adsorbent. Therefore high surface area solids are used as adsorbents, including activated carbon, silica gel, and zeolites.

1.1.2 Adsorption Isotherms

When considering adsorption in a gas-solid system, the equilibrium volume of gas adsorbed may be described by a function of temperature and pressure. At a constant temperature, the adsorption equilibrium becomes a function of pressure alone. This is known as an adsorption isotherm.

Two types of adsorption occur, namely physical adsorption (physiosorption) or chemical adsorption (chemisorption). In separation processes, only physical adsorption is encountered due to its reversibility. Chemisorption can be regarded as a chemical reaction and is avoided in separation processes due to the difficulty involved in removing the adsorbed molecules.

Physiosorption bonds are caused by van der Waals and coulombic forces. These forces are generally quite weak, and therefore easily reversed.

The deviation from adsorption equilibrium is the driving force for gas separation. Therefore

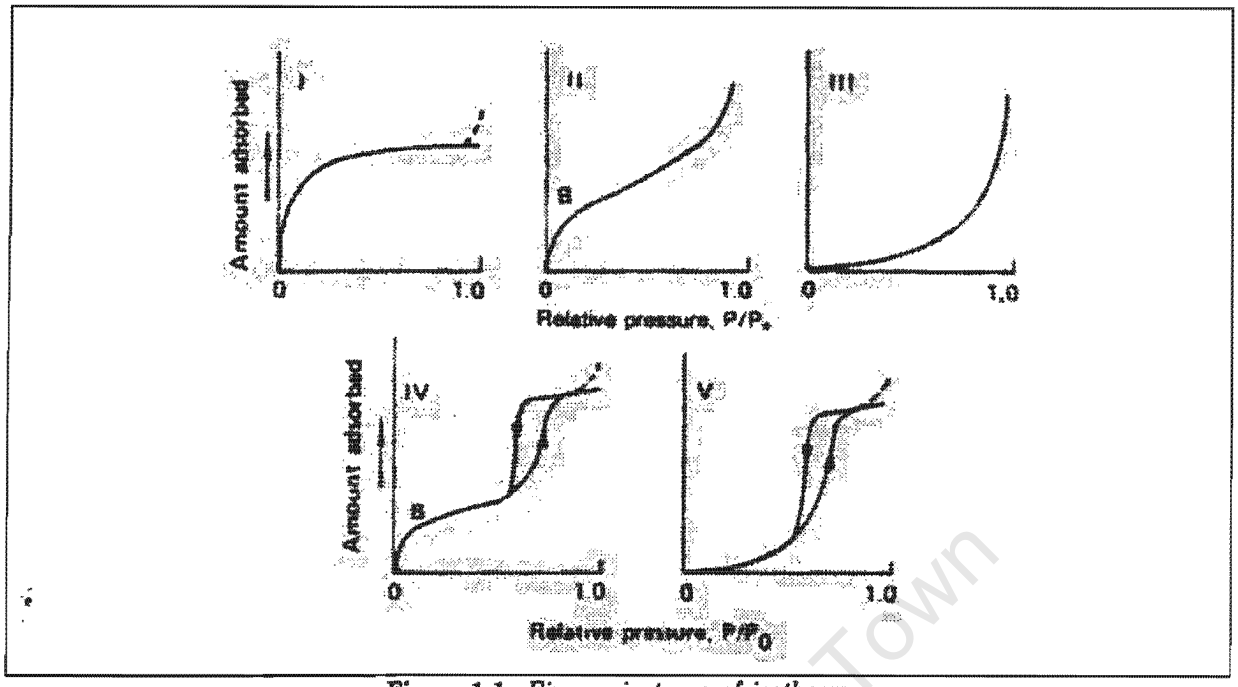

Figure 1.1: *Five main types of isotherm*

knowledge of equilibrium is vital to describe the process, and is provided by the adsorption isotherm. Experiments to-date have resulted in five different types of isotherm, as shown in Figure 1.1. Types I and II are the most common (Yang, 1987).

It is preferable to generate isotherms experimentally. However various isotherm models exist in varying degrees of applicability and use of use. In general, three different approaches have been used. They are the Langmuir Approach, the Gibbs Approach, and the Potential Theory.

Isotherms using the Langmuir Approach

This approach is based on a kinetic understanding of the equilibrium. A dynamic equilibrium is assumed, where the rate of condensation is equal to the rate of evaporation. Langmuir based isotherms remain the most useful for correlating data due to their ease of use and good fits for type I isotherms.

Langmuir Isotherm This is a mono-layer adsorption on homogeneous surface isotherm.

The basic assumptions used for this isotherm are:

- The adsorbed molecule is held at definite, localised sites
- Only one molecule can occupy each site

- The energy of adsorption is the same for all sites
- There is no interaction between neighbouring adsorbed molecules

The equation is as follows:

$$\theta = \frac{BP}{1 + BP} \tag{1.1}$$

B is known as the Langmuir Constant.

At low pressure this isotherm reverts to Henry's law, and for this reason B is also known as the Henry's Law Constant (normalised for q_s). At high pressure, θ tends to 1. B is temperature dependent, and is usually modelled according to an Arrhenius relation.

Langmuir-Freundlich Isotherm

Langmuir considered the case where each molecule occupied two sites. This case was then extended to multiple site adsorption. The equation derived has another parameter, n, which determines the number of sites each molecule occupies when adsorbed. Under normal circumstances, n is greater than unity for physiosorption.

By solving the Langmuir-Freundlich equation, a distribution function of energy of adsorption can be found. When solved, it shows a distribution that is extremely close to Gaussian.

Adsorption Isotherm for Heterogeneous Solid

This isotherm developed by Do and Do (1997) is for a heterogeneous solid, where the heterogeneity is represented by the variation in isosteric heat of adsorption as a function of loading. This heat of adsorption is assumed to be independent of the type of adsorbate used.

The heat of adsorption is modelled as a function of the heat of adsorption for zero loading, plus a variation in the heat of adsorption weighted according to a pattern of homogeneity.

An adsorbate-adsorbate interaction term was included to allow for interaction between adsorbed molecules.

The final isotherm reduces to many of the well known isotherms given certain parameter values (including Langmuir and Langmuir-Freundlich). It can be used to fit type I isotherm, and has been tested successfully on two types of activated carbon, and on H-mordenite.

General Gas Isotherm (Martinez and Basmadjian, 1996)

Martinez and Basmadjian (1996) have developed a general gas isotherm that takes into account effects such as adsorbate size, symmetry loss (or chemical dissociation), clustering, and molecular interactions between the adsorbed molecules. In certain limiting cases, this isotherm can be reduced to many of the well-known isotherms such as Langmuir.

Experiments show that this isotherm fits experimental data extremely well. In some cases no improvement over simpler isotherm models are obtained, but it does indicate what the causes for the deviations are. Thus the system's non-ideality can be analysed.

Gibbs Approach

The Gibbs Approach uses the Gibbs isotherm, and a two-dimensional equation of state. Integrating the Gibbs equation results in the isotherm - therefore there are as many isotherms as there are equations of state.

By considering the adsorbate (fluid) as a two-dimensional microscopic entity, classical thermodynamics can be used to model the system.

Gibbs adsorption isotherm is as follows:

$$-Ad\pi + nd\mu = 0 \tag{1.2}$$

where π is the spreading pressure (two-dimensional pressure) and μ is the chemical potential, or partial molar Gibbs free energy (Sandler, 1989). For pure, ideal-gas adsorption this equation becomes:

$$\frac{\pi A}{RT} = \int_0^P \frac{n}{P} dP \tag{1.3}$$

This isotherm is one of many that can be generated by the substitution of a valid equation of state.

Potential Theory Approach

This approach considers the solid surface to contain a gradual concentration of gas molecules, with the concentration decreasing with distance from the surface. This is similar to the atmosphere above the surface of a planet. This approach is not widely used for modelling zeolite adsorption.

Mixed Gas Adsorption Isotherms

We have discussed a few theories of pure component isotherms. It is obvious however, that separation processes involve mixtures and not pure components. Unfortunately, adsorption equilibria are not simply superpositions of the respective pure gas isotherms. There is a significant amount of interaction between adsorbed species. This makes mixed-gas isotherm predictions from pure-component isotherm data very difficult and often unsatisfactory. Nevertheless, the Langmuir isotherm has been extended to accommodate mixtures with some success with well behaved gas mixtures, as has the Langmuir-Freundlich equation. The potential theory approach has resulted in a number of isotherms for mixtures. There are also several isotherms based on other aspects of thermodynamics.

Adsorbed solution theory (Yang, 1987; Ruthven, 1984) The adsorbed solution theory by Myers and Prausnitz (1965) regards the mixed adsorbate as a solution in thermodynamic equilibrium with the gas phase. Classical thermodynamics can then describe the adsorbed phase.

The ideal adsorbed solution theory (IAST) regards the adsorbed phase as being thermodynamically ideal. This allows the adsorbed phase equilibrium to be derived directly from the pure-component isotherms. It has been shown that a number of systems do conform to the model of ideal behaviour.

Although a large number of multi-component isotherms have been developed, there is very little experimental data available to test the models. For this reason, choosing the best one requires careful analysis of the theoretical basis of that isotherm.

1.1.3 Fixed Bed Adsorbers

Overview

Fixed-Bed adsorbers have been thoroughly studied and a plethora of mathematical models for their performance are available. Ruthven (1984) and Yang (1987) have compiled discussed a large number of these. A few of the models they discuss as well as some of the more recent work on the subject will be dealt with in this discussion.

Analytical models

By making dramatic assumptions that are valid in only very special cases, models can be developed that are amenable to analytic solutions.

For example, exact, closed form expressions for the breakthrough curves of single component fixed-beds, exhibiting plug flow, isothermal operation and a linear driving force for mass transfer, have been developed (Walter, 1952; Furnas, 1930; Klinkenberg, 1954).

Lapidus and Amundsen (1952) and Levenspiel and Bischoff (1963) extended these models by incorporating axial dispersion. Rosen (1954) made use of the mass balance for mass transfer but assumed that intraparticle diffusion was rate controlling and developed his model in the case of plug flow. Rasmuson and Neretnieks (1980) did the same but allowed for axial diffusion. Rasmuson later improved on his model by incorporating macro- and micropore diffusion as well as external resistance (Rasmuson, 1982). An excellent review of the available analytical expressions is available in Ruthven (1984).

Mass Transfer Approximations

An area that has long been subjected to simplification is the transport of gaseous species from the bulk phase to the adsorption site. Now, while this process is well defined by a mass balance (1.4), solving the associated equations is computationally intense. Thus, approximations have been developed that drastically reduce computation time, the most popular being the linear driving force (LDF) model by Gluekauf (1955), given in (1.5).

$$\frac{\partial q}{\partial t} = \frac{1}{r^2}\frac{\partial}{\partial r}\left(Dr^2\frac{\partial q}{\partial r}\right) \tag{1.4}$$

$$\frac{d\bar{q}}{dt} = k\left(q^* - \bar{q}\right) \tag{1.5}$$

Here, the concentration profile inside the particle is assumed to be parabolic. The LDF eliminates the spatial dependency, reducing a differential equation to an algebraic expression. While the LDF model is very useful, it is not valid for the small times. It also assumes that no reaction takes place. Buzanowski and Yang (1991) extended the LDF model by assuming a more general cubic profile within the particle. Kim (1989) gave the following results for intraparticle mass

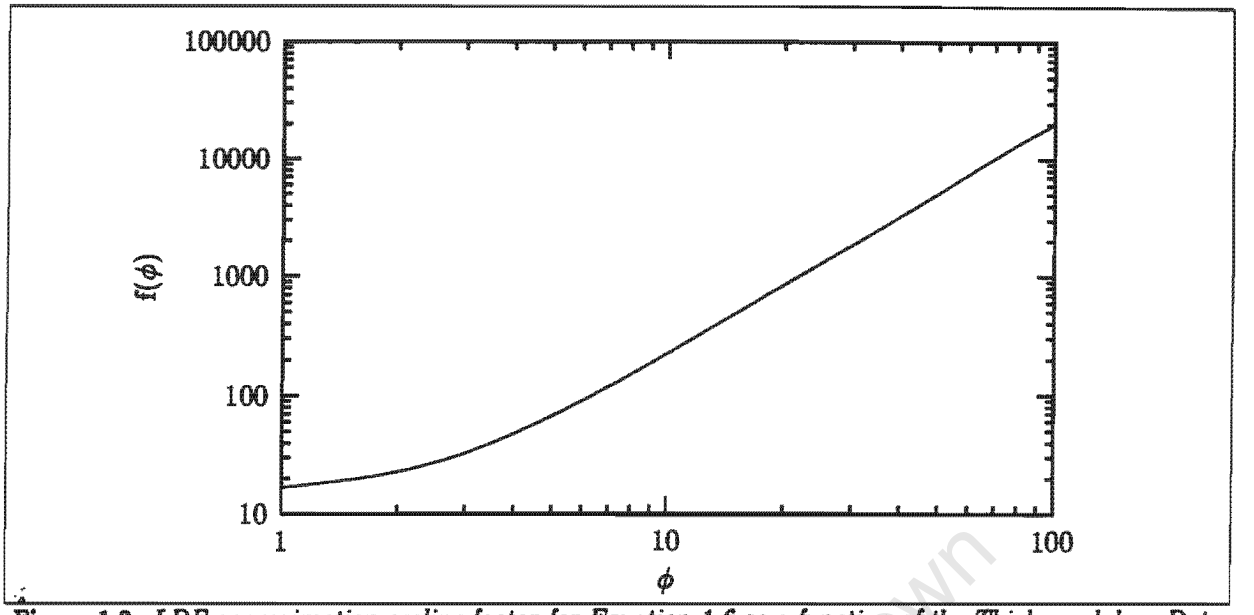

Figure 1.2: *LDF approximation scaling factor for Equation 1.6 as a function of the Thiele modulus. Data interpolated from (Kim, 1989).*

transfer which incorporate the Thiele modulus for reaction:

$$\frac{d\bar{q}}{dt} = f(\phi)\frac{\varepsilon_p D}{R^2\left[\varepsilon_p + (1-\varepsilon_p)B\right]}(q^* - \bar{q}) \qquad (1.6$$

The value of $f(\phi)$ for a given Thiele modulus can be read off figure 1.2.

Fixed-Bed Simulation

Fixed-Bed simulations have been carried out with considerable success. Applications include air separation (Farooq and Ruthven, 1991) and perhaps of greater interest in this study, the separation of normal and iso-paraffins using Pressure-Swing Adsorption by Silva and Rodriques (1998). Their model incorporated heat effects and used the linear driving force model and a multicomponent isotherm developed by Nitta and Shigetomi (1984). The model successfully predicted PSA performance and the fit to experimental data was very good.

In general finite element techniques are used to solve the large numbers of partial differential equations these models can potentially generate because they are more stable than their finite difference counterparts (Rice and Do, 1995). However, Sun and Meunier (1991) have obtained good agreement with experimental data in their modelling of multicomponent adsorption on 5A zeolite. They used Langmuir isotherms, LDF approximation as well as incorporating an energy balance in their model.

1.2 Pressure Swing Adsorption

1.2.1 Introduction

Pressure Swing Adsorption was patented in the late fifties by Skarstrøm and independently by Guerin de Montgareuil and Domine. Since then it has found particular application in air-drying, hydrogen purification, normal and iso-paraffin separation and air separation (Yang, 1987). Several different operating cycles have been implemented in the past but they all employ the same principle: A component is removed from a mixture by virtue of being more strongly adsorbed into a fixed bed. The product is recovered by desorbing the component at a lower pressure.

PSA systems operate cyclicly and for this reason there is normally more than one unit operating in parallel order to maintain continuous production.

1.2.2 Operating Principles

The Skarstrøm and Guerin cycles operate slightly differently. In the four-step Skarstrøm cycle, shown in Figure 1.3, two beds are run in parallel. During step one, the bed is fed with high pressure feed and adsorption of components takes place. Initially, only the feed side is open but the exit side is opened once the desired bed pressure is reached. The strongly adsorbing component, S is retained by the bed, while the weakly adsorbing component, W is recovered at the bed exit. After the adsorption step, the input stream is fed to the second bed and the first bed is depressurised, usually to atmospheric pressure. The strongly adsorbing component is desorbed and leaves the bed entrance in an almost pure form. The remaining S is purged using a small amount of the weakly adsorbing component in reverse flow. The bed is then ready for the next adsorption step. The cycle times for adsorption and regeneration are equal, since both beds need to operate concurrently.

Although not discussed here, the Guerin cycle is more versatile and designs of one to six beds have been proposed for various separations (Yang, 1987, ch7:p240). The Guerin cycle uses three steps: pressurisation with only the feed end open, cocurrent depressurisation, and evacuation under vacuum from the midpoint of the bed.

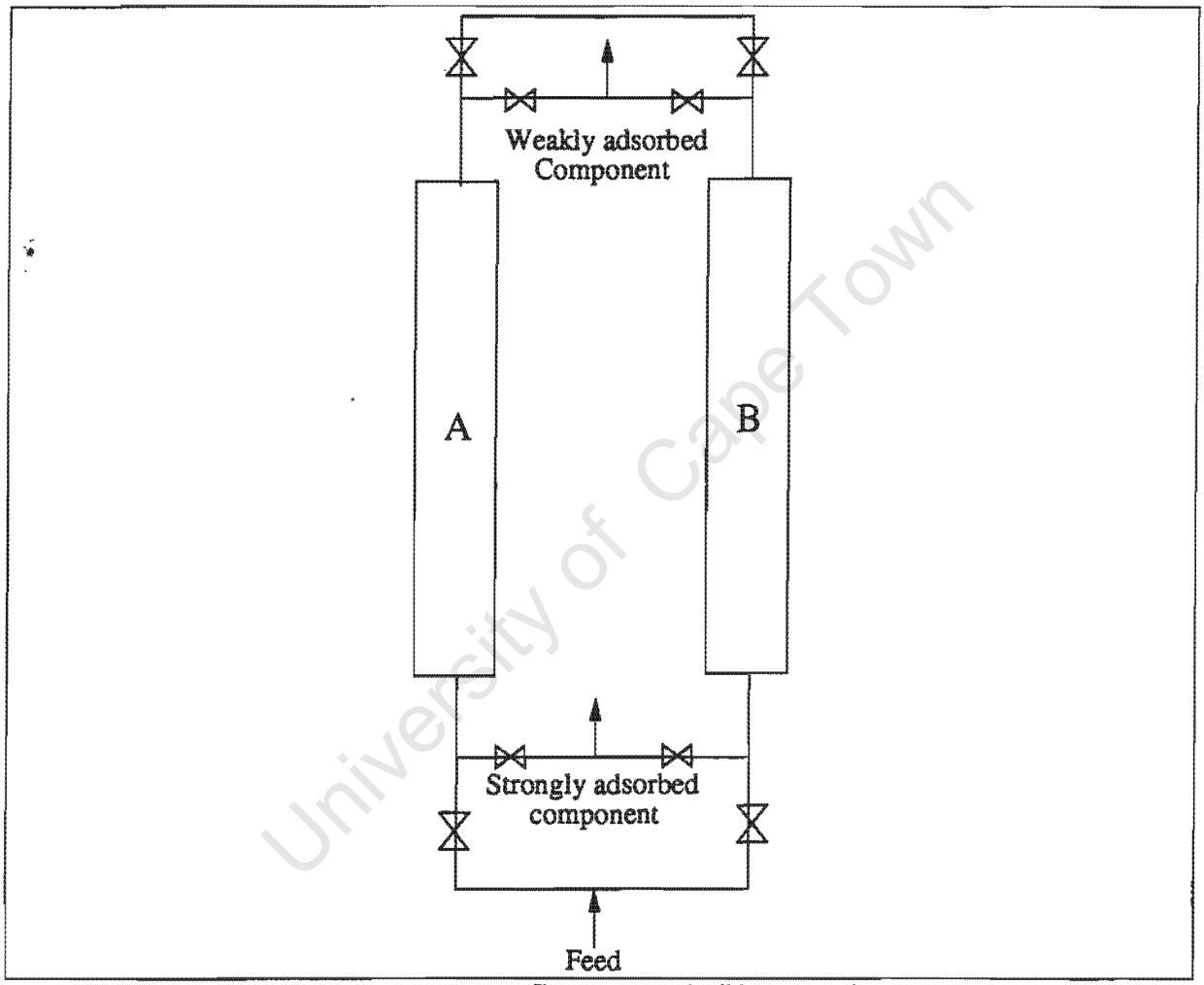

Figure 1.3: *The Skarstrøm cycle.(Yang, 1987)*

1.2.3 Operating considerations

Cocurrent Depressurisation

Since the original PSA patents, several improvements in operation have been developed. The first major improvement was with the introduction of a cocurrent depressurisation step. The step is introduced into the Skarstrøm cycle by cutting the adsorption step short, i.e. before the concentration front reaches the end of the bed. Then the bed is depressurised cocurrently before resuming the normal Skarstrøm purge step.

Cocurrent depressurisation improves the strong adsorptive purity and consequently the total recovery of the weakly adsorbed component (Yang, 1987).

Pressure Equalisation

Pressure equalisation was devised to conserve mechanical energy in PSA systems. It is largely due to this technique that PSA became economically feasible (Yang, 1987). At the end of every cycle, one bed is under pressure awaiting blowdown whilst the other is at atmospheric pressure awaiting repressurisation. Pumping costs can be reduced by equalising the pressure in the two beds before resuming normal operation.

Purge with strongly adsorbing component

If high purity of S is required, a high pressure purge step using pure S can be inserted after the adsorption step. This step can be used in conjunction with cocurrent depressurisation to optimise separation.

Temperature equalisation

Adsorption is an exothermic process and temperature gradients often develop within adsorption beds. The local temperature rise during adsorption and temperature drop during desorption are both detrimental to good separation. Isothermal operation is the most desirable case for adsorptive separation. This can be realised through short cycle times and low throughput per cycle (Yang, 1987). This is not always possible and other methods have been suggested to minimise temperature fluctuation during PSA cycles (Yang, 1987, ch7:pp249-252).

1.2.4 PSA Models

Analytical Model

Analytical studies have been carried out under the following assumptions (Chan et al., 1981; Yang, 1987):

1. Linear Isotherms are followed by both components, A and B. The strongly adsorbed component, A is highly dilute. Furthermore the two isotherms are independent.
2. Isothermal operation (i.e. short cycle times and low throughput)
3. Instantaneous gas-solid equilibrium.
4. The interstitial gas velocity is constant during constant pressure steps.
5. Plug flow is assumed, with no axial or radial dispersion.
6. The ideal gas law is applicable.
7. There is no significant pressure drop across the bed.

The mass balance for A is

$$\varepsilon\left[\frac{\partial C_A}{\partial t}+\frac{\partial(uC_A)}{\partial z}\right]+(1-\varepsilon)\frac{\partial q_A}{\partial t}=0 \tag{1.7}$$

and for B:

$$\varepsilon\left[\frac{\partial C_B}{\partial t}+\frac{\partial(uC_B)}{\partial z}\right]+(1-\varepsilon)\frac{\partial q_B}{\partial t}=0 \tag{1.8}$$

Under the above assumptions,

$$q_A = B_A C_A \quad ; \quad q_B = B_B C_B$$

$$Y_B \approx 1$$

where $B_A > B_B$. The equations are simplified and solved using the method of characteristics (Yang, 1987). The position of the concentration front is given by

$$Z_H = \left(\frac{\varepsilon}{\varepsilon+(1-\varepsilon)B_A}\right)u_H\Delta t \tag{1.9}$$

$$Z_L = \left(\frac{\varepsilon}{\varepsilon+(1-\varepsilon)B_A}\right)u_L\Delta t \tag{1.10}$$

during the high and low pressure steps respectively. The change in position of the concentration front over a pressure-change step is

$$\frac{Z_H}{Z_L} = \left(\frac{P_H}{P_L}\right)^{-\beta} \tag{1.11}$$

with $\beta = \frac{\epsilon+(1-\epsilon)B_B}{\epsilon+(1-\epsilon)B_A}$. The change in the mole fraction of A over a pressure change is

$$\frac{Y_H}{Y_L} = \left(\frac{P_H}{P_L}\right)^{\beta-1} \tag{1.12}$$

Finally, over a complete cycle, the change in position of the concentration front is

$$\Delta Z = Z_L - \left(\frac{P_H}{P_L}\right)^{\beta} Z_H \tag{1.13}$$

Due to the cyclic nature of PSA operation, the analytical solutions exhibit large errors over time when compared to experimental studies. More complex numerical models have had more success.

Numerical Model

Various researchers have modelled Pressure-Swing adsorption numerically according to different sets of assumptions. The following significant results were obtained:

The 'frozen concentration' assumption that the gas and adsorbed phase concentrations remain fixed during pressure change steps is poor. The frozen concentration assumption underpredicts separation if the mass transfer coefficient k is held constant. On the other hand, assuming that instantaneous equilibrium is obtained during pressure-change steps predicts overseparation, although the equilibrium assumption is far closer to experimental results (Yang, 1987).

In general, better agreement with experiment is obtained when k is made a function of pressure.

During the blowdown step, good agreement was obtained with the instant equilibrium assumption (Yang, 1987, Ch8,pp294-295).

The preceding simulations assumed isothermal operation. There are however, small temperature variations within PSA's that may be significant. Once reaction is introduced, temperature effects may become very important.

1.3 Simultaneous Reaction and Separation Operations

The idea of incorporating reaction and separation in one step refers primarily to reversible, equilibrium limited reactions. If the desired product can be continuously removed from the reaction mixture using one of the methods described above, then according to Le Chateliers principle, the reaction will continue to proceed in the desired direction. Since most industrial reactions are catalysed, a catalyst will also have to incorporated into the scheme. In some cases, the catalyst may also perform the separation. In most cases however, separate catalysts and separating agents will be used.

1.3.1 Catalytic Distillation

Catalytic Distillation (CD) is one reaction-separation scheme that has realised industrial success. Charter Oil commissioned the first CD unit for methyl tert-butyl ether (MTBE) synthesis in 1981. By combining reaction and separation in one unit, capital costs are reduced. During operation benefits of CD can include increased reaction conversion, increased catalyst life, improved selectivity and reduced fouling (Gildert, 1997).

Operation

A typical CD unit for MTBE production is shown schematically in figure 1.4. Feed is introduced below the catalyst section of the unit. MTBE, the heavy component, is removed from the bottom and the light components (methanol and C_4's) move to the top. The C_4-rich stream reacts in the catalyst bed, forming MTBE. Unreacted lights exit from the top and are recycled. With high reflux ratios, very high overall conversions of C_4's are achieved.

1.3.2 Simulated Moving Bed Reactors

Simulated Moving Bed Reactors (SMBR's) are a result of combining the philosophies of simulated moving beds (a separation scheme) and chromatographic reactors (a reaction/separation scheme), an idea that has been around since the sixties.

A pulse of feed is passed though a column containing a catalyst bed followed by a chromatographic region. The products are then recovered as two separate pulses.

Simulated moving beds (SMB) simulate the continuous countercurrent separation of liquid mixtures by a complicated process of rotating the positions of the feed, raffinate and extract

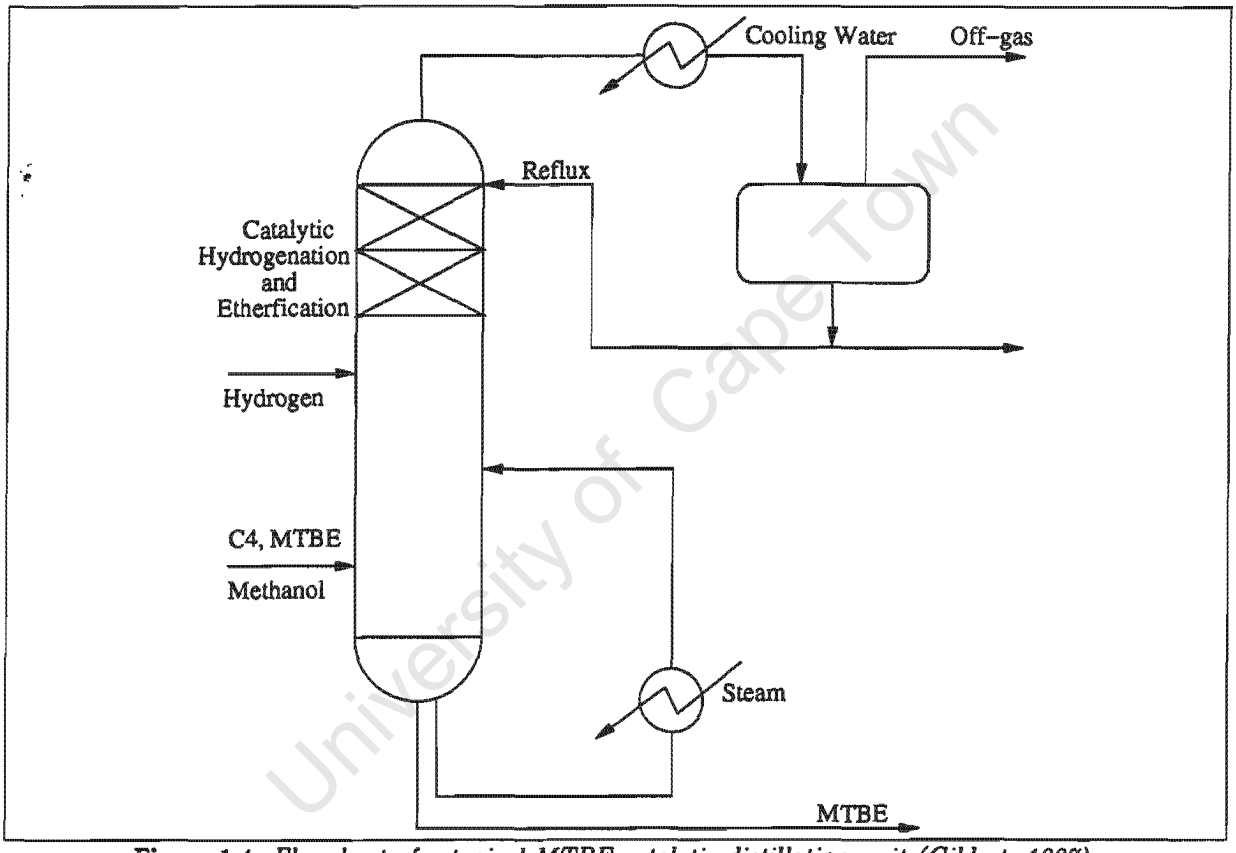

Figure 1.4: *Flowchart of a typical MTBE catalytic distillation unit (Gildert, 1997).*

streams. Despite the complex operation, the gains in separation performance justify industrial scale SMB's, an example of which is the Sorbex process.

In principle, SMBR's are simply SMB's containing a catalyst. Although no industrial applications have been developed yet, laboratory-scale results are promising (Mazotti et al., 1996; Migliorini et al., 1999). Developed for liquid phase reactions, SMBR's have been shown to effect complete conversion and separation for equilibrium limited reactions (Migliorini et al., 1999). They are also not energetically intensive.

The first true SMBR experiments, with catalyst and adsorbent mixed in the same column, were performed in 1995 (Ray and Carr, 1995). Mazotti et al. (1996) ran an SMBR containing Amberlyst 15, a resin that performs both catalysis and separation. In his investigation of the esterification of acetic acid, 100% conversion of acetic acid was achieved with complete separation of the products, water and ethylacetate.

The prospects of industrially feasible applications are positive.

1.4 Pressure Swing Reactors

A natural analogy of SMBR's and CD units to fixed-bed adsorption is the reactive Pressure Swing Adsorber, or Pressure Swing Reactors (PSR) as they have become known.

Very little work has been done in this area and what literature is available is limited to simulation and modelling. The precise nature of how best to build a PSR has not been established. There are several options available :

- A fixed-bed containing a zone of catalyst followed by a zone of adsorbent, in direct analogy to catalytic distillation.
- An admixture of catalyst and adsorbent throughout the bed as is the case in most SMBR's.
- An adsorbent that has catalytic properties throughout the bed.
- A hybrid of the previous suggestions.

The available literature generally describes systems of the second kind, although the first type has been mentioned. The prevailing attitude however, that better performance is obtained from a catalyst/adsorbent mixture (Lu and Rodrigues, 1994).

1.4.1 Overall review of previous work

The PSR appeared for the first time in 1984 in a paper by Lee and Kadlec (1984). The principles are the same, although Lee and Kadlec's PSR was operated slightly differently to the more conventional Skarstrøm cycle. In their study, the PSR cycle contains three steps, with product collected at the exit during the first (feed) step, and at both ends during the third (exhaust) step. The second step is termed a delay step during which the exit valve is closed, allowing the concentration front to penetrate deep into the reactor.

The primary assumptions of the Lee and Kadlec's PSR are

1. Instantaneous adsorption equilibrium
2. Isothermal operation
3. Simple Power Law Kinetics
4. No axial or radial pressure gradients
5. Ideal Gas behaviour
6. Flow described by Darcy's Law
7. Linear Isotherms
8. Ideal Solution behaviour
9. Perfect step response to pressure changes
10. No feed variations
11. No diffusion effects

Most of these assumptions are still in effect in current models. On the other hand, most current models include axial dispersion (assumption 11) and finite adsorption rates (assumption 1). The nonisothermal case has also been dealt with; Alpay et al. (1993) and Yongsunthon and Alpay (1999) include temperature effects in their models. Occasionally assumption 7, the linear isotherm constraint has been relaxed (Kodde et al., 2000). This is particularly important since it is the nonlinearities of adsorption and reaction that aid the reaction-separation process.

To date, no model has tried to improve the flow model, with some making even simpler assumptions, replacing assumption 6 with a constant velocity approach (Alpay et al., 1994).

At most, Yongsunthon and Alpay (1999) use the Ergun equation instead of Darcy's law to accommodate turbulent flow. There is no case in the literature of assumption 6 being relaxed completely by incorporating the Navier-Stokes equations into the frame. The Navier-Stokes equations are based on a fundamental momentum balance and as such, give a far more accurate description of the flow (Bird et al., 1960). In addition to this the Navier-Stokes equations allow more accurate descriptions of the boundary conditions during PSR operation.

1.4.2 Significant results

Lee and Kadlec (1984) modelled the equation $A \rightleftharpoons B \rightleftharpoons C$ with B being the desired product. The reactor contained various layers of adsorbents, selective towards individual species. Using this approach, the authors claimed an increase in overall conversion with a 64% selectivity towards B against an equilibrium selectivity of 33%.

Vaporciyan and Kadlec (1987) studied theoretical reversible reactions corresponding to isomerisation, dehydrogenation and disproportionation reactions. Their PSR was identical to that of Lee and Kadlec but with the added assumption that the reaction rate was sufficiently fast to assume local equilibrium. The authors discovered that the reaction terms resulted in numerical instabilities during simulations. These were overcome by changing the discretisation strategy. Their main findings were

- No improvements in conversion or separation were found for isomerisation reactions. Exit compositions were at equilibrium.
- Adsorbent capacity had significant effect on conversion

The authors were of the opinion that by allowing finite reaction rates these findings could be overturned.

Vaporciyan and Kadlec (1989) extended their model to include finite reaction rates. However, the main thrust of this study was to verify their model experimentally. Unfortunately, there was poor agreement between model and experiment. The commercial value of the experimental setup is also questionable. In an attempt to justify the assumptions made in the model, the reactants were highly diluted in an inert carrier. This kept the partial pressures of the reactants very low, maintaining linear isotherms and a constant overall gas velocity through the bed.

The same assumptions (constant velocity, dilute reactants) were made by Alpay et al. (1994)

in their PSR study using the Skarstrøm operating principles. In an investigation of the physical parameters of the system they found that

- There is an optimum reaction rate for PSR operation. Reaction rates that are too low are too far away from the equilibrium to achieve good conversions. Conversely, reactions that proceed too quickly tend to favour the reverse reaction too much and exit concentrations approach the equilibrium concentrations. This result was echoed in Vaporciyan and Kadlec (1987).
- At the optimum reaction rate, the equilibrium yield was exceeded for isomerisation and disproportionation reactions.
- Due to unfavourable pressure effects, dehydrogenation reactions in the PSR did not exceed equilibrium yields, but still outperformed the PFR.

Preliminary simulations of the hypothetical reaction $A \rightleftharpoons B + C$ revealed that conversions greater than equilibrium were possible in PSR's (Alpay et al., 1993; Chatsiriwech et al., 1994).

Lu and Rodrigues (1994) performed thorough investigations on the operation and performance of a single-bed PSR operating under a modified Skarstrøm process. The PSR operated under three steps; feed, delay and blowdown. Adsorption and catalysis were carried out by the same substance. The reaction under consideration was $A \rightleftharpoons B + C$ ($K_e = 1.48 \times 10^3$) under isothermal conditions. Furthermore, instantaneous equilibrium between adsorbed and gas phases was assumed. Two cases were examined: In the first B was the only adsorbable component; in the second, both A and B were adsorbed. In the first case conversions of between 10% and 20% above equilibrium were obtained. In the latter case, the improvement was 10%.

The main trends that were identified were:

- When blowdown times are very small, the inclusion of a purge step increases conversion.
- An increase in adsorption capacity, rate of reaction or feed flowrate increases overall conversion.
- Diluting the feed with inerts reduces overall conversion.
- Increasing the adsorbent affinity for A reduces overall conversion.

Cheng et al. (1998) modelled the reaction $2A \rightleftharpoons B + C$ so that pressure would have no effect on reaction equilibrium. The composition of the PSR was modelled as an admixture of catalyst and adsorbent. Mathematically, this model was equivalent to the previous case of catalyst/adsorbent combined. Whether this is physically accurate remains to be seen. The PSR was operated with two steps: Pressurise and blowdown. C was the only adsorbable component and isothermal operation was assumed. The model of Lu was extended somewhat by allowing for mass transfer resistances via the linear driving force (LDF) approximation. At cyclic steady state (reached after approximately 5000 cycles) the improvement over equilibrium conversion ($K_e = 0.0156$) was 32%.

Yongsunthon and Alpay (1999) applied this model to the dehydrogenation of methylcyclohexane (MCH) to toluene over Pt-Al_2O_3 catalyst and zeolite A5. According to the data presented, $K_e \rightarrow \infty$ at the given temperature (673K), i.e. the reaction is irreversible. In a five stage PSR system, MCH conversion of 59% with 72% near-pure toluene recovery (inert free basis) was obtained. This indicates that the PSR is kinetically constrained which casts doubt onto the feasibility of PSR for this reaction. It was claimed that an equivalent PFR would yield 23% conversion.

The study of irreversible reactions in PSR processes was continued by Kodde et al. (2000). In this case the challenge was to improve the intermediate product in the reaction $A \xrightarrow{+D} B \xrightarrow{+D} C$. The PSR was operated under the usual Skarstrøm conditions. The model contained the same assumptions as the Lee and Kadlec model except that

- Langmuir isotherms were used (assumption 7),
- Axial diffusion was included (assumption 11),
- Constant gas velocity throughout the bed (assumption 6), and
- LDF model was used to model the mass transfer limitations (assumption 1).

Kodde et al. found that selectivity over a PSA-PFR in series was improved but that the PSR offered lower productivity.

1.5 Summary

While there has been some work in the modelling and simulation of PSR's, there is still much scope for extension and investigation. In particular, temperature effects have yet to be fully considered, nonlinear isotherm models have had scant exposure, while flow models beyond the empirical are nonexistent.

The physical and economic feasibility of reaction-separation processes has already been established with simulated moving bed reactors and catalytic distillation. Pressure swing reactors are just a natural extension of these ideas. However, the complexity of the systems involve preclude any definite conclusions on the operability of such systems without performing rigorous simulations of the proposed systems. Unfortunately, the mathematical models are so exceedingly complicated that even numerical solutions have required sometimes restrictive assumptions to avoid such demons as numerical instability, erroneous oscillations and impractical running times.

Chapter 2

Theory

This chapter contains the theoretical background necessary for understanding where the PSR differential equation system comes from and how it relates to real-world physics. The equations are derived using transport phenomena balances.

The boundary conditions are particularly important since they describe the operation philosophy of the PSR.

Following the equation and boundary condition description is an overview of the FORTRAN numerical packages used to solve the PSR equations, PDASAC and PDECOL.

Finally, the phenomenon of numerical instability is investigated, how it originates and how it may influence numerical results.

2.1 Problem description

In this section the model for the Pressure Swing Reactor is described.

The equations describing the system will be derived using the differential volume approach, as shown in Figure 2.1. Before continuing with the derivation, it is instructive to examine the transport mechanisms that contribute to the physics of the reactor system.

2.1.1 Mass transfer

Most mass transfer takes place through bulk flow, as material moves along with the current into and out of the volume element. The rate of mass flux into the element is a function of the gas velocity and its concentration.

Diffusion can also be a significant contributor to the mass flux term. Following Fickian diffusion theory, the rate of mass flux into the volume element is proportional to the local concentration gradient at the element boundary.

The two chemical processes that characterise the PSR are reaction and adsorption.

Any reaction kinetics may be used in the system, but for this case, simple first-order reaction kinetics will be assumed. Mass transfer from the gas to the adsorbed phases will follow local isotherm equilibrium and kinetic relations. The linear driving force model (Gluekauf, 1955) will be used to describe the adsorption kinetics, again for simplicity. The adsorption equilibrium will be described by the multicomponent Langmuir isotherm (Yang, 1987).

2.1.2 Energy Transfer

Both adiabatic and the isothermal operation will be investigated. Isothermal operation does not require an explicit energy balance because the temperature profile is known *a priori*. For the adiabatic case, an energy balance is needed across the volume element. Bulk enthalpy flow, axial conduction and heat of reaction and adsorption will be taken into account. It is assumed that no heat is lost to the environment.

The bulk energy transfer is a function of the specific enthalpy of the gas, its concentration and velocity. Conduction follows Fourier's law and is proportional to the temperature gradient at the element boundaries. Thermal equilibrium between the solid and gas phases is assumed at all times.

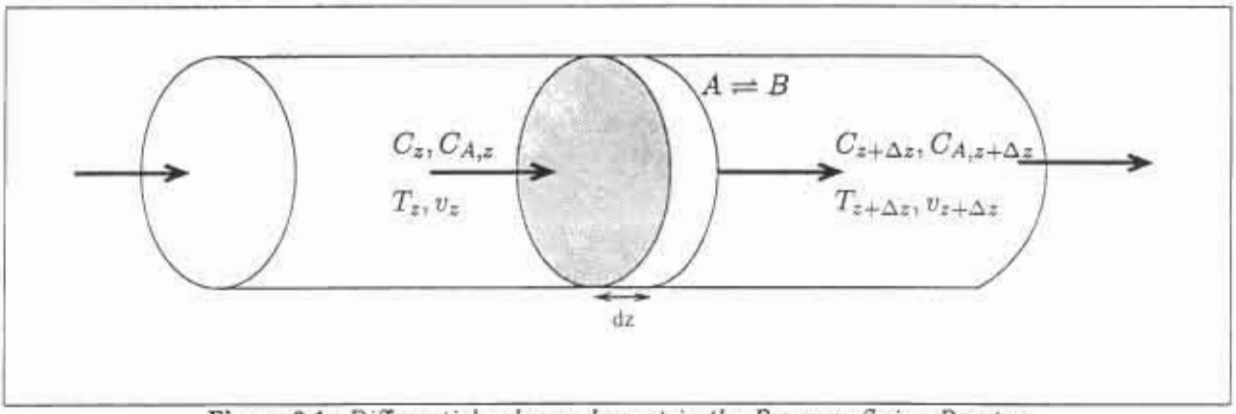

Figure 2.1: *Differential volume element in the Pressure Swing Reactor*

2.1.3 Flow

The gas flow, or velocity will be described by the Navier-Stokes equation. The Navier-Stokes equation makes allowances for viscous, compressible flow as well as contributions from advective terms and flow due to an external pressure driving force.

2.1.4 Summary of assumptions

To make the limitations of the model clear, all the assumptions that were made in the development of the model have been repeated below.

1. No radial pressure or concentration gradients. This reduces the problem to one spatial dimension.
2. All diffusion coefficients are constant and equal.
3. Diffusion follows Fick's law.
4. The reaction follows simple power law kinetics.
5. The reactor is operated either isothermally or adiabatically.
6. There is instantaneous thermal equilibrium between the gas and solid phases.
7. Adsorption kinetics follow a linear driving force model.
8. The adsorption isotherms are of the multicomponent Langmuir type.
9. The adsorbed phase concentration is locally homogeneous, i.e. $q_i = \overline{q}_i$.

10. The catalyst and adsorbent are uniformly distributed throughout the reactor length.

11. The reaction rate and the Henry's constants of adsorption have an Arrhenius temperature dependency.

12. The heat of reaction and adsorption are constant.

13. Gravitational forces are insignificant.

2.2 Formulation of the Model Equations

2.2.1 General Balance Equations

Material balances

A material balance is performed for each species taking part in reaction or adsorption as well as an overall mass balance. Naturally, one of these equations is redundant due to the restriction that the sum of the mole fractions of the components is necessarily unity, i.e.

$$\sum_{i=1}^{C} y_i = 1 \tag{2.1}$$

Thus one material balance equation, usually one of the species equations may be omitted for solution purposes. The absent component is easily recovered by invoking (2.1).

Referring to Figure 2.1, the overall mole balance in the gas phase consists of

$$\{\text{Accumulation}\} = \{\text{Net flux through element}\} - \{\text{Net loss to adsorption}\} + \{\text{Net increase through reaction}\} \tag{2.2}$$

$$\{\text{Accumulation}\} = \left\{ \varepsilon A \Delta z C \Big|_{t+\Delta t} - \varepsilon A \Delta z C \Big|_{t} \right\} \tag{2.3a}$$

$$\{\text{Net flux through element}\} = \left\{ C\varepsilon A v \Delta t \Big|_{z} - C\varepsilon A v \Delta t \Big|_{z+\Delta z} - D\frac{\partial \varepsilon C}{\partial z}\Big|_{z} + D\frac{\partial \varepsilon C}{\partial z}\Big|_{z+\Delta z} \right\} \tag{2.3b}$$

$$\{\text{ Net loss to adsorption}\} = \left\{ (1-\varepsilon)\rho_s \sum_{i=1}^{C} A \Delta z \bar{q} \Big|_{t+\Delta t} - (1-\varepsilon)\rho_s \sum_{i=1}^{C} A \Delta z \bar{q} \Big|_{t} \right\} \tag{2.3c}$$

$$\{\text{Net increase through reaction}\} = 0 \tag{2.3d}$$

The net mole increase due to reaction is taken from the reaction stoichiometry and is zero for the reaction $A \rightleftharpoons B$. Replacing each term in (2.2) with the expressions in (2.3), dividing through by $\varepsilon A \Delta z \Delta t$ and taking the limits as Δz and Δt tend to zero, the following partial differential equation is obtained.

$$\frac{\partial C}{\partial t} = D_z \frac{\partial^2 C}{\partial z^2} - \frac{\partial C v}{\partial z} - \frac{(1-\varepsilon)}{\varepsilon} \sum_{i=1}^{C} \rho_s \frac{\partial \bar{q}_i}{\partial t} \tag{2.4}$$

The species mole balances follow the same procedure, except in this case the reaction term must be included. The partial differential equation describing the evolution of each species is then

$$\frac{\partial C_i}{\partial t} = D_{z,i} \frac{\partial^2 C_i}{\partial z^2} - \frac{\partial C_i v}{\partial z} - \frac{(1-\varepsilon)}{\varepsilon} \rho_s \left(\frac{\partial \bar{q}_i}{\partial t} + r_i \right), \quad i = 1 \ldots C \tag{2.5}$$

where

$$r_i = r(T, C_1, C_2, \ldots, C_C) \tag{2.6}$$

in general.

For elementary first-order reversible reaction kinetics and two reacting species

$$-r_A = k_f C_A - k_r C_B \tag{2.7}$$

$$= k_f C_A - \frac{k_f}{\mathrm{Ke}}(C - C_A) \tag{2.8}$$

The adsorption rates follow the linear driving force model (Gluekauf, 1955):

$$\frac{\partial \overline{q}_i}{\partial t} = k(q_i^* - \overline{q}_i) \tag{2.9}$$

and the multicomponent Langmuir isotherm is employed for the adsorption equilibria:

$$q_i* = q_{s,i}\frac{B_i C_i}{1 + \sum_{j=1}^{C} B_j C_j} \tag{2.10}$$

Energy balance

The adiabatic energy balance described above is given by the following equation,

$$\left(\frac{(1-\varepsilon)}{\varepsilon}\rho_s Cp_s + M_r CCp\right)\frac{\partial T}{\partial t} = -M_r CCp\frac{\partial Tv}{\partial z} + k_z\frac{\partial^2 T}{\partial z^2} - r\frac{(1-\varepsilon)}{\varepsilon}\rho_s \Delta H_{rxn} - \sum_{i=1}^{C}\frac{(1-\varepsilon)}{\varepsilon}\rho_s \Delta H_{ads}\frac{\partial \overline{q}_i}{\partial t} \tag{2.11}$$

Momentum balance

The momentum balance, which describes the Pressure drop inside the reactor vessel or in this case the velocity profile, is given by the Navier-Stokes-Duhem equation for compressible flow (Bird et al., 1960). This is a vector-valued equation, but since only one spatial dimension is considered, only one component is required.

$$\rho\frac{D\mathbf{v}}{Dt} = \rho\mathbf{b} - \nabla p + \mu\nabla(\nabla\cdot\mathbf{v}) + \mu\nabla(\nabla\mathbf{v})^T \tag{2.12}$$

of which only consider the z component is needed,

$$\rho\left[\frac{\partial v}{\partial t} + v\frac{\partial v}{\partial z}\right] = -\frac{dP}{dz} + 2\mu\frac{\partial^2 v}{\partial z^2} \tag{2.13}$$

Gravitational and other body forces, b_z have been neglected.

Table 2.1: *Definition of dimensionless variables*

$x = \frac{z}{L}$	$\tau = \frac{v_0 t}{L}$	$u = \frac{v}{v_0}$
$\phi = \frac{\bar{q}}{q_s}$	$\Pi = \frac{P}{P_H}$	$\theta = \frac{T}{T_0}$
$\varphi = \frac{C}{C_0}$	$\sigma = \frac{\rho_s L}{v_0 C_0} r$	

2.2.2 Dimensionless equations

To get a clearer picture of the important parameters in the equation set, it is useful to rewrite it in dimensionless form. To do this, we first define the dimensionless variables listed in Table 2.1.

Then, by substituting into equations (2.4) to (2.13) and dividing to remove coefficients on the left-hand sides, the desired dimensionless equations are obtained. The coefficients of the terms on the right-hand side of the equations, which are also dimensionless, are redefined as dimensionless groups. The dimensionless equations as well as their corresponding dimensionless groups are given below.

Mole Balances

The overall dimensionless mole balance is given by (2.14) and the dimensionless species balances by (2.18).

$$\frac{\partial \varphi}{\partial \tau} = \frac{1}{\mathrm{Pe_m}} \frac{\partial^2 \varphi}{\partial x^2} - \frac{\partial (\varphi u)}{\partial x} - \sum_{i=1}^{C} \mathrm{Qa}_i \frac{\partial \phi_i}{\partial \tau} \tag{2.14}$$

with

$$\frac{\partial \phi_i}{\partial \tau} = \kappa_i (\phi_i^* - \phi_i) \tag{2.15}$$

and

$$\phi_i^* = \frac{\beta_i y_i \varphi}{1 + \sum \beta_j y_j \varphi} \tag{2.16}$$

The Henry's constants are temperature dependent and for the adiabatic case are modelled

as

$$\beta_i = \beta_{i,\text{ref}} e^{\text{Br}\left(\frac{1}{\theta}-1\right)} \tag{2.17}$$

where $\beta_{i,\text{ref}}$ is the Henry's constant at the inlet temperature, T_{in}.

The species mole balances are

$$\frac{\partial(\varphi_i)}{\partial\tau} = \frac{1}{\text{Pe}_\text{m}}\frac{\partial^2(\varphi_i)}{\partial x^2} - \frac{\partial(\varphi_i u)}{\partial x} - \text{Qa}_i\frac{\partial\phi_i}{\partial\tau} + \text{Rn}\sigma_i \tag{2.18}$$

For the isothermal case, $\text{Rn} = \text{Rn}_{\text{iso}}$ and

$$\sigma_A = \frac{1}{\text{Ke}}\Big(\varphi - \varphi_A(\text{Ke}+1)\Big) \tag{2.19}$$

$$\sigma_B = -\sigma_A \tag{2.20}$$

For the adiabatic case, $\text{Rn} = \text{Rn}_{\text{ad}}$ and

$$\sigma_A = e^{\frac{\text{Ke}0}{\theta}} e^{\frac{-\text{Ea}0}{\theta}}\left(\varphi - \varphi_A\left(e^{\frac{-\text{Ke}0}{\theta}}+1\right)\right) \tag{2.21}$$

Dimensionless Energy Balance

The dimensionless form of (2.11) is

$$(\text{Cr}+\varphi)\frac{\partial\theta}{\partial\tau} = -\varphi\frac{\partial(\theta u)}{\partial x} + \frac{1}{\text{Pe}}\frac{\partial^2\theta}{\partial x^2} + \text{Hr}\,\sigma_A - \sum_{i=1}^{C}\text{Qa}_i\text{Ha}\frac{\partial\phi_i}{\partial\tau} \tag{2.22}$$

Momentum Balance

The Navier-Stokes-Duhem equation for this system becomes

$$\frac{\partial u}{\partial\tau} = -u\frac{\partial u}{\partial x} - \frac{\text{Eu}}{\varphi}\frac{d\Pi}{dx} + \frac{2}{\text{Re}\,\varphi}\frac{\partial^2 u}{\partial x^2} \tag{2.23}$$

The dimensionless groups represented in (2.14) to (2.23) are defined in Table 2.2. The Reynolds, Euler and Peclet numbers are familiar and typically found in fluid flow equations.

Table 2.2: *Definition of the Dimensionless groups seen in* (2.14) *to* (2.23)

$\mathrm{Pe_m} = \dfrac{v_0 L}{D_z}$	$\mathrm{Qa_i} = \dfrac{(1-\varepsilon)}{\varepsilon}\dfrac{\rho_s q_{s,i}}{C_0}$	$\mathrm{Cr} = \dfrac{(1-\varepsilon)}{\varepsilon}\dfrac{\rho_s Cp_s}{M_r C_0 Cp}$
$\mathrm{Pe} = \dfrac{M_r C_0 L Cp\, v_0}{k_z}$	$\mathrm{Hr} = \dfrac{\Delta H_{\mathrm{rxn}}}{M_r Cp T_0}$	$\mathrm{Ha} = \dfrac{\Delta H_{\mathrm{ads}}}{Cp\, T_0 M_r}$
$\mathrm{Eu} = \dfrac{P_H}{M_r C_0 v_0}$	$\mathrm{Re} = \dfrac{\rho v_0 L}{\mu}$	$\kappa_i = \dfrac{k_i L}{v_0}$
$\mathrm{Rn_{ad}} = \dfrac{(1-\varepsilon)}{\varepsilon}\dfrac{A_0 \rho_s L}{v_0}$	$\mathrm{Rn_{iso}} = e^{-Ea0}\mathrm{Rn_{ad}}$	$\mathrm{Br} = \dfrac{\Delta H_{\mathrm{ads}}}{RT_{\mathrm{in}}}$
$\beta_i = B_i C_o$	$\mathrm{Ke0} = \dfrac{\Delta G_{\mathrm{rxn}}}{RT_{\mathrm{in}}}$	$\mathrm{Ea0} = \dfrac{\Delta E_A}{RT_{\mathrm{in}}}$

2.3 Formulation of the Boundary Conditions

While the model equations, viz. the governing partial differential equations, describe the physics of the system, and form the deterministic basis for how it behaves, the boundary conditions fulfill the role of describing the operating principles of the process. The PDE's describing the PSR are second order in space. This imposes the need for two boundary conditions for each equation, one at each end of the reactor corresponding to $z = 0$ and at $z = L$. The evolution of the adsorbed phases are given by (2.9). Since this is an ordinary differential equation with time as the independent variable, no boundary conditions are necessary for ϕ_i.

Additionally, since each of the four steps of the Pressure Swing Reaction process is operated differently, there will be four sets of boundary conditions. The formulation of theses conditions are described here.

2.3.1 Pressurisation Step

During pressurisation, the reactor outlet is closed. Pure reactant is pumped into the reactor at high pressure, P_H and at the inlet interstitial velocity, v_0 and temperature, T_0. The concentration is assumed to be continuous across the reactor inlet. This models the case where a short bed of inert material of the same porosity is placed before the reactor inlet (Barber et al., 1998).

Formulation

In terms of the normal variables of the system, the boundary conditions are then:

$$z = 0: \quad y_A = 1 \qquad (2.24a) \qquad\qquad z = L: \quad \frac{\partial y_A}{\partial z} = 0 \qquad (2.25a)$$

$$C = \frac{P_H}{RT_0} \qquad (2.24b) \qquad\qquad \frac{\partial C}{\partial z} = 0 \qquad (2.25b)$$

$$T = T_0 \qquad (2.24c) \qquad\qquad \frac{\partial T}{\partial z} = 0 \qquad (2.25c)$$

$$v = v_0 \qquad (2.24d) \qquad\qquad v = 0 \qquad (2.25d)$$

Dimensionless Boundary Conditions

Using the definitions supplied in Table 2.1 the dimensionless boundary conditions for the Pressurisation step are:

$$x = 0: \quad y_A = 1 \qquad (2.26a) \qquad\qquad x = 1: \quad \frac{\partial y_A}{\partial x} = 0 \qquad (2.27a)$$

$$\varphi = 1 \qquad (2.26b) \qquad\qquad \frac{\partial \varphi}{\partial x} = 0 \qquad (2.27b)$$

$$\theta = 1 \qquad (2.26c) \qquad\qquad \frac{\partial \theta}{\partial x} = 0 \qquad (2.27c)$$

$$u = 1 \qquad (2.26d) \qquad\qquad u = 0 \qquad (2.27d)$$

2.3.2 Adsorption Step

The adsorption step begins when the exit valve is opened allowing product to be collected. Pure feed is still introduced at the reference pressure and temperature. Thus, the inlet boundary conditions for this step do not change. At the outlet, the velocity is allowed to take on a nonzero value

$$z = L: \quad \frac{\partial v}{\partial z} = 0 \qquad (2.28)$$

and the other boundary conditions are unchanged.

In dimensionless terms, the adsorption step boundary conditions are

$$x = 1: \quad \frac{\partial u}{\partial x} = 0 \qquad (2.29)$$

2.3.3 Blowdown Step

The blowdown step sees the exit valve being closed off, the feed supply stopped and the reactor entrance pressure reduced to P_{iL}. This causes desorption of reactant and product from the

adsorbent and some purging of the reactor vessel. The corresponding boundary conditions are

$$z = 0: \quad \frac{\partial y_A}{\partial z} = 0 \qquad (2.30a) \qquad z = L: \quad \frac{\partial y_A}{\partial z} = 0 \qquad (2.31a)$$

$$\frac{\partial C}{\partial z} = 0 \qquad (2.30b) \qquad \frac{\partial C}{\partial z} = 0 \qquad (2.31b)$$

$$\frac{\partial T}{\partial z} = 0 \qquad (2.30c) \qquad \frac{\partial T}{\partial z} = 0 \qquad (2.31c)$$

$$\frac{\partial v}{\partial z} = 0 \qquad (2.30d) \qquad v = 0 \qquad (2.31d)$$

The equivalent dimensionless boundary conditions for the Blowdown step are

$$x = 0: \quad \frac{\partial y_A}{\partial x} = 0 \qquad (2.32a) \qquad x = 1: \quad \frac{\partial y_A}{\partial x} = 0 \qquad (2.33a)$$

$$\frac{\partial \varphi}{\partial x} = 0 \qquad (2.32b) \qquad \frac{\partial \varphi}{\partial x} = 0 \qquad (2.33b)$$

$$\frac{\partial \theta}{\partial x} = 0 \qquad (2.32c) \qquad \frac{\partial \theta}{\partial x} = 0 \qquad (2.33c)$$

$$\frac{\partial u}{\partial x} = 0 \qquad (2.32d) \qquad u = 0 \qquad (2.33d)$$

2.3.4 Purge Step

To prepare the reactor bed for the next cycle, a purge step is necessary. This involved back-flushing the bed with product at low pressure, P_L and at the reference velocity, $-v_0$ to remove any feed still in the reactor. The inlet conditions remain unchanged from the blowdown step.

$$z = L: \quad y_A = 0 \qquad (2.34a)$$

$$C = \frac{P_L}{RT_0} \qquad (2.34b)$$

$$T = T0 \qquad (2.34c)$$

$$v = -v_0 \qquad (2.34d)$$

The exit end dimensionless equivalents are

$$x = 1: \quad y_A = 0 \qquad (2.35a)$$

$$\varphi = \frac{P_L}{P_H} = \mathrm{P_{iL}} \qquad (2.35b)$$

$$\theta = 1 \qquad (2.35c)$$

$$u = -1 \qquad (2.35d)$$

2.4 Numerical Methods

Two numerical engines were used to solve the PSR system. In this section they are described and their solution strategies briefly discussed.. Deviations from the original set of equations and any additional assumptions that are imposed will also be covered.

2.4.1 PDECOL

Description

PDECOL is a partial differential equation solver originally written in FORTRAN. It is capable of handling coupled second-order equations. It does this by converting the spatial component of the equations into algebraic equations using collocation on finite elements. The resulting first order, coupled and generally stiff, ordinary differential equations are then integrated using Gear's method (Madsen and Sincovec, 1992).

Form of Boundary Conditions for PDECOL

PDECOL requires continuity between the initial conditions and the boundary conditions. In addition, the boundary conditions are required to remain continuous as a function of time. This is a potential problem at the switchover point of any of the steps and certainly between the adsorption and blowdown steps.

In order to overcome these constraints, the boundary conditions were implemented slightly differently than stated in Section 2.3. Wherever a potential discontinuity seemed likely, the boundary condition variables were not set to their new values immediately in a discontinuous fashion, but rather approached them asymptotically using exponential functions. For example if the boundary condition were to change X from 0 to 1, it would be coded as $X = 1 - e^{\alpha t_{ref}}$. It may be argued that this is in fact a more realistic model for the boundary step changes.

The duration of each step in the cycle was specified by the user in the simulation specifications.

All simulations performed under PDECOL utilised the adiabatic version of the PSR equations.

2.4.2 PDASAC

Description

PDASAC is a more modern partial differential equation solver, developed specifically to deal with reaction-diffusion systems. The acronym PDASAC stands for Partial-Differential-Algebraic Sensitivity Analysis Code (Stewart et al., 1996).

PDASAC utilises the method of lines. This involves the use of finite differences to approximate the x derivatives. The resulting ordinary differential equations are solved using a modified version of the implicit integrator DDASSL (Petzold, 1982). This integrator is able to handle stiff systems of coupled equations and is a more advanced variant of Gear's method. It employs a variable-order, variable-step predictor-corrector approach. The time derivatives are approximated by backward difference formulae and the resulting algebraic corrector equations are solved by a modified Newton's method. The step-size and approximation order are automatically adjusted during the integration.

Special Conditions for PDASAC

The simulations run on PDASAC were all based on the isothermal equations for the PSR.

Since PDASAC allows step changes in boundary conditions, they were coded as they stand in Section 2.3.

The step durations for the adsorption and purge step were specified by the simulation parameters. However, PDASAC's boundary condition handlers allowed the user to set flags to terminate the other steps. The pressurisation step was set to end when the pressure at the reactor exit came within 5% of the inlet pressure. The blowdown step terminated when the entrance pressure was within 10% of the desorption pressure.

2.5 Numerical Instability

2.5.1 Introduction

In this section, the phenomenon of numerical instability and particularly nonlinear instability is explained and discussed. This explanation will require a short digression into the subject of Fourier modes and analysis. The mechanisms that cause instability are identified and discussed

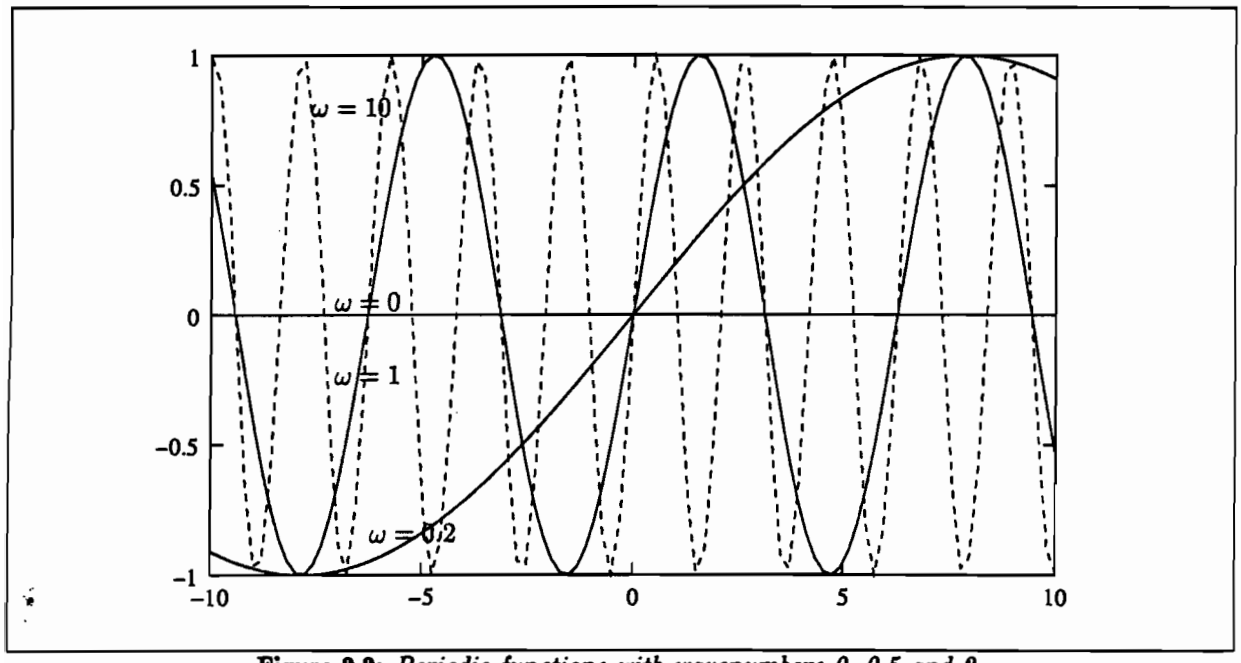

Figure 2.2: *Periodic functions with wavenumbers 0, 0.5 and 2.*

and some suggestions from literature on how to reduce or preferably, eliminate the instability are offered.

Instability is recognisable in a few ways, but common to all forms of instability is evidence of counter-intuitive or physically absurd results. Without going into a formal definition, numerical instability causes "blowup", spurious oscillations (wiggles) or both. "Blowup" occurs when small truncation errors from numerical routines are amplified instead of damped out. This leads to parts of the numerical solution becoming exponentially large very quickly, causing results to explode or "blow up". Oscillations result from poor handling of high frequency harmonics of the system by numerical schemes. These harmonics drift out from their correct position, resulting in waves in what would otherwise be quiescent parts of the solution.

2.5.2 Fourier Transforms

In the same way that functions can be broken down into a linear combination of polynomial functions (in a Taylor series), functions can also be be represented as a sum of periodic, or wavelike functions, such as those in figure 2.2. In fact any absolutely integrable function can be written as the sum of an infinite number of periodic functions each with a unique frequency. This is done through the Fourier Transform and is written as (Haberman, 1987)

$$F(\omega) = \frac{1}{2\pi}\int_{-\infty}^{\infty} f(x)e^{i\omega x}dx \tag{2.36}$$

The inverse Fourier transform is very similar to 2.36 and is given by

$$f(x) = \int_{-\infty}^{\infty} F(\omega)e^{-i\omega x}d\omega \tag{2.37}$$

This indicates that a function is the sum of all waves $e^{-i\omega x}$ with the wavenumber, ω varying across the Real domain. The amplitude of each wave is given by $F(\omega)$. The functions $f(x)$ and $F(\omega)$ form a unique pair called the Fourier transform pair. The wavelength, λ is related to the wavenumber by

$$\lambda = \frac{2\pi}{\omega} \tag{2.38}$$

Clearly, if one has access to the Fourier transform of a function it is easy to see its dependence on various frequencies or frequency ranges. Electrical engineers, for instance use Fourier transforms to eliminate noise from a signal by converting a function to its Fourier transform, setting the harmonics corresponding to the noise to zero, and then applying an inverse Fourier transform to obtain a new, clean signal.

2.5.3 Oscillations

Consider a simple, linear diffusion system

$$\frac{\partial C}{\partial t} = \frac{\partial^2 C}{\partial x^2} - U\frac{\partial C}{\partial x} \tag{2.39}$$

where C is the gas concentration, U is the velocity of the gas and D is the diffusivity. Let $C_0(x)$ describe the initial concentration distribution. Written in the frequency or Fourier domain this becomes

$$C_0(x) = \int_{-\infty}^{\infty} \rho_0(\omega)e^{-i\omega x}d\omega \tag{2.40}$$

The solution of (2.39) can then be written terms of the Fourier integral,

$$C(x,t) = \int_{-\infty}^{\infty} \rho(\omega,t)e^{-i\omega x}d\omega \tag{2.41}$$

It follows that the derivatives of (2.39) are

$$\frac{\partial C}{\partial t} = \int_{-\infty}^{\infty} \frac{\partial \rho}{\partial t} e^{-i\omega x} d\omega \tag{2.42}$$

$$\frac{\partial C}{\partial x} = \int_{-\infty}^{\infty} -i\omega\rho e^{-i\omega x} d\omega \tag{2.43}$$

$$\frac{\partial^2 C}{\partial x^2} = \int_{-\infty}^{\infty} -\omega^2\rho e^{-i\omega x} d\omega \tag{2.44}$$

Substituting (2.42) to (2.44) into (2.39),

$$\int_{-\infty}^{\infty} \left[\frac{\partial \rho}{\partial t} - i\omega U\rho + \omega^2 D\rho\right] e^{-i\omega x} d\omega = 0$$

In order for the integral to exist, the expression in brackets must be zero for all ω. Thus for any fixed ω, the following must hold:

$$\frac{d\rho}{dt} - i\omega U\rho + \omega^2 D\rho = 0$$

and hence

$$\rho = \rho_0 e^{(i\omega U - \omega^2 D)t} \tag{2.45}$$

Placing (2.45) into (2.41) and rearranging,

$$C(x,t) = \int_{-\infty}^{\infty} \left[\rho_0(\omega) e^{-\omega^2 Dt}\right] e^{-i\omega(x-Ut)} d\omega \tag{2.46}$$

It is evident from (2.46) that the waves making up the initial distribution are transported with velocity U, while they are simultaneously decaying exponentially at a rate $\omega^2 D$.

When numerical algorithms are implemented, the system domain is necessarily discretised. This discretisation places a limit on the number of wavelengths that are allowed in (2.46) and the integral becomes a sum. In fact, if the domain is divided into N equal samples, then the sampling interval is $h = 1/N$ and the maximum wavenumber allowed is πN (Adam, 1985). This corresponds to a wavelength of $2/N$, twice the sampling interval. Any function containing waves with shorter wavelengths will not be correctly represented by the numerical scheme.

In most schemes, waves with $\lambda < 6h$ are not handled well, with damping being either too large or too small and the speed of propagation either incorrect or even in the wrong direction.

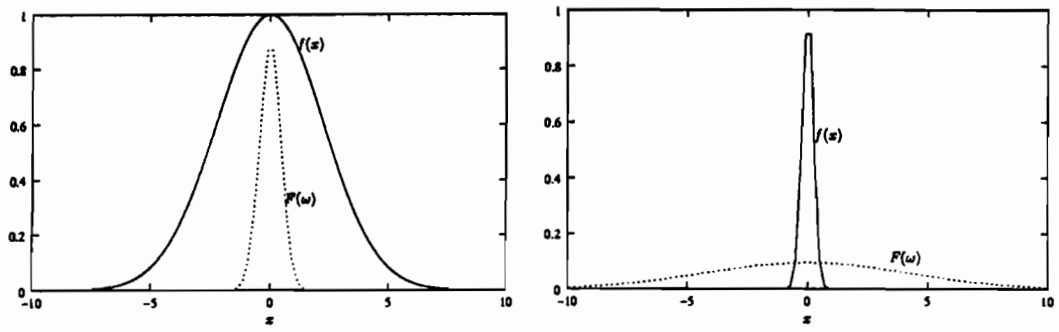

(a) Shallow gradient, steep frequency profile

(b) Steep gradients have wide frequency distributions

Figure 2.3: *The effect of gradient on the Fourier Transform*

The Crank-Nicholson scheme, for instance has $\frac{u^*}{U} < 0.9$ for $\lambda < 10h$, where u^* is the speed of propagation generated by the scheme. Even worse inaccuracies are present in the Lax-Wendroff scheme, where the numerical waves move in the wrong direction for $2h < \lambda < 4h$. This distortion leads to the creation of wiggles and negative concentrations (Adam, 1985).

Effect of gradients on Fourier transform and stability

Based on the discussion in the previous section, the effect the steepness of the concentration profile will have on stability is evident. Figure 2.3 has two illustrations of this effect. In the first, the concentration profile has a gentle gradient. Its associated plot in the frequency domain is highly localised. This indicates that there are very few waves with short wavelengths and that numerical integration will be stable far fairly large values of h. The second plot, however has steep gradients; the associated Fourier plot is widely dispersed, with many high frequency wave contributions. As a result, numerical algorithms will struggle to maintain stability without resorting to very small values of h.

Although the functions in figure 2.3 are idealised, the principle holds for any arbitrary function: Steep gradients lead to instabilities, and as gradients increase, so does the instability. The limiting case for all of this is a vertical gradient, corresponding to the Dirac delta function. The Fourier function for $\delta(x)$ is $\frac{1}{2\pi}$. This means that there are contributions from the entire wave spectrum, $-\infty < \omega < \infty$ and instabilities for any value of h will arise eventually.

The analysis here has been performed on nonlinear equations but the argument is easily extended to nonlinear equations. Any continuous nonlinear system can be linearised at arbitrary

points, causing the same oscillations as before. Experience has shown that nonlinear terms amplify these disturbances rather than damping then out (Whitham, 1974).

Chapter 3

Analytical Results

This chapter provides insight into the PSR equations that were derived in Chapter 2 by examining the model from a mathematical perspective. This approach has the advantage of giving general results, from which trends and interesting cases may be spotted far more easily than would be the case if only numerical experiments were used.

It is obvious however, that the system of equations must be simplified before analysis is carried out, or there would be no need for numerical computation in the first place. The results below examine special cases of the PSR system as well as some fundamental aspects of PSR operation. This is done with the aim that they will provide a guide for the selection of parameters in the numerical experiments.

3.1 Steady-State Solutions

To confirm the integrity of the coded model, the steady-state profile after a long adsorption step can be compared to the analytical steady state solutions. The underlying equations are the same for each step in the PSR process; only the boundary conditions differ. For this reason, a good agreement here over a range of parameters will be deemed sufficient proof that the model has been coded and implemented correctly. The boundary conditions can be confirmed by more intuitive arguments and by simple inspection of the results.

In addition, a PSR with an infinitely long adsorption step is equivalent to a fixed-bed reactor. Since a major aim of this study is to identify regions of the PSR parameter space that outperform a fixed-bed reactor, the steady-state solution provides an important benchmark against which to measure performance.

The steady state equations are found by setting the left-hand side (i.e. the time derivatives) of equations (2.14) to (2.23) to zero. The following system is then obtained:

$$\frac{1}{\mathrm{Pe_m}}\frac{d^2\varphi}{dx^2} - \frac{d(\varphi u)}{dx} = 0 \tag{3.1}$$

$$\frac{1}{\mathrm{Pe_m}}\frac{d^2(y_A\varphi)}{dx^2} - \frac{d(y_A\varphi u)}{dx} + \mathrm{Rn}\,\sigma_A = 0 \tag{3.2}$$

$$\frac{1}{\mathrm{Pe}}\frac{d^2\theta}{dx^2} - \varphi\frac{d(\theta u)}{dx} + \mathrm{Hr}\sigma_A = 0 \tag{3.3}$$

$$\frac{2}{\mathrm{Re}\,\varphi}\frac{d^2u}{dx^2} - u\frac{du}{dx} - \frac{\mathrm{Eu}}{\varphi}\frac{d\Pi}{dx} = 0 \tag{3.4}$$

Solving a system of nonlinear, coupled equations such as these analytically is a difficult, if not impossible task. To make some headway, some simplifying assumptions are required.

Assumption: The steady-state total concentration is one; $\varphi = 1$

This is an entirely reasonable assumption because although reaction may be taking place, the overall number of moles is conserved, adsorption is at equilibrium and no accumulation is occurring in the reactor.

Substituting $\varphi = 1$ into equation (3.1) one obtains:

$$u' = 0 \tag{3.5}$$

which when combined with the boundary conditions, $u(0) = 1$ and $u'(1) = 0$ becomes

$$u = 1 \tag{3.6}$$

Taking equation (3.4) and noting that for an ideal gas

$$\frac{d\Pi}{dx} = \theta\frac{d\varphi}{dx} + \varphi\frac{d\theta}{dx}$$

after substituting (3.6) and simplifying the notation, one obtains

$$\theta' = 0$$

$$\Rightarrow \theta = 1 \tag{3.7}$$

after inclusion of the boundary conditions. Consider equation (3.3). Substituting $\theta = \varphi = u = 1$, the resulting equation is simply $\mathrm{Hr}\,\sigma = 0$. Since the reactor is not at equilibrium along its entire length, $\sigma \neq 0$ and so Hr= 0. Thus these conditions can only occur if the system is isothermal. This then is the second assumption:

Assumption: The dimensionless heat of reaction is zero; $Hr = 0$

Finally, taking (3.2) and noting that

$$(y_A\varphi)'' = (y_A\varphi' + y_A'\varphi)' \tag{3.8}$$

$$= y_A\varphi'' + 2y_A\varphi + y_A''\varphi \tag{3.9}$$

after cancelling equation (3.1),

$$\frac{1}{\mathrm{Pe_m}}y_A'' - y_A' + \mathrm{Rn}\,\sigma = 0 \tag{3.10}$$

Substituting equation (2.21), (3.10) becomes

$$y_A'' - \mathrm{Pe_m}y_A' - \mathrm{Pe_m}\mathrm{Rn}\,\alpha_1\alpha_2 y_A = -\mathrm{Pe_m}\mathrm{Rn}\,\alpha_1 \tag{3.11}$$

with

$$\alpha_1 = e^{-\mathrm{Ea0}+\mathrm{Ke0}}, \tag{3.12}$$

$$\alpha_2 = 1 + e^{-\mathrm{Ke0}} \tag{3.13}$$

for the adiabatic model equations and

$$\alpha_1 = \frac{1}{\mathrm{Ke}}, \tag{3.14}$$

$$\alpha_2 = 1 + \mathrm{Ke} \tag{3.15}$$

for the isothermal model.

This is a non-homogeneous linear second-order ordinary differential equation. The general solution is:

$$y_A = y_{Ac} + y_{Ap} \tag{3.16}$$

where y_{Ac} is the solution to the homogeneous part of equation (3.11) and y_{Ap} is any solution to (3.11) that is linearly independent of y_{Ac}. It is straightforward to confirm that

$$y_{Ac} = e^{\frac{\mathrm{Pe_m}}{2}x} B\{\cosh(\Delta x) - A\sinh(\Delta x)\} \tag{3.17a}$$

where

$$A = \frac{\frac{\mathrm{Pe_m}}{2}\cosh(\Delta) + \Delta\sinh(\Delta)}{\frac{\mathrm{Pe_m}}{2}\sinh(\Delta) + \Delta\cosh(\Delta)}, \tag{3.17b}$$

$$B = 1 - \frac{1}{\alpha_2} \tag{3.17c}$$

and

$$\Delta = \sqrt{\left(\frac{\mathrm{Pe_m}}{2}\right)^2 + \mathrm{Pe_m Rn}\,\alpha_1\alpha_2} \tag{3.17d}$$

A particular solution, y_{Ap} is found by inspection:

$$y_{Ap} = \frac{1}{\alpha_2} \tag{3.18}$$

Thus the final form of the steady-state mole fraction is specified by equations (3.16), (3.17) and (3.18) under the two assumptions specified above. This solution can be written more concisely if Δ is large and $A \approx 1$. $\Delta > 3$ can be considered large since this corresponds to $A > 0.995$. Simplifying some more,

$$y_A = e^{\left\{\left(\frac{Pe_m}{2}-\Delta\right)x\right\}}\left(1-\frac{1}{\alpha_2}\right)+\frac{1}{\alpha_2} \tag{3.19}$$

In the special case of isothermal operation the steady-state solution is

$$y_A = \frac{1+e^{\left\{\left(\frac{Pe_m}{2}-\Delta\right)x\right\}}\mathrm{Ke}}{1+\mathrm{Ke}} \tag{3.20}$$

3.2 Short results

Several unrelated results are presented that are too short to command their own section. Two of the analyses identify the conditions necessary in the kinetics and adsorption equilibrium expression to obtain enrichment of product in the low pressure steps, viz. blowdown and purge. The final part proves that the model parameters are independent.

3.2.1 Pressure and adsorption equilibrium concentration

Pressure Swing Adsorbers and by inference, Pressure Swing Reactors rely on the change in adsorption properties with pressure for their operation.

In order to collect the strongly adsorbed component, one seeks a situation where a given drop in pressure results in an even larger drop in the adsorption equilibrium concentration, relatively speaking. To be more precise, the ratio of the adsorption equilibrium concentration at the high and low pressure must be greater than one for any enrichment of A to occur during the low pressure steps.

Let

$$\phi_1^* = \frac{\beta_i \varphi_i}{1+\sum \beta_j \varphi_j} \tag{3.21}$$

be the adsorption equilibrium concentration at the low pressure stage of operation, φ. Then if the high pressure concentration is φ' they can be related by

$$\varphi_i' = n\varphi_i; \quad n > 1 \tag{3.22}$$

where $n = \frac{P_H}{P_L}$ and consequently the high pressure adsorption equilibrium concentration is given by

$$\phi_2^* = \frac{\beta_i \varphi_i'}{1 + \sum \beta_j \varphi_j'} \tag{3.23}$$

Substituting (3.22) into (3.23) to get

$$\phi_2^* = \frac{n\beta_i \varphi_i}{1 + n\sum \beta_j \varphi_j} \tag{3.24}$$

and the adsorbed concentration equilibrium ratio is then

$$\frac{\phi_2^*}{\phi_1^*} = n\frac{1+\chi}{1+n\chi} \tag{3.25}$$

where $\chi = \sum \beta_j \varphi_j$.

High Pressures and/or steep Isotherm gradients

For $\chi \to \infty$

$$\begin{aligned} \frac{\phi_2^*}{\phi_1^*} &= n\frac{1+\chi}{1+n\chi} \\ &= n\frac{\chi}{n\chi} && (3.26) \\ &= 1 && (3.27) \end{aligned}$$

For high pressures, or when the isotherm gradient for one or more of the components is large (indicated by a large Henry's constant), the adsorption equilibrium concentration remains constant. Therefore no product is released to the gas phase during the low pressure steps and no enrichment occurs. To give an idea of constitutes high pressure, $\chi \geq 6$ is sufficiently large for $n = 1.5$ to limit the drop in adsorption equilibrium concentration by 5%. Values for β can lie anywhere between 0 and 20000, so in general low partial pressures are required to achieve any notable enrichment in the strongly adsorbed component. This argument applies to both PSA and PSR operation. In PSA operation this fact can generally be ignored, since it is usually the weakly adsorbed component that is of interest, while the strongly adsorbed component is discarded.

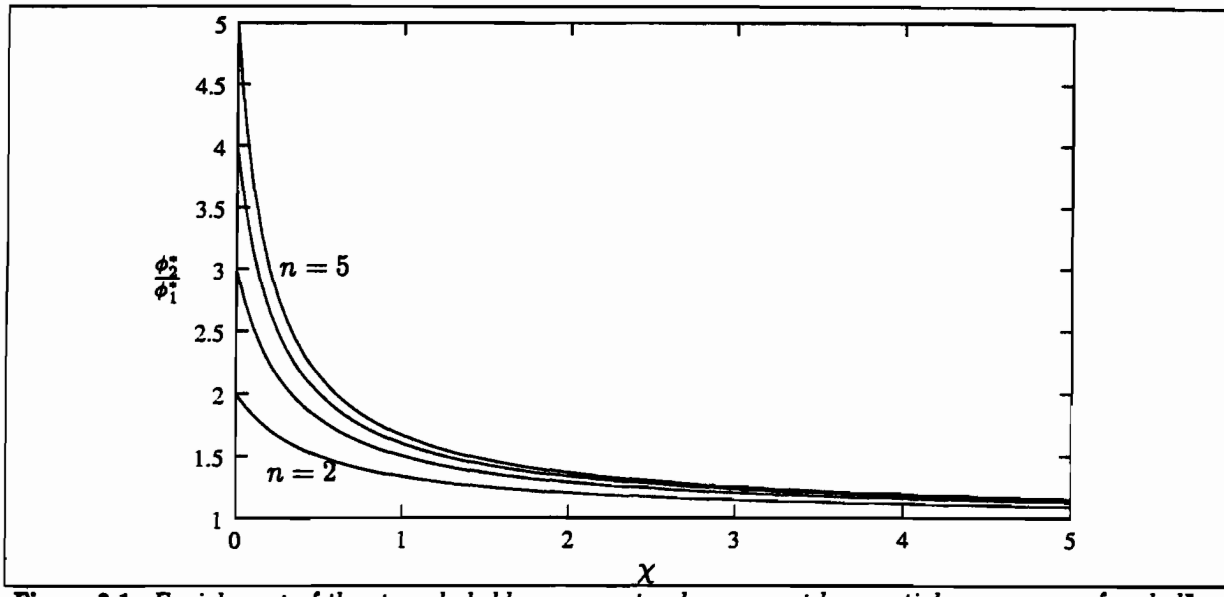

Figure 3.1: *Enrichment of the strongly held component only occurs at low partial pressures or for shallow isotherm gradients.*

Low Pressures and/or shallow Isotherm gradients

In the other extreme, for $\chi \ll 1$,

$$\frac{\phi_2^*}{\phi_1^*} \approx n\big(1+\chi\big)\big(1-n\chi\big) \tag{3.28}$$

$$= n\Big(1+(1-n)\chi - n\chi^2\Big) \tag{3.29}$$

$$\approx n - n(n-1)\chi \tag{3.30}$$

(3.28) has been plotted for $n = 2 \ldots 5$ in Figure 3.1. There the enrichment of the strongly adsorbed component at low partial pressures is evident, but this effect diminishes rapidly as χ increases. The effect also decreases with decreasing n, requiring possibly expensive pressure ratios to achieve acceptable separation.

It should be noted that this analysis was performed under the assumption that the multi-component Langmuir model is a good approximation of the adsorption behaviour. At very low partial pressures, the isotherms may well become linear, in which case the drop in equilibrium concentration is linearly proportional to the drop in pressure. This particular result has been expressed before in texts on adsorption (Ruthven, 1984; Yang, 1987).

3.2.2 Pressure and reaction rate

As was mentioned in the previous section, the difference between the adsorbing and desorbing pressure must provide the driving force for separation. When reactions are added to the system, one needs to consider whether the reaction will be detrimental to the separation process, enhance it, or play no significant role in either direction.

If product is to be collected during the low pressure steps, the reaction rate must have a super-linear dependency on the pressure. If this is not the case, then all the gains made in the adsorption step will be lost in the blowdown and purge steps due to the reverse reaction. Ideally, one would want the case where the reaction proceeds fairly quickly during the adsorption step, but comes to a near halt in the reverse flow steps so that the separation work isn't ruined by the reverse reaction.

The effect of pressure on the reaction rate will now be considered for the kinetics that are used in this system, viz. reversible first order. This is an extremely simple result and is found in many reactor design texts (Smith, 1981; Fogler, 1992).

If the reaction rates at the lower and higher pressures are denoted σ_1 and σ_2 respectively then from (2.19),

$$\sigma_1 = \mathrm{Rn}\left(\frac{\varphi}{\mathrm{Ke}} - \left(\frac{\mathrm{Ke}+1}{\mathrm{Ke}}\right)\varphi_A\right) \tag{3.31}$$

Keeping the same notation as before,

$$\varphi'_A = n\varphi_A; \quad n > 1 \tag{3.32}$$

$$\varphi' = n\varphi \tag{3.33}$$

Thus

$$\sigma_2 = \mathrm{Rn}\left(\frac{\varphi'}{\mathrm{Ke}} - \left(\frac{\mathrm{Ke}+1}{\mathrm{Ke}}\right)\varphi'_A\right) \tag{3.34}$$

$$= \mathrm{Rn}\left(\frac{n\varphi}{\mathrm{Ke}} - n\varphi_A\left(\frac{\mathrm{Ke}+1}{\mathrm{Ke}}\right)\right) \tag{3.35}$$

$$= n\sigma_1 \tag{3.36}$$

$$\therefore \frac{\sigma_2}{\sigma_1} = n \tag{3.37}$$

It is clear from (3.37) that simple first-order kinetics are linearly proportional to the pressure

ratio and as such neither aid nor hinder separation. In the system under investigation, the reaction proceeds at relatively the same rate no matter what the pressure is. It is important to keep in mind that catalysed reactions rarely, if ever, follow simple first-order kinetics. The kinetics were chosen to keep the DAE system fairly simple. More accurate and undoubtedly nonlinear reaction kinetics will give different results. Favourable reactions for PSR-type processes are those that predict $\frac{\sigma_2}{\sigma_1} = \kappa n$ with $\kappa > 1$ or preferably $\frac{\sigma_2}{\sigma_1} = \mathcal{O}(n^2)$ or even higher orders. The larger the dependency on pressure, the better the PSR will perform because the reverse reaction gets stunted to a far greater degree than the corresponding drop in pressure.

3.2.3 Independence of Dimensionless Groups

It would defeat the purpose of the numerical study if one of the variables in the equation set inadvertently was a function of one or more of the other variables. It is therefore imperative that the independence of the dimensionless groups be established. By making sure that all the dimensionless groups are independent, one may vary each of them at will without being concerned that this will impact any of the other groups.

Another way of approaching the problem is to ensure that the smallest number of dimensionless variables possible have been selected, given the set of reference variables chosen and that they are sufficient to describe all the physical cases of our system.

Since each equation in (2.14) to (2.23) has at least one term with a coefficient of 1, there can be no more algebraic manipulation to further reduce the set. Thus it remains to prove that the groups are mutually independent.

If a group were dependent, it would be possible to write it as a product of a subset of the remaining dimensionless parameters.

Determining Independence

Let there be n dimensionless groups, denoted $\Pi_1, \Pi_2, \ldots, \Pi_n$. Now assume that these groups are products of m independent process variables, denoted $x_1, x_2, ..., x_m$. Then each dimensionless group can be written as

$$\Pi_j = x_1^{a_{1j}} x_2^{a_{2j}} \ldots x_m^{a_{mj}}, \quad a_{ij} \in \mathbb{R}$$

If a dimensionless group is *dependent* on any combination of the other dimensionless groups,

it can be written as a product of those groups:

$$\Pi_k = \Pi_1^{b'_1}\Pi_2^{b'_2}\ldots\Pi_{k-1}^{b'_{k-1}}\Pi_{k+1}^{b'_{k+1}}\cdots\Pi_n^{b'_n}$$

where at least one exponent on the righthand side is nonzero. Dividing both sides by Π_k the following general expression is obtained:

$$\Pi_1^{b_1}\Pi_2^{b_2}\cdots\Pi_n^{b_n} = 1 \tag{3.38}$$

The groups are independent if and only if $b_1 = b_2 = \cdots = b_n = 0$. Expanding each group in terms of its variables,

$$(x_1^{a_{11}}x_2^{a_{21}}\cdots x_m^{a_{m1}})^{b_1}\,(x_1^{a_{12}}x_2^{a_{22}}\cdots x_m^{a_{m2}})^{b_2}\cdots(x_1^{a_{1n}}x_2^{a_{2n}}\cdots x_m^{a_{mn}})^{b_n} = 1 \tag{3.39}$$

and collecting exponents together one obtains the following set of equations:

$$a_{11}b_1 + a_{12}b_2 + \ldots + a_{1n}b_n = 0 \tag{3.40a}$$

$$a_{21}b_1 + a_{22}b_2 + \ldots + a_{2n}b_n = 0 \tag{3.40b}$$

$$\vdots$$

$$a_{m1}b_1 + a_{m2}b_2 + \ldots + a_{mn}b_n = 0 \tag{3.40c}$$

(3.40) can be represented more concisely in matrix notation,

$$A\mathbf{b} = \mathbf{0} \tag{3.41}$$

where

$$A = \begin{bmatrix} a_{11} & a_{12} & \cdots & a_{1n} \\ \vdots & & \ddots & \\ a_{m1} & a_{m2} & \cdots & a_{mn} \end{bmatrix}$$

and

$$\mathbf{b} = \{b_1, b_2, \ldots, b_n\}^T$$

For an independent set, $\mathbf{b} = \mathbf{0}$, which is true if and only if the rank$(A) = n$. Otherwise, the set contains dependent groups with the number of dependent groups being $n - \text{rank}(A)$.

Application to PSR equations

When the dimensionless groups associated with the PSR equations, (2.14) to (2.23) are arranged into the matrix system described by (3.41), A is a 23x14 matrix with rank 14. Therefore, all the dimensionless groups in (2.14) to (2.23) are linearly independent. The calculation can be found in Appendix A.

3.3 Perturbation analysis

3.3.1 Introduction

Tremendous strides have been made in the models of physical processes over the last century. This has inevitably led to the equations representing these theories to become more and more complex. While solutions to linear differential equations can be found in most cases, the same is certainly not true for nonlinear equations. However, this has not dampened the enthusiasm of physicists to try and extract as much information about the systems that they're modelling as possible. In some instances, approximate solutions to the models are more than adequate. One very powerful technique that has emerged to produce approximate solutions of differential equations is Perturbation Theory. This theory is based on the fact that physical systems often operate over several scales varying across several orders of magnitude with different mechanisms dominating in each domain. By joining the various domains together an overall approximate solution of the entire system can be obtained.

The equations that govern the Pressure Swing Reactor are highly nonlinear thanks mainly to the presence of the Navier-Stokes equation, the nonlinear adsorption isotherms and the reaction term. Finding an analytical solution of the complete system in closed form is a hopeless task, but Perturbation Theory may offer some respite.

For an excellent introduction and overview of Perturbation techniques, see the books by Nayfeh (1981) and Cole (1968).

3.3.2 Analysis

Formal definition of the problem

Consider the following system of partial differential equations governing the isothermal PSR, with the adsorption and reaction terms replaced by the general functions, f and g.

$$\varphi_t = a\varepsilon\varphi_{xx} - (\varphi u)_x - f(\varphi, \varphi_A) \tag{3.42}$$

$$\varphi_{At} = a\varepsilon\varphi_{Axx} - (\varphi_{Au})_x - g(\varphi, \varphi_A) \tag{3.43}$$

$$\varphi u_t = \varepsilon u_{xx} - u\varphi u_x - b\varphi_x \tag{3.44}$$

Here a and b are positive constants with $b = \mathrm{Eu}$. The small parameter, $\varepsilon = \frac{2}{\mathrm{Re}} \ll 1$ and $\{a : a\varepsilon = \frac{1}{\mathrm{Pe_m}}, a = \mathcal{O}(1)\}$. The system (3.42) to (3.44) is subject to the initial and boundary conditions of the PSR.

Form of Solutions

The solution takes the form

$$\varphi(x,t) = \varphi_0(x,t) + \varepsilon\varphi_1(x,t) + \varepsilon^2\varphi_2(x,t) + \ldots \tag{3.45}$$

$$\varphi_A(x,t) = \varphi_{A0}(x,t) + \varepsilon\varphi_{A1}(x,t) + \varepsilon^2\varphi_{A2}(x,t) + \ldots \tag{3.46}$$

$$u(x,t) = u_0(x,t) + \varepsilon u_1(x,t) + \varepsilon^2 u_2(x,t) + \ldots \tag{3.47}$$

Derivation of Perturbed Equations

The perturbed form of the solutions, (3.45) to (3.47) are substituted into the governing equations (3.42) to (3.44). Since $\varepsilon \ll 1$, only terms up to $\mathcal{O}(\varepsilon)$ are kept. Higher order terms are assumed

to be negligibly small and have no significant contribution to the solution:

$$(\varphi_0 + \varepsilon\varphi_1)_t = a\varepsilon\,(\varphi_0)_{xx} - [(\varphi_0 + \varepsilon\varphi_1)\,(u_0 + \varepsilon u_1)]_x - f\,(\varphi_0 + \varepsilon\varphi_1, \varphi_{A0} + \varepsilon\varphi_{A1}) \tag{3.48}$$

$$(\varphi_{A0} + \varepsilon\varphi_{A1})_t = a\varepsilon\,(\varphi_{A0})_{xx} - [(\varphi_{A0} + \varepsilon\varphi_{A1})\,(u_0 + \varepsilon u_1)]_x - g\,(\varphi_0 + \varepsilon\varphi_1, \varphi_{A0} + \varepsilon\varphi_{A1}) \tag{3.49}$$

$$(\varphi_0 + \varepsilon\varphi_1)\,(u_0 + \varepsilon u_1)_t = \varepsilon\,(u_0)_t - (\varphi_0 + \varepsilon\varphi_1)\,(u_0 + \varepsilon u_1)\,(u_0 + \varepsilon u_1)_x - b\,(\varphi_0 + \varepsilon\varphi_1)_x \tag{3.50}$$

To carry out the expansion, it is necessary to linearise f and g about φ_0 and φ_{A0}. Expanding f and g in a Taylor series, they become, respectively

$$f\,(\varphi_0 + \varepsilon\varphi_1, \varphi_{A0} + \varepsilon\varphi_{A1}) = f\,(\varphi_0, \varphi_{A0}) + \varepsilon\varphi_1 \left.\frac{\partial f}{\partial \varphi}\right|_{\varphi_0,\varphi_{A0}} + \varepsilon\varphi_{A1} \left.\frac{\partial f}{\partial \varphi_A}\right|_{\varphi_0,\varphi_{A0}} + \text{h.o.t} \tag{3.51}$$

$$\approx f_0 + \varepsilon\,\mathbf{u_1}\cdot\nabla f|_{\varphi_0,\varphi_{A0}} \tag{3.52}$$

$$g\,(\varphi_0 + \varepsilon\varphi_1, \varphi_{A0} + \varepsilon\varphi_{A1}) = f\,(\varphi_0, \varphi_{A0}) + \varepsilon\varphi_1 \left.\frac{\partial f}{\partial \varphi}\right|_{\varphi_0,\varphi_{A0}} + \varepsilon\varphi_{A1} \left.\frac{\partial f}{\partial \varphi_A}\right|_{\varphi_0,\varphi_{A0}} + \text{h.o.t} \tag{3.53}$$

$$\approx g_0 + \varepsilon\,\mathbf{u_1}\cdot\nabla g|_{\varphi_0,\varphi_{A0}} \tag{3.54}$$

where $f_0 = f(\varphi_0, \varphi_{A0})$, $g_0 = g(\varphi_0, \varphi_{A0})$ and $\mathbf{u_1}^T = \{\varphi_1, \varphi_{A1}, u_1\}$.

The perturbed equations are finally obtained by multiplying out and collecting terms of like orders of ε:

Order ε^0:

$$\varphi_{0t} + (\varphi_0 u_0)_x + f_0 = 0 \tag{3.55a}$$

$$\varphi_{A0t} + (\varphi_{A0} u_0)_x + g_0 = 0 \tag{3.55b}$$

$$\varphi_0 u_{0t} + u_0 \varphi_0 u_{0x} + b\varphi_{0x} = 0 \tag{3.55c}$$

Order ε^1:

$$\varphi_{1t} + (\varphi_1 u_0)_x = -(\varphi_0 u_1)_x - \mathbf{u_1} \cdot \nabla f_0 + a\varphi_{0xx} \tag{3.56a}$$

$$\varphi_{A1t} + (\varphi_{A1} u_0)_x = -(\varphi_{A0} u_1)_x - \mathbf{u_1} \cdot \nabla g_0 + a\varphi_{A0xx} \tag{3.56b}$$

$$u_{1t} + (u_0 u_1)_x = (u_{0t} + u_{0x} u_0) \frac{\varphi_1}{\varphi_0} - \frac{b\varphi_{1x}}{\varphi_0} - \frac{u_{0xx}}{\varphi_0} \tag{3.56c}$$

The overall result of this process is to reduce the second order partial differential equations to a first order system.

Solutions of the perturbed equations

Consider the system of equations in (3.55). In the analysis, only (3.55a) and (3.55c) will be considered, since (3.55a) and (3.55b) are qualitatively the same and should thus have similar solutions. It is more convenient to write (3.55) in vector notation. Hence after moving all terms to the left and dividing (3.55c) through by φ_0,

$$\mathbf{u}_t + A\mathbf{u}_x + \mathbf{b} = 0 \tag{3.57}$$

where $\mathbf{u}^T = \{\varphi_0, u_0\}$, $\mathbf{b}^T = \{f(\varphi), 0\}$ and $A = \begin{bmatrix} u & \varphi_0 \\ \frac{b}{\varphi_0} & u \end{bmatrix}$.

Multiplying (3.57) with a row vector $\mathbf{f}$, one obtains

$$\mathbf{f}\mathbf{u}_t + \mathbf{f}A\mathbf{u}_x + \mathbf{f}\mathbf{b} = 0 \tag{3.58}$$

If $\mathbf{f}$ is chosen (Barashenkov, 2001a) such that

$$\mathbf{f} \cdot A = c\mathbf{f} \tag{3.59}$$

i.e. if $\mathbf{f}^T$ is an eigenvector of A^T, then (3.58) becomes

$$\mathbf{f}(\mathbf{u}_t + c\mathbf{u}_x) + \mathbf{f}\mathbf{b} = 0 \tag{3.60}$$

If c is defined such that $\frac{dx}{dt} = c$ then $\mathbf{u}_t + c\mathbf{u}_x = \frac{d\mathbf{u}}{dt}$ and (3.60) becomes

$$\mathbf{f} \cdot \frac{d\mathbf{u}}{dt} + \mathbf{f} \cdot \mathbf{b} = 0 \tag{3.61}$$

The eigenvalues of A^T are found by solving (3.59) for c. That is when

$$\begin{vmatrix} u-c & \frac{b}{\varphi_0} \\ \varphi_0 & u-c \end{vmatrix} = 0 \tag{3.62}$$

$$\Rightarrow c_\pm = u \pm \sqrt{b} \tag{3.63}$$

The eigenvectors are found by substituting (3.63) back into (3.59) to obtain

$$\mathbf{f}_\pm^T = \begin{pmatrix} \pm\frac{\sqrt{a}}{\varphi_0} \\ 1 \end{pmatrix} \tag{3.64}$$

Now if $J^\pm$ is defined such that

$$J^\pm = \mathbf{f}^\pm \frac{d\mathbf{u}}{dt} \tag{3.65}$$

$$= \frac{\sqrt{a}}{\varphi_0}\frac{d\varphi_0}{dt} + \frac{du}{dt} \tag{3.66}$$

$$= \frac{d}{dt}\left(u \pm \sqrt{a}\ln\varphi\right) \tag{3.67}$$

then (3.61) becomes the following set of *ordinary* differential equations:

$$\frac{dJ^\pm}{dt} \pm \sqrt{a} f(\varphi) = 0 \tag{3.68a}$$

$$\frac{dx}{dt} = c^\pm \tag{3.68b}$$

where $J^\pm$ are known as the Riemann Invariants of the system (Barashenkov, 2001a), although in this case they are not constant due to the presence of the nonzero function $f(\varphi)$. Unfortunately, there is little hope of finding a closed form solution to (3.68) (Barashenkov, 2001b) except under very simple initial and boundary conditions; this is not the case for the PSR.

What *is* known however is this: For every x in the domain there are two curves, c^+ and c^-, known as characteristics that are governed by (3.68b). Along these curves the equations in (3.68a) hold, with initial conditions given by $c^\pm|_{t=0}$. This situation is shown schematically in Figure 3.2. In principle, the system (3.68) could be solved for every point on the x-axis with each point resolving to its own initial conditions.

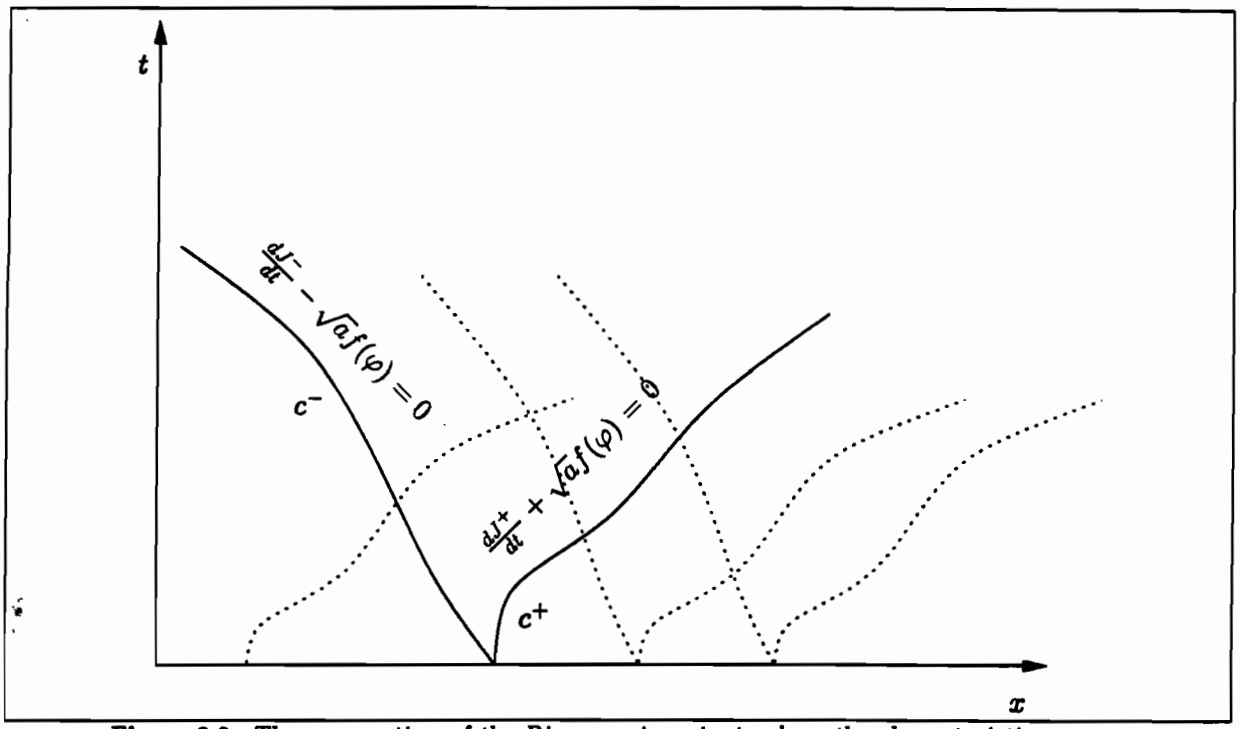

Figure 3.2: *The propagation of the Riemann invariants along the characteristic curves.*

3.4 Conclusions

In this section, several results were obtained including the steady-state profile of the adsorption step of the PSR and reduction of the PDE system to a set of ODE's through the theory of Perturbations. A few smaller results involving behavioural characteristics of the PSR were also obtained.

The system of partial differential equations were shown to be linearly independent. It was also shown that the set of parameters for the system contains the minimum number of elements.

3.4.1 Steady-state solution

The steady-state solutions for the adsorption step provide a benchmark for performance. This was found analytically in a closed form for the isothermal case. If by implementing periodic and reverse-flow operation, conversion and purity of the product may be increased, then the PSR philosophy can, in principle at least, be regarded a success. Obviously this study does not take economic or operation considerations into account but from a purely performance based evaluation, the bar set by the steady-state solution.

3.4.2 Reaction and adsorption properties

The Langmuir isotherm model predicts that separation performance is better at low partial pressures of the key components. This suggests the use of low total pressures or the introduction of an inert species into the reactor. The multi-component Langmuir isotherm predicts lower separation performance than linear isotherms.

First-order reversible kinetics yield simple linear mathematical expressions. As a result the dependence of the reaction rate on the pressure drop between the adsorption and desorption step is linear. This means that relatively speaking, the reaction rate remains constant, irrespective of the pressure. Thus, the low pressure steps do not slow the reaction rate sufficiently to improve separation. Kinetics on heterogeneous catalysts are usually highly nonlinear and thus may well play a significant role in the separation performance of the PSR; whether it improves or degrades would depend on the specific reaction. However, it is a relatively simple task to perform an analysis analogous to the one above to determine the suitability of a candidate reaction.

The overall performance of the PSR will depend to a large extent on the combined dependence of adsorption and reaction rate on pressure. Future candidate reactions can be subjected to the two analyses described above to give a rough idea of whether they are suitable for PSR or not.

3.4.3 Perturbation analysis

The presence of the small parameter in the Navier-Stokes equation immediately suggests the method of Perturbations. The perturbation analysis was carried out with the express hope of finding an approximate analytical to the PSR equations. This was found to be impossible.

After the zeroth-order expansions, the system was reduced to a set of coupled first order ordinary differential equations for which there are no analytical solutions. The first order expansions are even more difficult. However, the analysis does lend itself to numerical computation. Equations (3.68) may be used in cases where use of the small parameter (2/Re) leads to numerical problems, such as instability, in the original PSR equations.

Chapter 4

Numerical Results

Using the analytical results as a guideline, the numerical simulations set out to explore the characteristics of the PSR model, discover the important parameters and quantify the performance of the Pressure Swing Reactor model.

4.1 Operating philosophy

There are two qualitatively different approaches to running the PSR in the following simulations. In the first approach (Approach A), the desired product was selected as the strongly held component.

In this case, the forward reaction is constantly favoured by removing the product as it forms. The product is retrieved during the low pressure steps by desorbing the product. Ideally there is a favourable nonlinear relationship between pressure and reaction rate and the product can be collected before any significant reverse reaction occurs. The major drawback to this approach is that low yields can be expected due to low throughput during the low pressure steps.

The other approach (approach B) involves adsorbing the feed rather than the product. The disadvantage to this technique is that one is constantly battling against Le Chatelier's principle but this can be overcome by selecting the adsorbent in a such a way that adsorption is much faster than reaction. Yields can also be expected to be higher using this approach since product is primarily collected during the adsorption step when flowrates are the highest. In addition, this approach facilitates easy recycle of unreacted feed, since this is collected at the feed end of the reactor.

4.2 Typical parameter values

Typical values for the equation parameters are listed in Table 4.1. The numbers used were chosen as a rough guide and should not be considered hard and fast limits on what is permissible. Values were based on the isomerisation reaction of butene to isobutene.

The equivalent ranges for the dimensionless groups are given in Table 4.2. As these numbers indicate, there is a wide range of values spanning several orders of magnitude for some of the parameters.

4.3 General discussion and physical interpretation

This section addresses the interpretation of the underlying physics of Pressure Swing Reactor operation. One specific run is taken from the isothermal model simulations, the parameters for which are listed in Table 4.3.

The plots in this section are profile plots and present cross-sections of the reactor at specific

Table 4.1: *Typical values for the equation parameters*

Symbol	Variable	Value	
ϵ	voidage	0.4	
L	Reactor Length	0.5 - 10	m
u_0	Inlet interstitial velocity	0.1 - 2	m/s
D_z	Diffusion coefficient	10^{-4} - 10^{-5}	m^2/s
ρ	Average Gas density	0.5 - 10	kg/m^3
P_{in}	Adsorption Pressure	1 - 10	bar
C_p	Average gas heat capacity	120 - 160	J/kg.K
$C_{p,s}$	Solid heat capacity	800 - 1000	J/kg.K
k_z	Gas thermal conductivity	0.01 - 0.04	W/mK
$q_{s,i}$	Adsorption capacity	4 - 10	mol/kg
ρ_s	Solid density	1400 - 1800	kg/m^3
k_i	Adsorption rate constant	0.05 - 5	s^{-1}
β_i	Henry's adsorption constant	20 - 50	m^3/mol
ΔG_{rxn}	Gibb's free energy of reaction	-20	kJ/mol
E_A	Activation energy	$30 \cdot 10^3$ - $90 \cdot 10^3$	J/mol
ΔH_{rxn}	Heat of reaction	-15 - -30	kJ/mol
ΔH_{ads}	Heat of adsorption	-0.1 - -200	kJ/mol
μ	Viscosity	10^{-5} - $5 \cdot 10^{-5}$	J/mol
T_{in}	Inlet Temperature	300 - 500	K

Table 4.2: *Typical values for the dimensionless groups*

Group	Range
Pe_{m}	$5 \cdot 10^3$ - $2 \cdot 10^8$
Re	$5 \cdot 10^2$ - $2 \cdot 10^7$
Eu	$5 \cdot 10^2$ - $2 \cdot 10^7$
Pe	85 - $3 \cdot 10^6$
Qa	20 - 230
κ_i	0.013 - 50
β_i	0 - $2 \cdot 10^4$
Ke0	-0.69 - 1.4
Ea0	7.2 - 36
Ke	2 - 8
Rn_{ad}	48000
Rn_{iso}	0 - 35
Br	-0.02 - -80
Hr	-0.005 - -0.02
Cr	1200 - $4 \cdot 10^4$
Ha	$-3 \cdot 10^{-5}$ - -0.1

Table 4.3: *Operating parameter values for case study*

Parameter	Value
Pe_m	1000.0
Re	1.0
Eu	1.0
Qa_A	50.0
Qa_B	50.0
κ_A	0.5
κ_B	0.5
β_A	200.0
β_B	0.0
Ke	9.0
Rn	2.0
τ_{ads}	25.0
τ_{prg}	25.0
P_{iL}	0.1

moments during the operation cycle. To give an impression of the reactor dynamics, several snapshots are given at once. In addition, to make the interactions between the major state variables as clear as possible, several variables have been plotted simultaneously where this did not clutter the plots.

4.3.1 Breakthrough curve

Figure 4.1 shows the breakthrough curve at the reactor exit for the simulation. There is a distinct transient phase before cyclic steady-state is reached after 6 cycles. The first five cycles are very short with the total concentration increasing steadily during the transient period.

The reasons for this are evident when the profiles during the transient phase are compared those at cyclic steady-state. Figure 4.2 shows the concentration and adsorbed phase profiles during cycle 4 of the case study. It is clear the adsorbent is not fully loaded at this point of operation. Since the adsorbed component is essentially in liquid phase, giving the adsorbent far greater capacity than the void areas of the reactor, reaching adsorption equilibrium requires a large volume of feed, more than can be provided in one PSR cycle. For this reason, the total concentration remains low in the latter part of the bed, facilitating short purge times. The adsorbed phase concentration front advances with each successive cycle, primarily during the adsorption step until the entire bed is 'full' at which point cyclic steady state follows within one or two cycles. Figure 4.3 contains the cyclic steady-state adsorbed phase profile, where the bed is fully loaded.

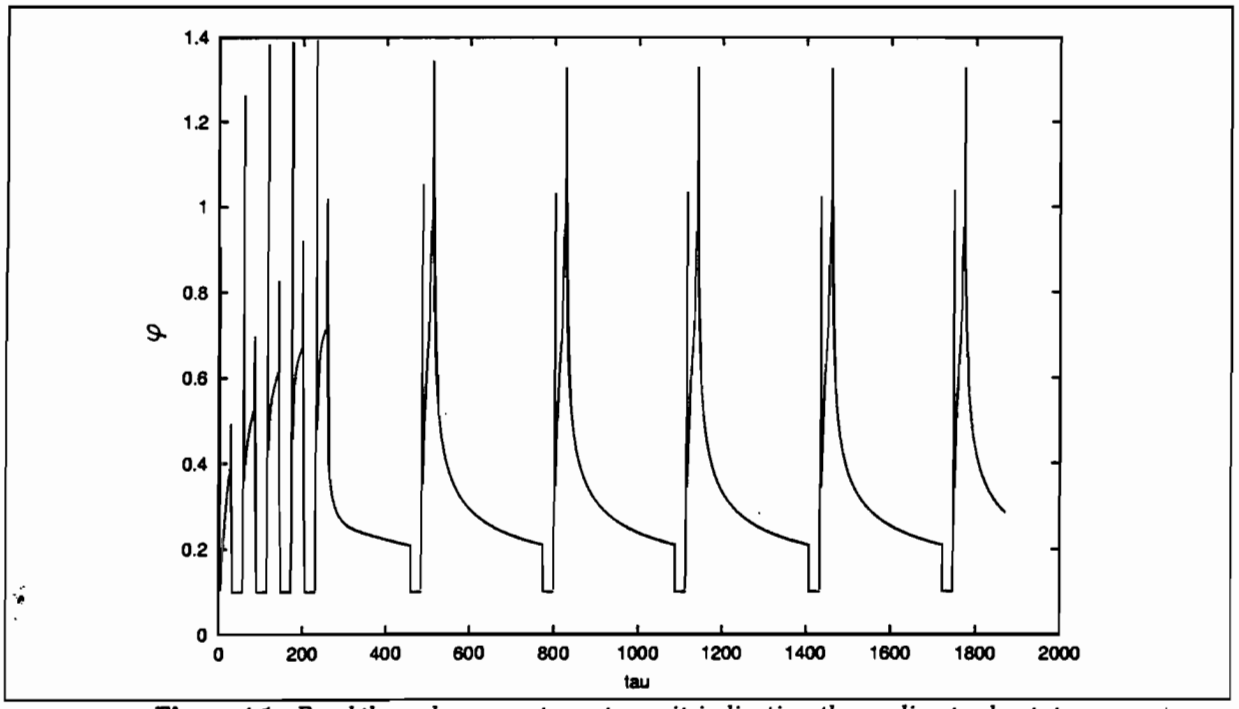

Figure 4.1: *Breakthrough curve at reactor exit indicating the cyclic steady state.*

4.3.2 Pressurisation step

The cyclic steady-state profiles for the pressurisation step are plotted in Figure 4.3. The arrows indicate the direction of increasing time and reference times have also been annotated.

The velocity profile is nearly linear. This is due to the use of a very small Reynolds number in the simulations. This was necessary because of the numerical algorithm's instability when higher Reynolds number were used. Since Re^{-1} plays the role of the diffusion constant in the Navier-Stokes equation, a small value will lead to severe 'backmixing' of momentum. This will serve to flatten the velocity profile out. Since the boundary conditions for the pressurisation step fix the velocity profile at 1 and 0 at the left and right boundaries respectively, a linear profile represents the flattest gradient that is available. Higher Reynolds numbers result in steeper profiles and are covered below.

In this case study, the low pressure adsorbed phase surface coverage, ϕ_A, is 80%. This is high for a $\frac{P_L}{P_H}$ ratio of 0.1. It effectively means that only 20% of the adsorbent surface is available for carrying out separation mechanics (At the adsorption pressure, $\phi_A \approx 1$). The rest of the adsorbent surface is dead weight and only serves to permanently hold a large quantity of feed. This ratio can be improved by implementing the measures discussed in section 3.2.1.

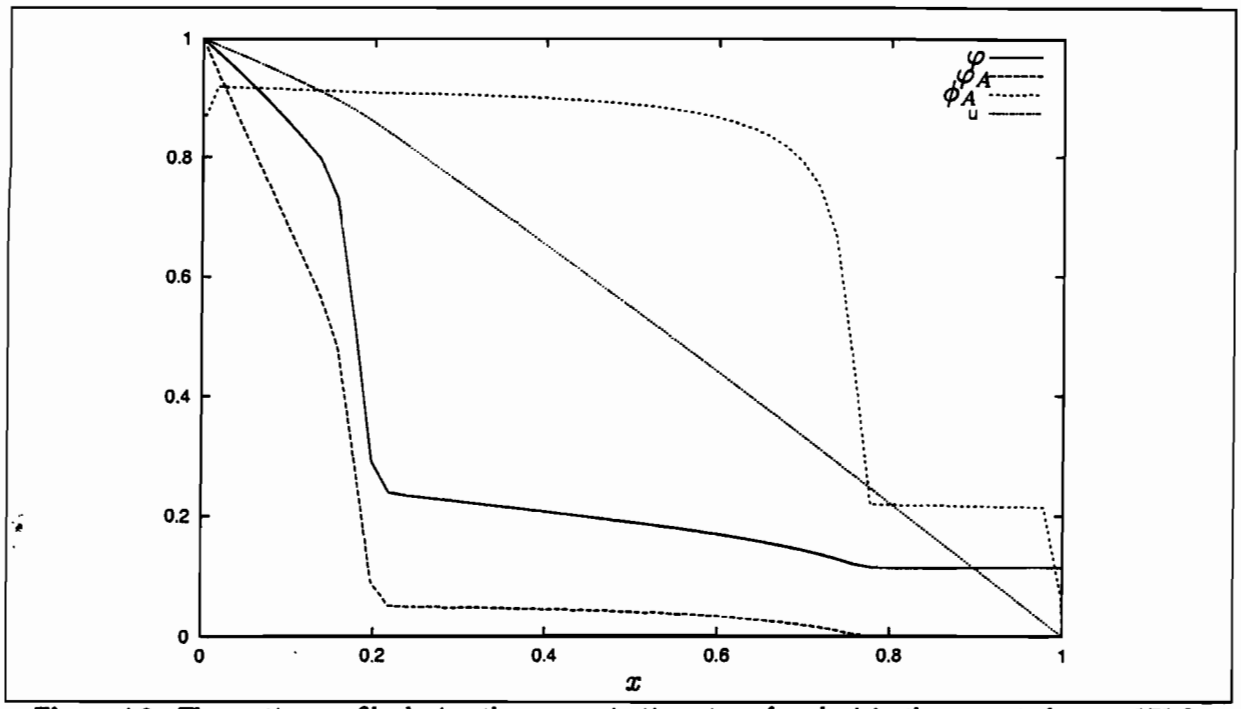

Figure 4.2: *The section profile during the pressurisation step of cycle 4 in the case study.* $\tau = 171.8$.

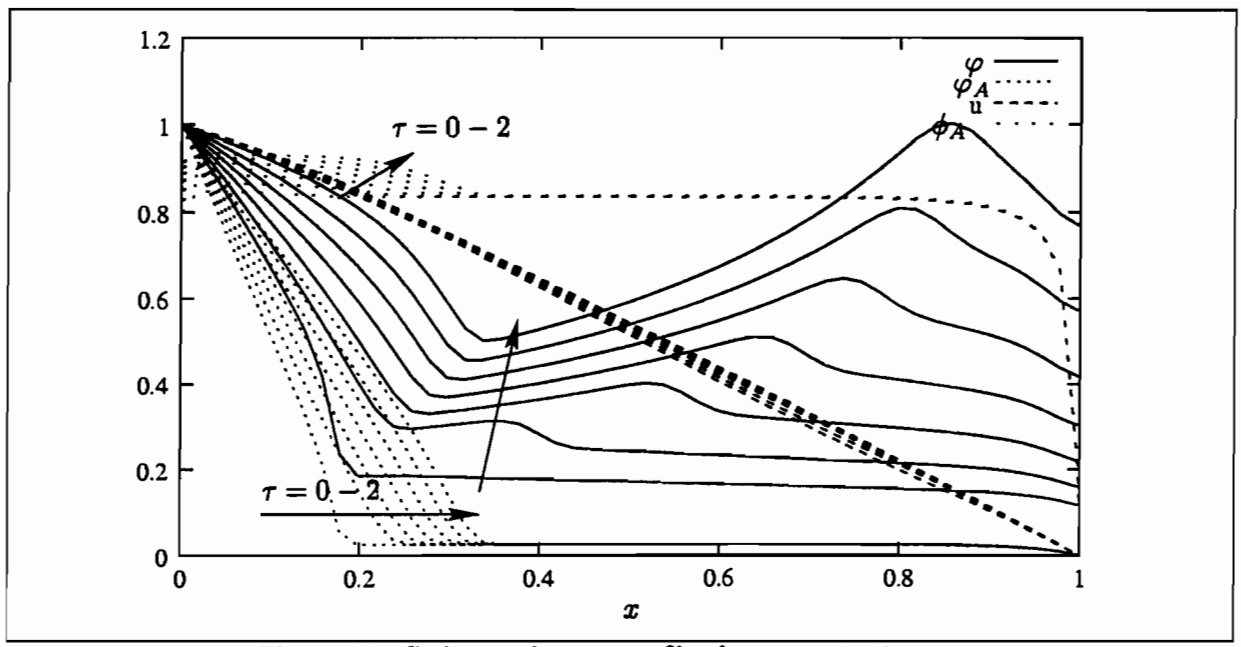

Figure 4.3: *Cyclic steady-state profiles for pressurisation step.*

During the pressurisation step, the bed contains two zones; an adsorption zone and a compression zone.

The adsorption zone occupies the first part of the bed up until the point that the adsorbed phase concentration descends to its low pressure equilibrium.

The gas concentration front in the adsorption zone is quite diffuse. This is caused by the tandem effects of molecular diffusion, reaction and adsorption.

The adsorption rate is quite high. This can be seen from the rate at which the concentration front is advancing. The dimensionless time unit is based on the residence time of the reactor, assuming no holdup. The pressurisation step is two time units in duration, yet the concentration front only advances a quarter of the way through the bed. This indicates severe holdup, explained by rapid adsorption of the feed gas. It will be shown later that the value of 0.1 for κ_A indicates effectively instantaneous adsorption equilibrium.

Reaction is occurring in this zone as can be seen from the fact that the φ_A profile is dropping faster than the total concentration profile. Since the adsorbent is completely selective towards A, the presence of B must be due to reaction.

The behaviour that is depicted here is very different to that predicted by the incompressible gas model (Yang, 1987, pp144-145): If the pressure is forced to remain constant, a drop in the gas phase concentration of the adsorbable component necessitates an increase in velocity to maintain the mass balance. For compressible flow, this restriction is not necessary since the total pressure may vary, as happens in Figure 4.3.

The compression zone occupies the latter portion of the bed.

In the compression zone, there is no adsorption taking place, the velocity is positive and the total concentration is increasing with time. Furthermore, the increase is uneven and the concentration profile in the compression zone does not remain flat. Intuition indicates that a flat concentration profile should increase linearly and remain flat in the presence of a linear velocity profile. The reason that this is not the case is twofold: The boundary condition at the end of the bed is unusual, and the adsorption zone contributes a secondary concentration front.

Under a linear velocity profile and the assumption that no adsorption or reaction is taking place, the PSR overall mass balance equation (2.14) becomes a separable second order partial differential equation. Besides the reaction assumption, these are precisely the conditions in the compression zone. Unfortunately, the solution is very messy and not given here. What is significant is that *under the pressurisation step boundary conditions*, the solution is exponential

in the spatial variable and not constant as intuition suggests. There is definite evidence of exponential growth in the concentration profile in the compression zone of Figure 4.3.

There is also formation of a secondary concentration front at the beginning of the compression zone, primarily from product formed in the adsorption zone and any feed that escaped adsorption. This front moves through the bed at roughly the gas velocity, growing in size as it progresses, becoming a large hump that builds up at the reactor exit. The reasons for this hump formation are the twin actions of the exponential growth of the concentration profile (due to the reactor exit being closed off) and molecular diffusion trying to spread the front out. In practical terms this represents a dangerous situation as the gas pressure may be significantly higher inside the reactor than at the reactor exit.

4.3.3 Adsorption Step

During the adsorption step, flow is permitted from the reactor exit and the adsorbed phase concentration front that characterised the adsorption zone in the pressurisation step rapidly advances through the bed until the adsorbent reaches saturation. Under these boundary conditions, the behaviour of the concentration and velocity profiles match the constant pressure model more closely; the velocity profile, although nonlinear, is greater than unity when adsorption is taking place and falls back to the inlet conditions as the adsorbent becomes saturated. Figure 4.4 illustrates the evolution of the adsorption step. The adsorbed phase and velocity profiles have not been included to avoid clutter.

Towards the end of the adsorption step, the total and feed concentrations approach the steady-state profiles of section 3.1 as expected.

The first profile, at $\tau = 2.2$ is the cause of the 'spikes' seen in the breakthrough curve, Figure 4.1. This spike is due to the disruption caused by the sudden change in boundary conditions. It is a numerical error and not as a result of any physical process. The error introduced by this spike is insignificant and its effects are negligible.

4.3.4 Blowdown step

Besides the same numerical 'spike' that occurred in the adsorption step, the blowdown step evolution is very simple. Figure 4.5 depicts the progress of all the state variables throughout the blowdown step.

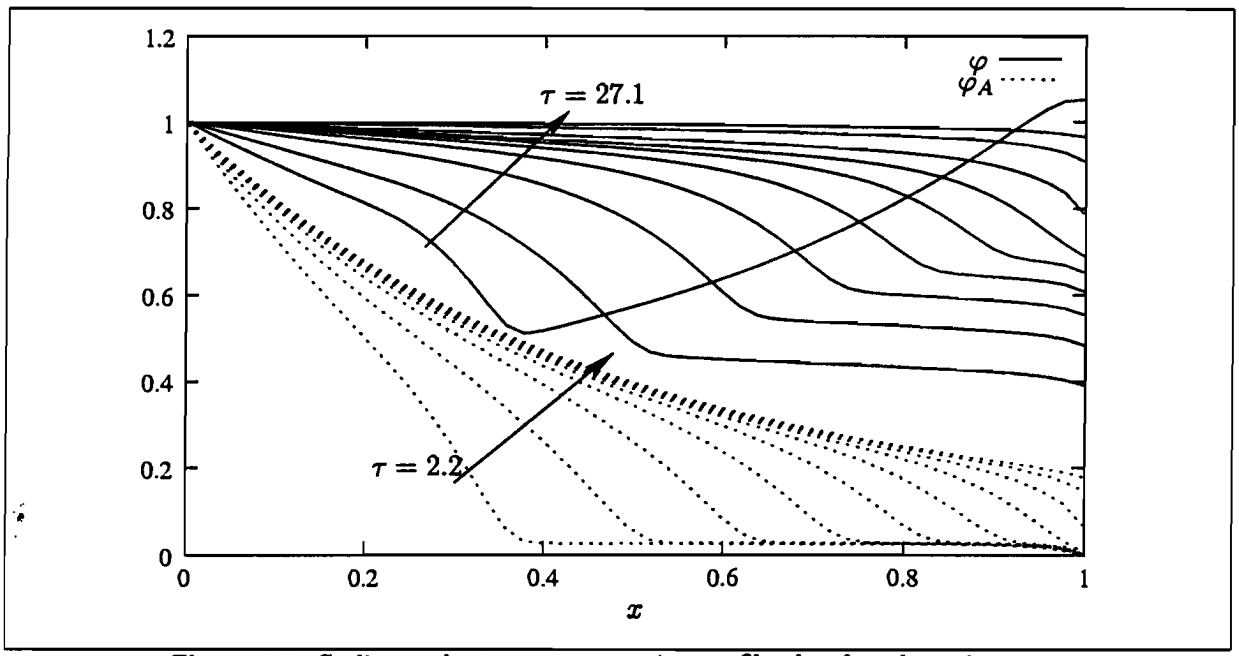

Figure 4.4: *Cyclic steady-state concentration profiles for the adsorption step.*

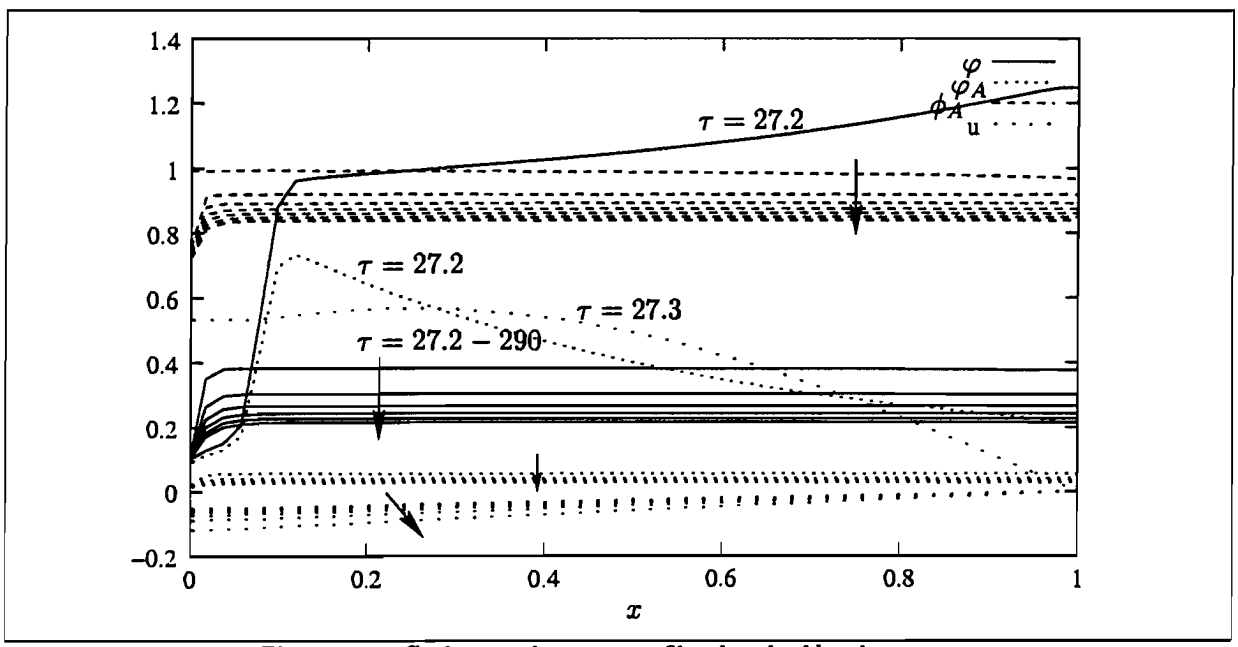

Figure 4.5: *Cyclic steady-state profiles for the blowdown step.*

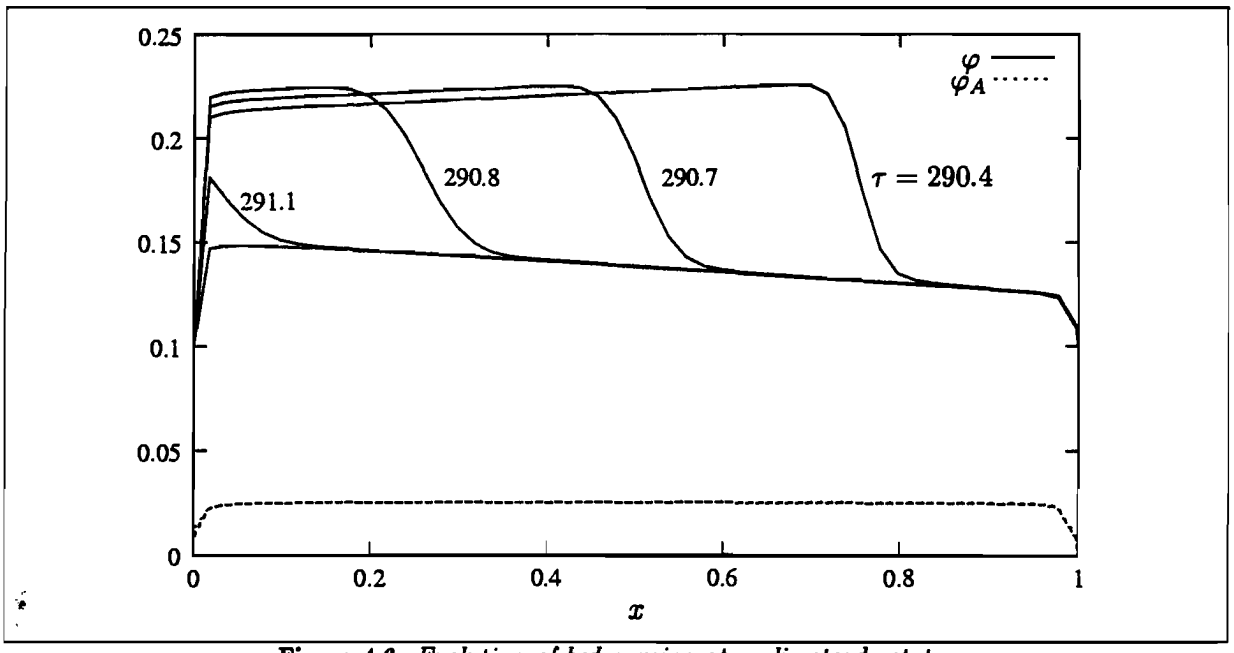

Figure 4.6: *Evolution of bed purging at cyclic steady-state.*

The velocity profile is linear once again. However, since flow is permitted at the reactor entrance, the constant pressure model applies and the concentration profiles remain flat, gradually decreasing as the bed depressurises. φ_A is also decreasing due to the outflow of gas, but the reverse reaction and the desorption of feed means that the mole fraction of A is increasing.

4.3.5 Purge Step

Figure 4.6 demonstrates the flushing action of the purge step. This happens very quickly, as a glance at the time labels attest. The whole process take approximately 1 dimensionless time unit (the residence time), indicating that there is very little holdup or adsorption taking place.

Reverse reaction ensures that the bed is never completely clean. There is also a slight concentration gradient across the bed after the flush. This gradually recedes as the purge continues, but long purge times are required to drive the concentration to a uniform P_{iL} and is probably not necessary.

The velocity profiles have been left off to improve clarity and because they are uninteresting; the velocity is constant at -1 for the entire duration.

4.4 The Euler and Reynolds parameters

Typical values for the Reynolds and Euler numbers for the PSR range from 500 to $1 \cdot 10^6$. Unfortunately, the reactor equations become unstable for any values of Eu or Re greater than $\mathcal{O}(1)$.

The instability arises due to the steep velocity gradients generated for large Reynolds numbers in (2.23). The Reynolds number (or more precisely, its inverse) plays the part of the diffusion coefficient in the Navier-Stokes equation. Large values reduce the stabilising effect of diffusion and numerical instability of the type described in Section 2.5 may occur.

The numerical scheme also becomes unstable for large values of the Euler number. The reasons for this are less clear but a large dependency of the velocity on the pressure gradient will cause rapid changes in the substantial derivative of the velocity. This results in steep velocity gradients as well as rapid fluctuations. It is already known that steep gradients cause problems. Extremely rapid changes in the temporal derivative may also introduce truncation errors into the numerical solution, further exacerbating numerical instability. PDASAC does employ a variable time-step algorithm to try and eliminate such errors. Even so, the required resolution may well push the precision limits of the computer. The maximum allowable time-step computed for simulations using large Euler numbers was typically in the order of 10^{-9}. On an Intel processor, the machine precision is generally 10^{-16} but underflow errors have been known to creep in at values as high as 10^{-10}, uncomfortably close to the required stable time-step interval. No problems were found for smaller Euler numbers, for which the required time-step interval was of the order 10^{-6}.

The instability caused by large Euler and Reynolds numbers meant that unrealistically small values of these parameters had to be used to generate results. This may well have jeopardised the meaningfulness of the results that were generated but this study is more concerned about the qualitative trends that can be deduced from the model and less about the actual numbers generated. It can be argued that the numbers in any model of this complexity are suspect, regardless of the accuracy of the system parameters because it is a fact that highly nonlinear systems (such as this one) often produce chaotic results making long term accurate predictions about performance impossible. The fallibility of weather prediction is a testament to this, despite the use of highly detailed models and the most powerful computers in the world.

4.4.1 The effect of the Euler number

The effect the Euler number has on the velocity and concentration profiles is shown in Figures 4.7 through 4.10. In these graphs, the Reynolds number was set at 0.005. This was done to allow the simulations with large Euler numbers to compute. Figure 4.7 shows the concentration and velocity profiles at the end of the pressurisation step for values of the Euler number ranging from 10 to 500. Numerical computation could not be completed for larger values. There is little change in either the velocity or the concentration profile during the pressurisation step. At the end of the adsorption step (Figure 4.8), the velocity profile begins to show positive deviation for large Euler numbers. However, the impact on the concentration is minimal, as can be seen from Figure 4.8(b). The variation becomes a little more exaggerated during the blowdown step (Figure 4.9(b)) for Eu > 100 but the deviation tends to converge at higher values. A similar trend is noted for the purge step. There is negligible difference in the velocity profiles, but the concentration is overestimated for low Euler numbers. Once again, there is little difference between the results for Eu =100 and Eu =500.

Thus, although there are discrepancies in the results, there is good reason to believe that qualitative trends will not be destroyed through the use of small Euler numbers for the sake of numerical stability. These results indicate that using small Euler numbers in the simulations will not cause significant gross error in further simulations and that any trends will remain valid.

4.4.2 The effect of large Reynolds numbers

Several simulations were performed using a range of Reynolds numbers, from Re =1 to Re=5000. The Euler number was set at 1 for all simulations. The results, presented as the velocity profile at τ=0.6 are shown in Figure 4.11. The profiles were necessarily taken near the beginning of the simulations since most runs were unstable. In fact for Re=5000, signs of instability are already evident. The graph shows that the velocity profiles become steeper as the Reynolds number increases.

The mixing of components in reactors is well known to have a negative effect on performance. Analogously, it is argued that small Reynolds numbers underestimate PSR performance due to the excessive 'backmixing' that occurs in the velocity profile.

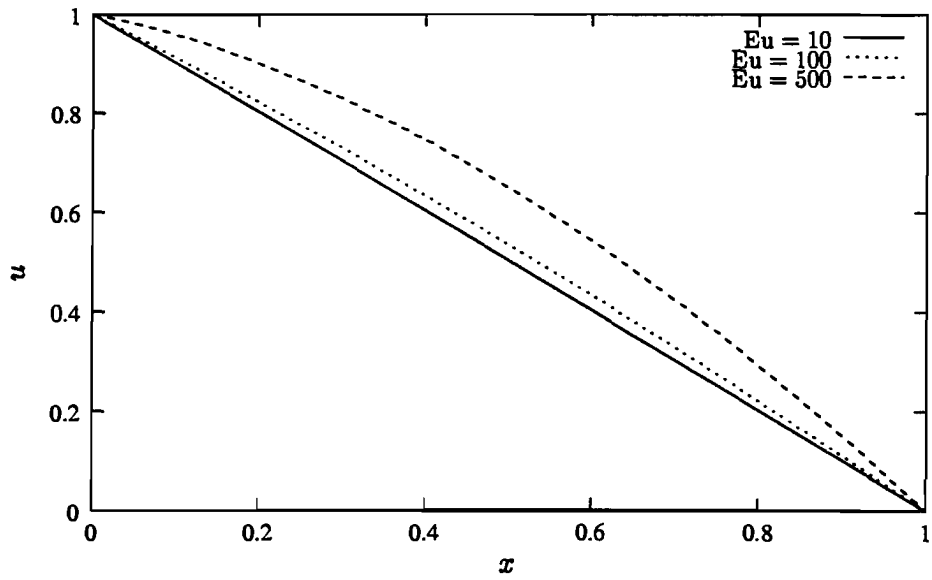

(a) The effect of the Euler number on the velocity profile

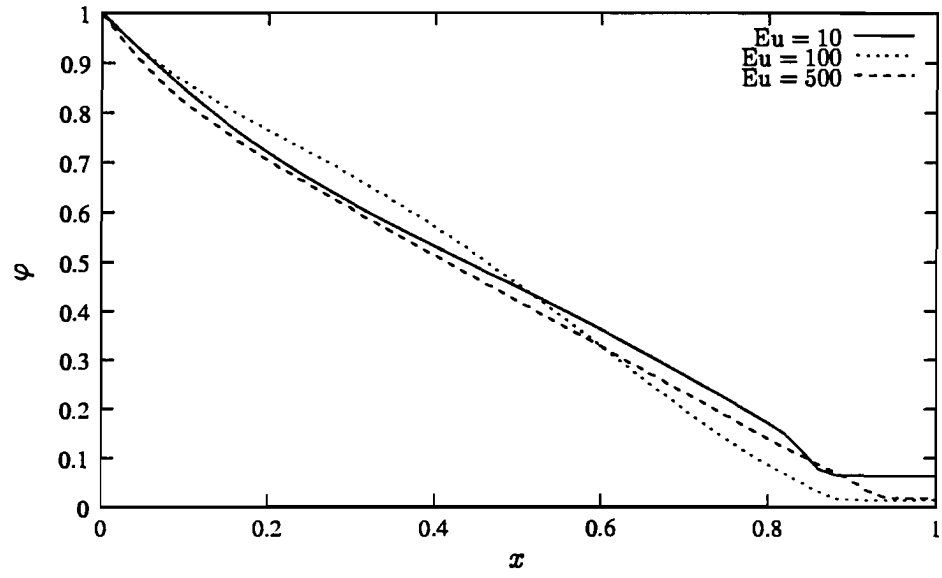

(b) The effect of the Euler number on the concentration profile

Figure 4.7: *Velocity and concentration profiles at the end of the pressurisation step for* Re = 0.005.

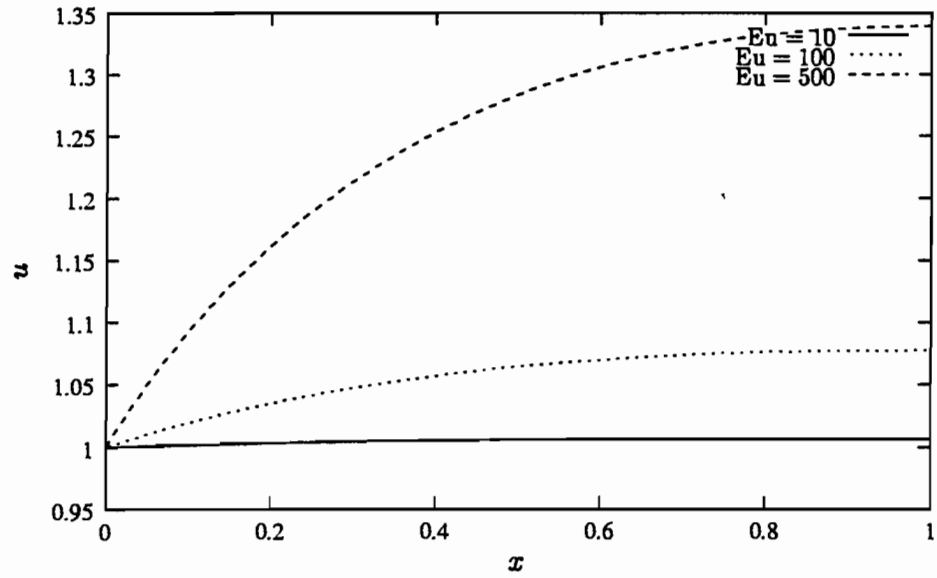

(a) The effect of the Euler number on the velocity profile

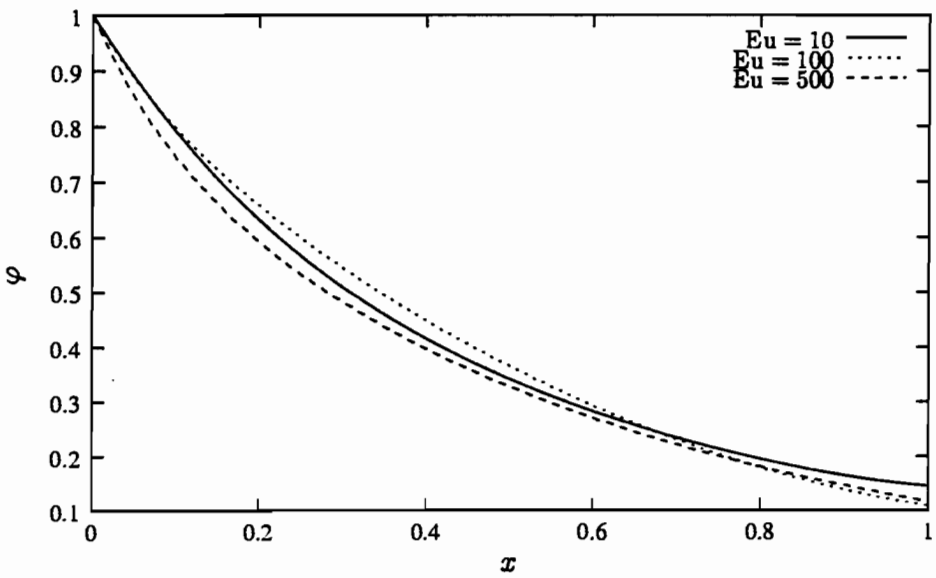

(b) The effect of the Euler number on the concentration profile

Figure 4.8: *Velocity and concentration profiles at the end of the adsorption step for* $\mathrm{Re} = 0.005$.

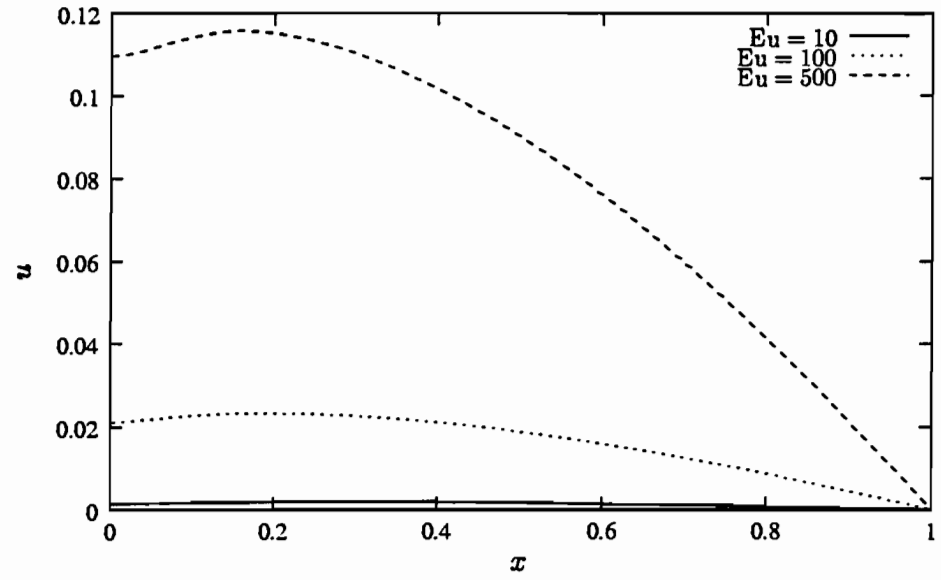

(a) The effect of the Euler number on the velocity profile

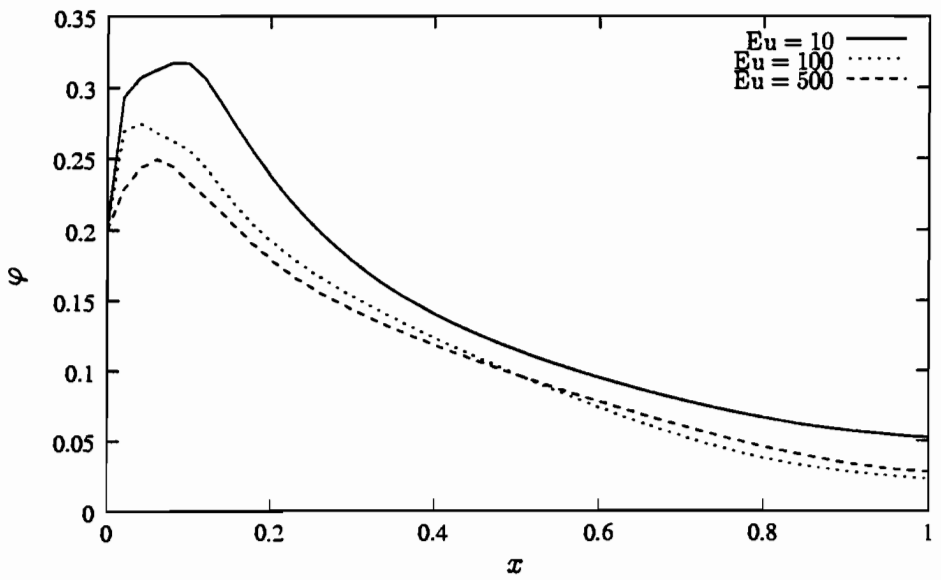

(b) The effect of the Euler number on the concentration profile

Figure 4.9: *Velocity and concentration profiles at the end of the blowdown step for* Re = 0.005.

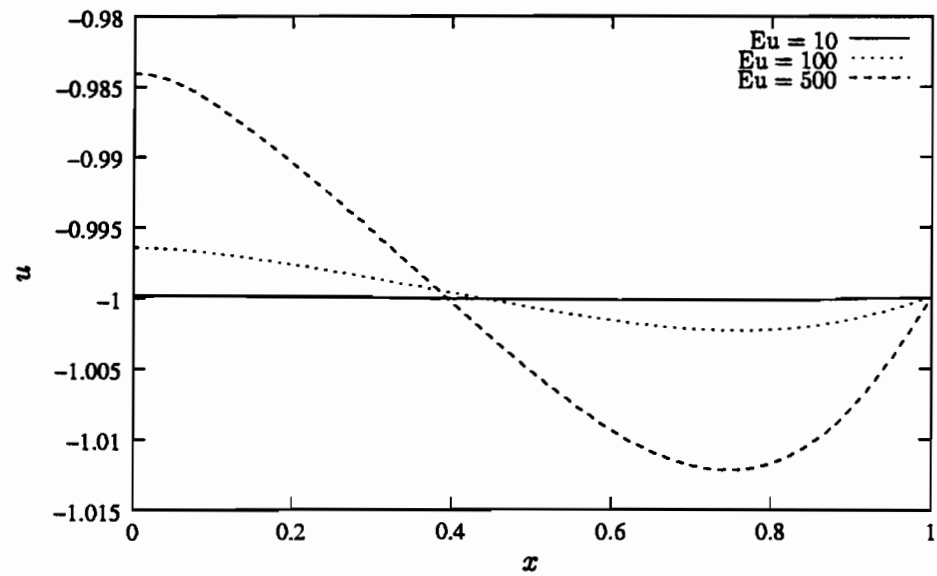

(a) The effect of the Euler number on the velocity profile

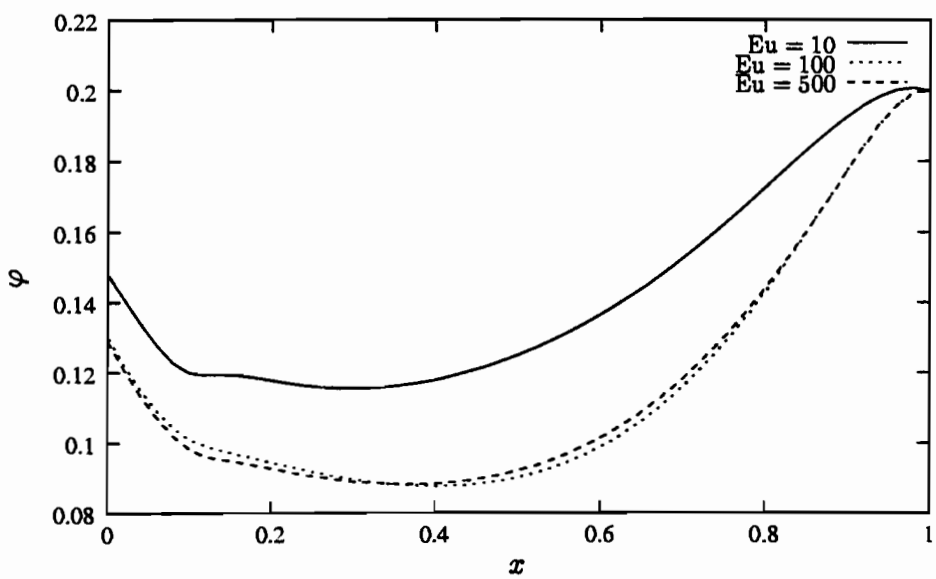

(b) The effect of the Euler number on the concentration profile

Figure 4.10: *Velocity and concentration profiles at the end of the desorption step for* $\mathrm{Re} = 0.005$.

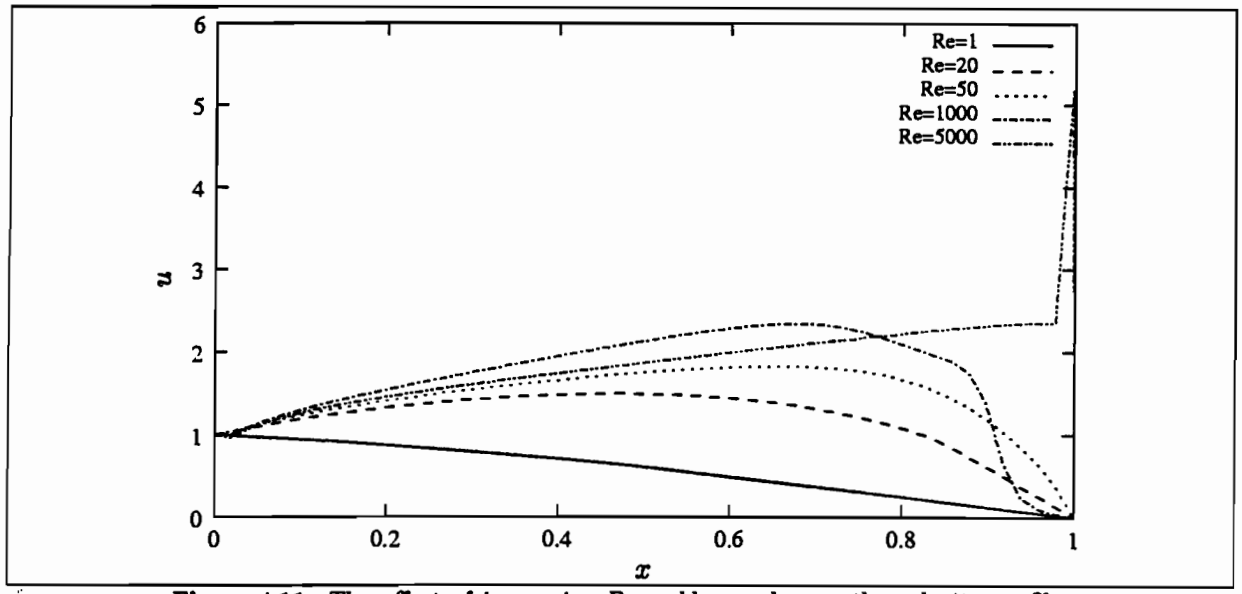

Figure 4.11: *The effect of increasing Reynolds number on the velocity profile.*

4.4.3 Possible solutions to the problem

There are several approaches that may overcome the numerical instability:

1. Improve the temporal and spatial resolution of the problem.
2. Use finite elements to solve the equations.
3. Make use of approximate solutions, such as (3.68)
4. Avoid using the Navier-Stokes equations to describe flow.

PDASAC, as has been mentioned, already uses as fine a time step as is practicably possible. Increasing the spatial resolution did not improve matters satisfactorily. In addition, computation time and storage requirements became prohibitive (on an AMD-K7 Athlon 500MHz processor).

The use of finite element techniques appear the most promising. The reason they were not used for this work is that they were too slow for the amount of computation required, compared to the usual finite difference and collocation techniques.

The approximate solutions to the perturbed equations of the PSR explicitly require a large Reynolds number. Therefore the numerical solutions to (3.68) should be more stable, the equations being first order. However, implementing the boundary conditions in a solution making use of the method of characteristics is a challenging task made even more difficult by the fact that first order equations have only one boundary condition. Therefore either the left or right

set of conditions have to be neglected (the exact choice depends on where the concentration front lies) and this choice will change over time.

Approximate expressions for flow, such as the Ergun equation is a final solution to the problem. Unfortunately, since a PDE is replaced by an algebraic expression, the choice of boundary conditions become limited and impractical and expedient flow specifications have to be prescribed at the reactor exit. This has been the case in all previous work on this subject; either the Ergun equation or Darcy's law has been used describe the flow.

4.4.4 Conclusion

To summarise, large Reynolds and Euler numbers cause catastrophic numerical instabilities. To circumvent this situation, it was decided to use stable values for these parameters with the belief that qualitative trends will be preserved and furthermore, the use of more realistic boundary conditions is preferable to using the Ergun equation or Darcy's law to describe the flow.

4.5 Temperature Effects

The adiabatic model was implemented and run under PDECOL. Results were qualitatively similar to those of the isothermal model however cyclic steady-state was not reached before the end of the simulation. This was due to the build up of heat inside the reactor.

The agreement for the first few cycles of the adiabatic and isothermal results were reasonably good. Because the isothermal simulations reach cyclic steady state so rapidly this model was used for all the remaining simulations. This reduced computation time by at least an order of magnitude and allowed a more comprehensive study of the important parameters.

4.6 Performance Characterisation

The performance of the PSR will be characterised according to two quantifiable factors, purity and yield.

The purity is defined as the average mole fraction of B that has been collected over a specific step, or in case of the overall average purity, over the entire operation cycle at cyclic steady

state. Thus

$$P_S = 1 - \left.\frac{\int_S \varphi_A u d\tau}{\int_S \varphi u d\tau}\right|_{x=i} \tag{4.1}$$

where $S \in (ads, blw, prg)$ referring to the adsorption, blowdown and purge steps respectively and

$$i = \begin{cases} 0 & S = blw, prg \\ 1 & S = ads, \end{cases} \tag{4.2}$$

refers to the end of the reactor at which the integral is evaluated.

The average purity for the entire cycle is

$$P_{ave} = 1 - \frac{\left[\int_{ads} \varphi_A u d\tau\right]_{x=1} + \left[\int_{blw+prg} \varphi_A u d\tau\right]_{x=0}}{\left[\int_{ads} \varphi u d\tau\right]_{x=1} + \left[\int_{blw+prg} \varphi u d\tau\right]_{x=0}} \tag{4.3}$$

The yield is defined as the number of moles of B recovered per mole A fed into the reactor and is written as

$$Y_{ads} = \frac{\left[\int_{ads} (\varphi - \varphi_A) u d\tau\right]_{x=1}}{\left[\int_{prs+ads} \varphi u d\tau\right]_{x=0}} \tag{4.4}$$

$$Y_{blw} = \frac{\left[-\int_{blw} (\varphi - \varphi_A) u d\tau\right]_{x=0}}{\left[\int_{prs+ads} \varphi u d\tau\right]_{x=0}} \tag{4.5}$$

$$Y_{prg} = \frac{\left[-\int_{prg} (\varphi - \varphi_A) u d\tau\right]_{x=0} + \left[\int_{prg} \varphi u d\tau\right]_{x=1}}{\left[\int_{prs+ads} \varphi u d\tau\right]_{x=0}} \tag{4.6}$$

$$Y_{ave} = Y_{ads} + Y_{blw} + Y_{prg} \tag{4.7}$$

The yield is reduced by the presence of the purge step, since some product is used to carry out the purge. The negative signs in (4.5) and (4.6) are required since flow is reversed in those steps i.e. $u < 0$.

4.6.1 Comparative Performance

The PSR needs to be compared to the performance of an equivalent fixed-bed reactor and/or separator. Roughly speaking, the purity index gives an indication of separation performance, while the yield rates the reaction performance.

Direct comparisons are difficult because product can be collected at both the feed and exit ends of the reactor. There is a choice between keeping the components collected during the blow-down and purge steps, discarding them, or recycling back into the feed. The PSR performance will depend to some extent on the choice made. In any case, the relative importance of high product purity and high yield must be weighed up against each other since there is normally an inverse relationship between the two.

In the plots that follow, the average purity and yield have been used to determine the performance of the PSR. The performance benchmarks for purity are the equilibrium mole fraction and the steady-state mole fraction, calculated at the exit from (3.19).

The steady-state concentration represents par performance for the PSR. Obtaining an average purity greater than the steady-state indicates that there is some separation taking place. If the purity is greater than the equilibrium concentration, then the separation performance can be considered exemplary. Most results can be expected to lie between the two benchmarks.

4.7 Sensitivity Analysis

The effect on PSR performance was calculated for most of the parameters in the PSR. In most cases, a pair of related parameters were investigated simultaneously to expose any possible co-dependence. For each parameter investigation, several simulations were carried out. The performance indices, (4.1) to (4.7) were calculated for each simulation and summarised on the performance plot (Figures 4.12 through 4.24). Interesting cases have been examined more minutely and have been supplemented with tabulated data and breakthrough curves.

Results were taken at cyclic steady-state, which was usually achieved after 3 to 8 operating cycles (Figure 4.1).

Table 4.4: *Base case variables for simulations*

Pe_m	1000	κ_A	0.1
Re	1.0	κ_B	0.5
Eu	1.0	β_A	0 or 200
Qa_A	0.1	β_B	60 or 0
Qa_B	100	Ke	9.0
τ_{ads}	25	Rn	2.0
τ_{prg}	25	P_{iL}	0.1

4.7.1 Base case parameters

Typical ranges for the dimensionless groups present in the governing equations are listed in Table 4.2. Most simulations were based on the set of base case of parameters given in Table 4.4. These values were selected to compromise between relevance and stability. Most of the parameters lie well within the ranges listed in Table 4.2.

The dimensionless Henry's constants, β_i, were chosen according to the operating approach in effect at the time.

4.8 Operating parameter sensitivity

4.8.1 Step duration

Approach A was used in this section's simulations.

Figure 4.12 indicates that longer adsorption and purge steps improve purity. Figure 4.13 on the other hand, shows that while longer adsorption steps improve yield, longer purge steps hurt the product yield. This is to be expected because

1. some product has to be used up in the purge step.

2. the cycle time is lengthened for very little return in terms of product collected at the reactor entrance during low-pressure steps.

The overall performance is not spectacular. The mole fraction of product collected (Figure 4.12) approaches the steady-state value asymptotically. Thus the best performance for this scenario would be to operate the PSR as a fixed-bed reactor. This suggests that it is the reaction parameters and not the operating conditions that are important when considering the use of PSR for a particular reaction.

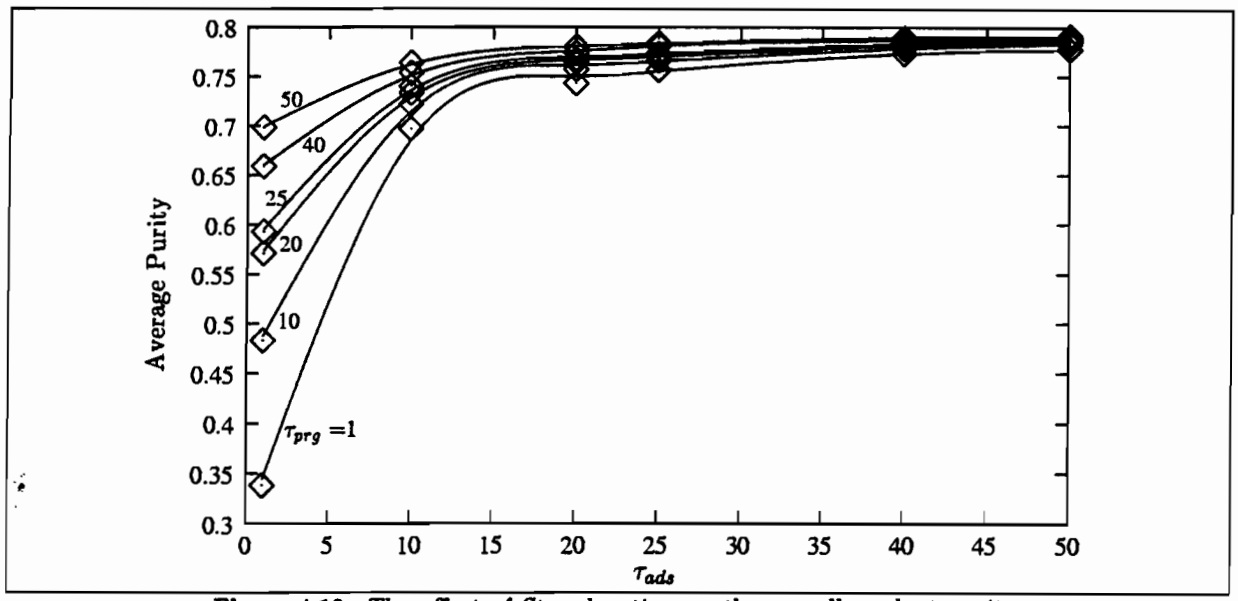

Figure 4.12: *The effect of Step duration on the overall product purity.*

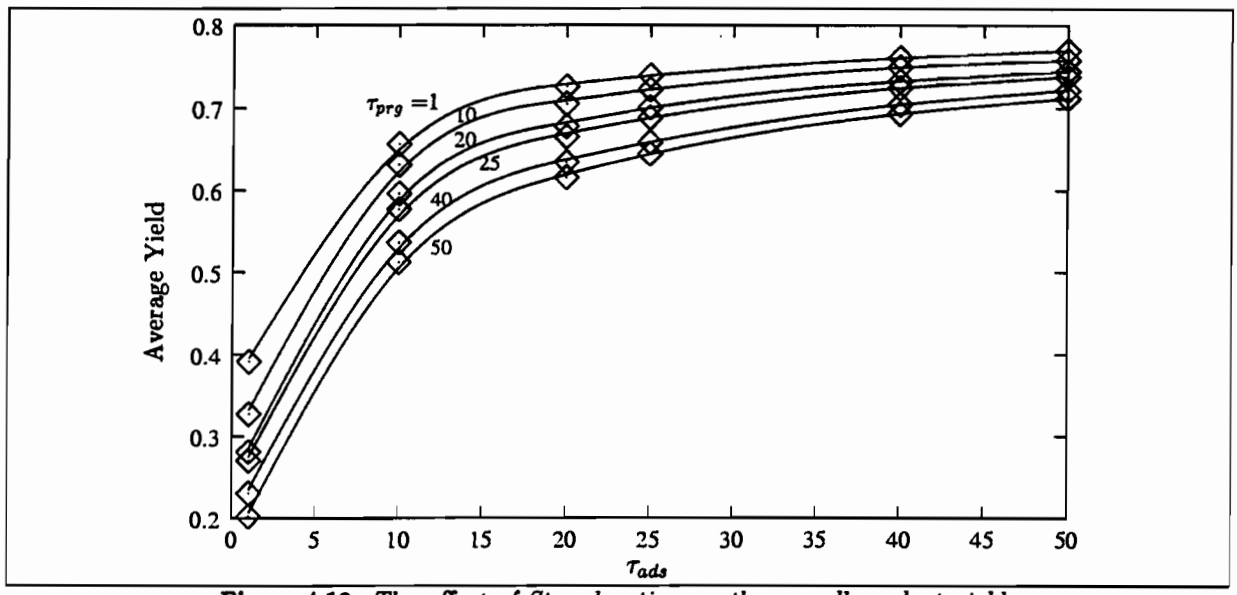

Figure 4.13: *The effect of Step duration on the overall product yield.*

4.8.2 Desorption Pressure

The desorption pressure, P_{iL} did not play a major role in reactor performance. However, this may be due more to the use of linear reaction kinetics in the simulations, as discussed in Section 3.2.2, than an actual negative result. The primary goal in this parameter study was to obtain good product purity at the feed end of the reactor during blowdown and purge, using Approach A. It was found that as P_{iL} decreases, increasing the product purity, the quantity of product collected rapidly decreases to the point of impracticality.

It is clear that the lower the value of P_{iL}, the better the regeneration of adsorbent during the low pressure steps, thus aiding separation during the adsorption step.

4.9 Physical parameter sensitivity

The dependence on PSR separation performance by physical parameters was far more noticeable than for the operating parameters. In many cases, steady-state concentrations were exceeded and in a few cases, almost perfect separation was achieved during the adsorption step.

4.9.1 Adsorption parameters

Adsorption capacity of feed component

In this section both components were adsorbed to varying degrees.

The adsorption capacity of the feed component was varied across a range of 1 to 1000. The Henry's constant was also varied between 5 and 100 to generate the graphs in Figure 4.14.

Figure 4.14 plots the average mole fraction, or purity, of the product B across the entire operation cycle. One notes that for small Henry's constants, very poor performance is obtained. All simulations returned purity results below the steady-state concentration with a maximum average purity approaching the steady-state concentration for Qa_A =50-100. For higher Henry's constants, results were generally above steady-state, but well below the equilibrium concentration of 0.9.

It is evident from the plot that there is an optimum adsorption capacity for purity performance. At low values of Qa_A, the reactor behaves much like a fixed-bed reactor and the resulting purity figures approach steady-state in the adsorption step. For high adsorption capacities, the reaction is hindered by excessive removal of feed from the gas phase, enhancing the reverse reac-

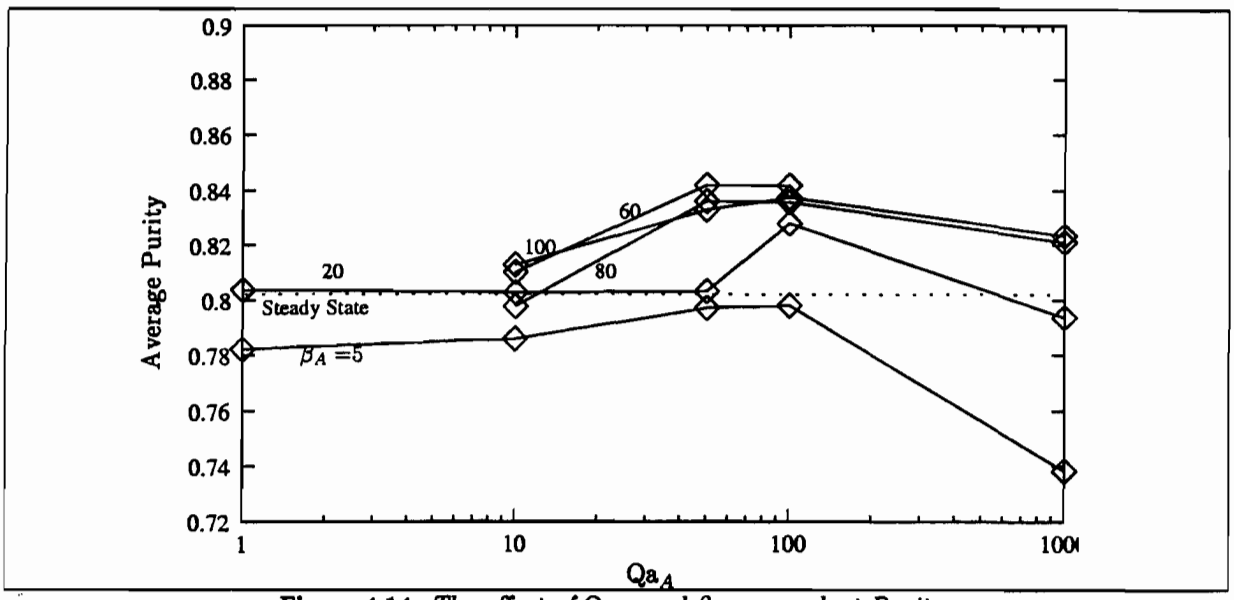

Figure 4.14: *The effect of* Qa_A *and* β_A *on product Purity.*

tion and reducing overall purity. This effect was also reflected in the yields for these simulations, which lay around 10%.

Adsorption capacity of product

This section examines the relationship between the adsorption capacity of B, its isotherm gradient and performance. Approach A was used in these simulations.

Looking at the results, the adsorption capacity for product has an inverse relationship on PSR performance, as Figures 4.15 to 4.17 show. The average purity drops of steadily as Qa_B is increased, as shown in Figure 4.15. This trend is independent of the Henry's constant for the product, although higher Henry's constants produce better results.

Figure 4.17 shows average yields lying between 69% and 76%.

One would expect higher purities in the blowdown step than in the adsorption step, yet this only happens in the case of $Qa_B = 10$ (See Table 4.5 and Figure 4.16). Higher adsorption capacities serve to decrease the blowdown purity. This must be due to the fact that the reverse reaction happens to an appreciable extent during the low pressure steps, contrary to what was proposed. Evidence of this lies in the fact that although the blowdown yield increases with increasing adsorption capacity, the overall yield decreases, thus product must be lost to reverse reaction. Recall that the kinetics used in this model does not predict a favourable nonlinear decrease in reaction rate.

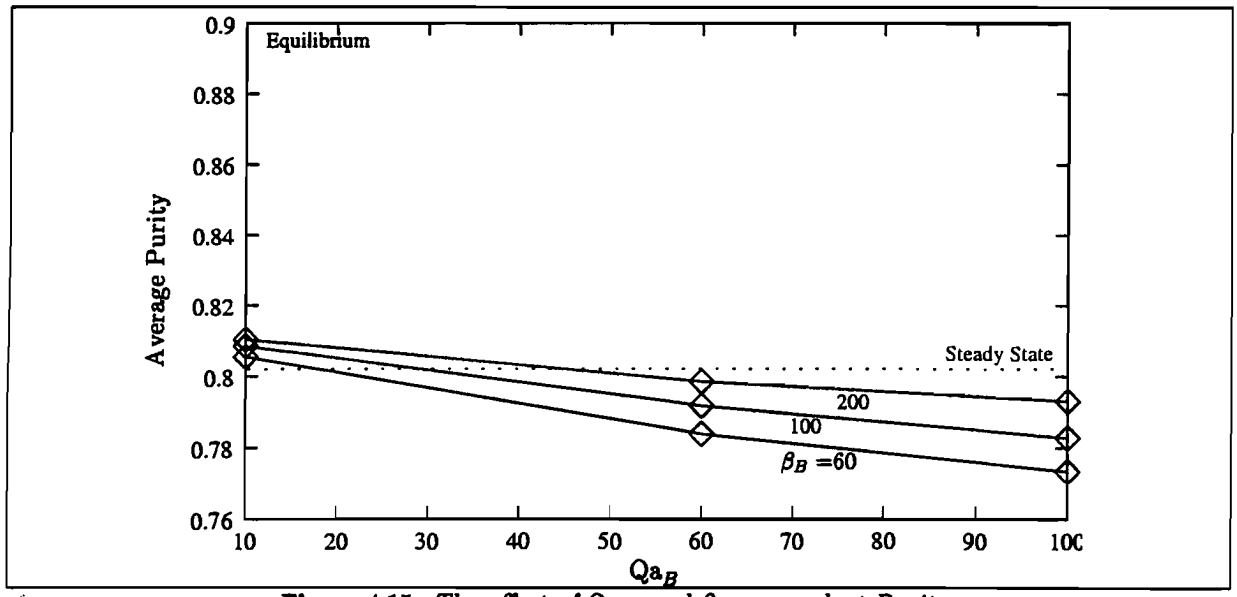

Figure 4.15: *The effect of* Qa_B *and* β_B *on product Purity.*

Table 4.5 gives a more detailed look at the PSR performance for this set of simulations. There is significant recovery in the blowdown step but overall yields and purities suggest that this is not the ideal way to run the PSR, at least not with the form of reaction kinetics used in the simulations. Purities generally lie below the benchmark steady-state level, indicating poor separation performance.

From the results in the last three sections, it is evident that Approach A is not suitable for PSR operation. Even the proposed benefits of negligible reverse reaction occurring during the low pressure steps were not obtained and the flowrate at the reactor entrance during the blowdown step is negligible.

Most throughput occurs during the adsorption step (around 95% of all traffic). The gas collected during the low pressure steps can be considered bonus, or used as recycle or vented off. This suggests the use of the second approach, which will be examined in the following few sections.

Henry's constants

In the results presented so far, higher Henry's adsorption constants produce better overall results. This section compares the relative performance of the two Henry's constants on PSR performance. Values of β_A and β_B were varied between 0 and 200. Adsorption capacities for each component were set at 100. The average purity of the simulations are summarised in Fig-

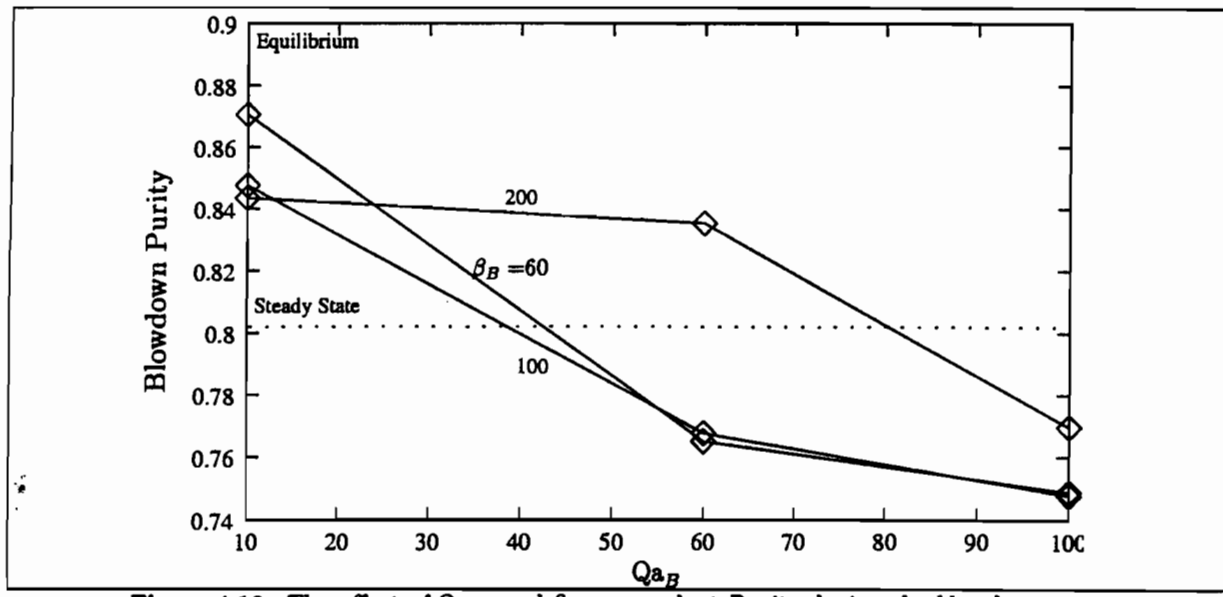

Figure 4.16: *The effect of* Qa_B *and* β_B *on product Purity during the blowdown step.*

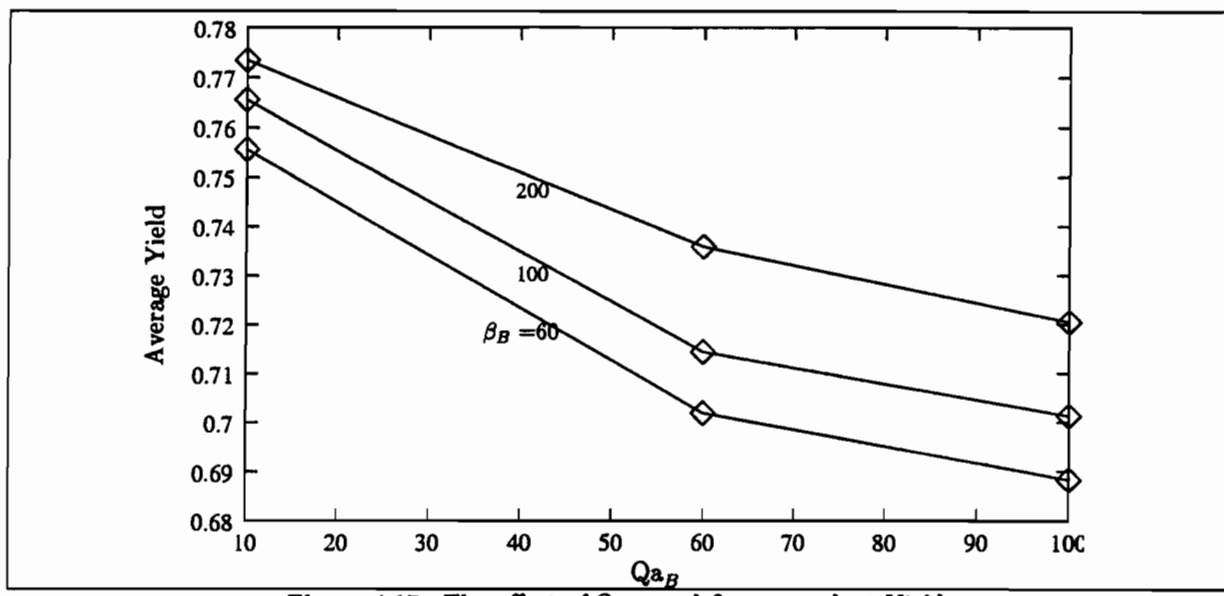

Figure 4.17: *The effect of* Qa_B *and* β_B *on product Yield.*

Table 4.5: *Performance Data for* Qa_B *and* β_B *parameter analysis*

Qa_B	AdsYld	BlwYld	DesYld	**AveYld**	AdsPur	BlwPur	DesPur	**AvePur**
β_B =60								
10	0.752	0.0108	-0.00783	0.755	0.805	0.870	0.916	0.805
60	0.679	0.0295	-0.00638	0.701	0.806	0.765	0.917	0.783
100	0.654	0.0409	-0.00575	0.688	0.812	0.748	0.915	0.773
β_B =100								
10	0.764	0.0088	-0.00799	0.765	0.807	0.847	0.914	0.808
60	0.700	0.0207	-0.00684	0.714	0.803	0.767	0.919	0.791
100	0.677	0.0299	-0.00631	0.701	0.807	0.747	0.917	0.782
β_B =200								
10	0.774	0.0072	-0.0082	0.773	0.807	0.843	0.912	0.810
60	0.728	0.0150	-0.0073	0.735	0.802	0.835	0.919	0.798
100	0.708	0.0193	-0.0069	0.720	0.803	0.769	0.919	0.793

ure 4.18. Previous results, indicating a positive relationship between separation performance and Henry's constant are confirmed. Most results beat the steady-state concentration. In addition for the cases $\beta_B = 0$ and $\beta_A > 70$, the average exit mole fraction of B exceeded equilibrium concentrations. In fact, looking at Table 4.6, the separation during the adsorption step is nearly perfect with exit mole fractions exceeding 99% for $\beta_A \geq 40$. The overall purities are reduced by the significantly lower purities in the blowdown and desorption steps.

The separation performance of this configuration is due to the PSR acting as two units in series: a reactor followed by a separator. The reaction takes place in the first part of the reactor along the concentration front. The rest of the reactor acts as a separator, with the very high adsorption affinity for A effectively mopping up all the unreacted feed. The adsorption step is terminated before the concentration front reaches the end of the reactor. Continued performance is maintained through effective regeneration during the low pressure steps.

One major drawback to this operation is that the overall conversion of feed is low, as pictured in Figure 4.19. The average yields for runs with superior separation performance produced yields of around 30%.

Further simulations using a feed-only selective adsorbent produced better results, listed in Table 4.6. Here yields improved to 58% for an exit purity of 99.8% at the exit. With unspent feed easily collected and recycled, there appears to be definite potential for PSR's in isomerisation reaction and separation applications.

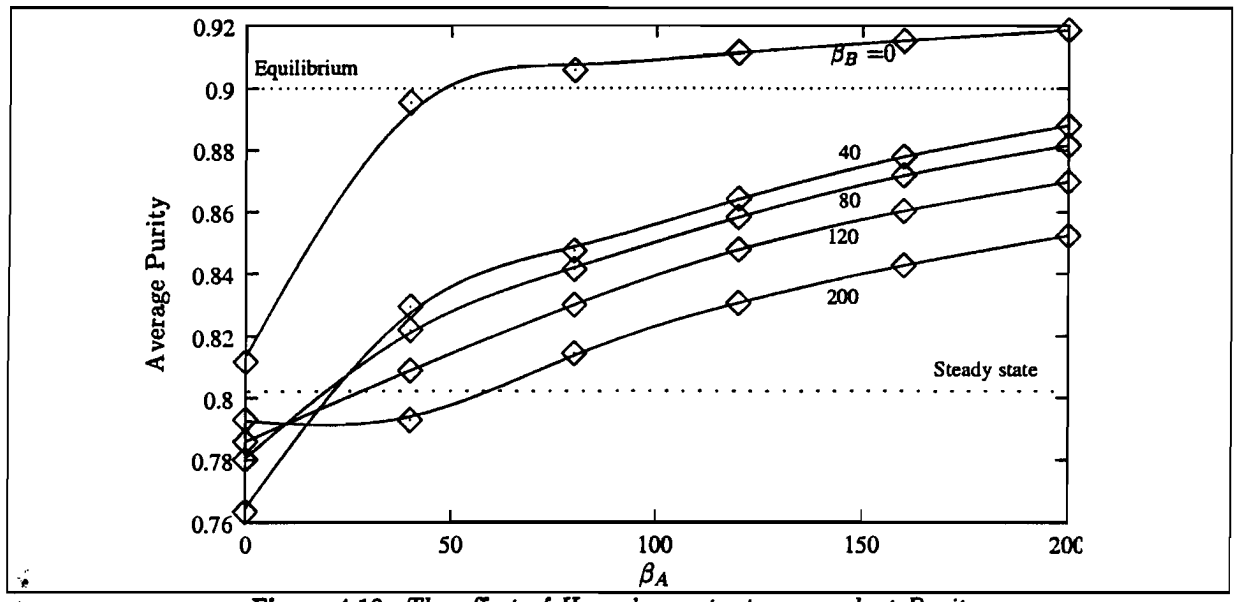

Figure 4.18: *The effect of Henry's constants on product Purity.*

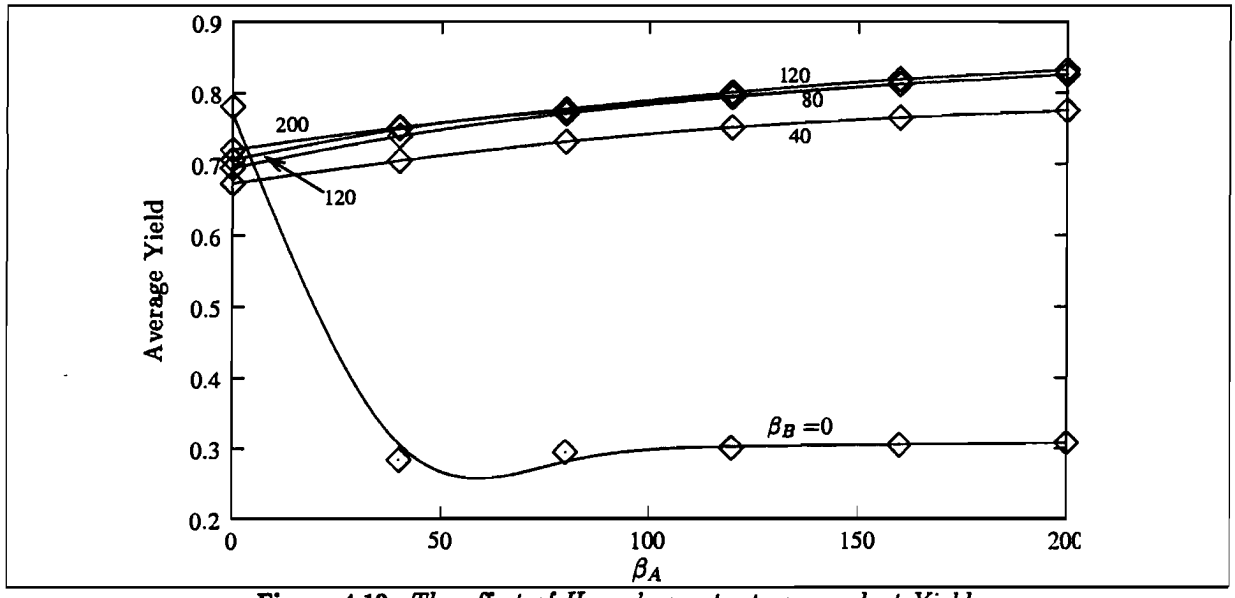

Figure 4.19: *The effect of Henry's constants on product Yield.*

Table 4.6: *Performance Data for β_A parameter analysis ($\beta_B = 0$)*

β_A	AdsYld	BlwYld	DesYld	**AveYld**	AdsPur	BlwPur	DesPur	**AvePur**
0	0.784	0.0056	-0.0084	0.781	0.807	0.840	0.910	0.811
40	0.522	0.0033	-0.0371	0.488	0.994	0.689	0.616	0.931
80	0.559	0.0029	-0.0342	0.528	0.996	0.752	0.644	0.941
120	0.581	0.0026	-0.0324	0.551	0.997	0.764	0.661	0.947
160	0.595	0.0028	-0.0312	0.566	0.998	0.775	0.673	0.949
200	0.605	0.0025	-0.0302	0.577	0.998	0.78	0.683	0.952

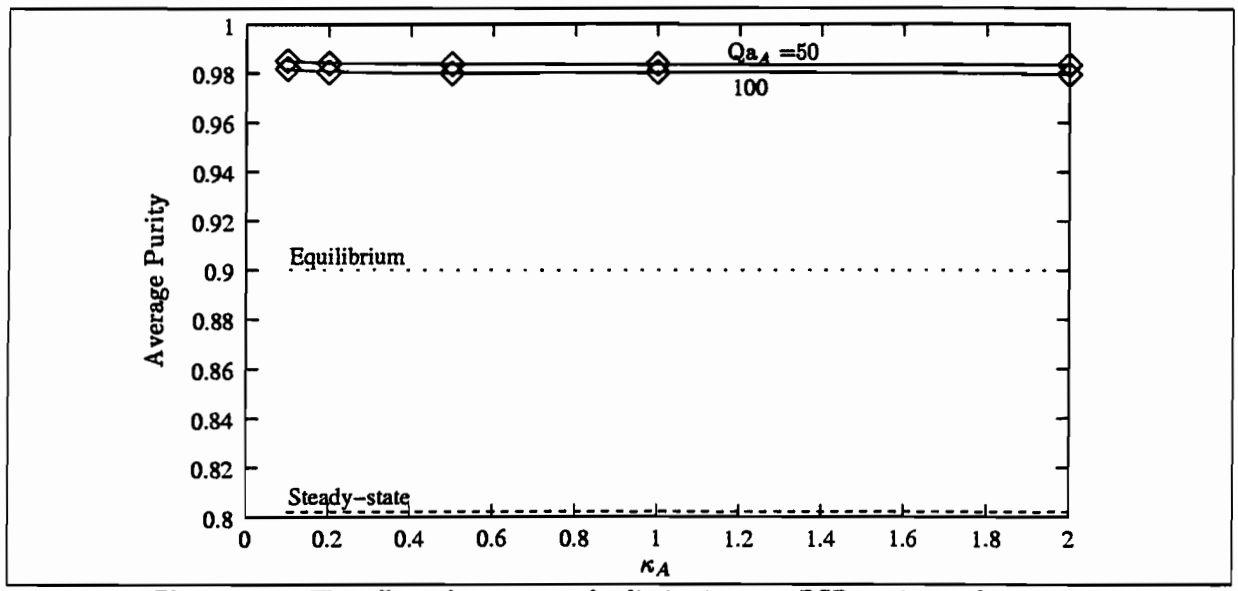

Figure 4.20: *The effect of mass transfer limitations on PSR purity performance.*

4.9.2 Mass Transfer limitations

Approach B was used in these simulations.

One would expect high mass transfer limitations to hinder PSR separation performance. In Figures 4.20 and 4.21 the adsorption rate constant, κ_A has been varied and the performance results plotted.

Different adsorption parameters were used in these simulations to try and reproduce or improve on the excellent performance obtained in the previous section. Henry's constants of 200 and 0 were used for A and B respectively. The dimensionless purge time was also dropped to 5. Values of $\mathrm{Qa}_A = 50$ and 100 were used to compare the effect of increasing the adsorption capacity.

The separation performance is excellent for both adsorption capacities over the entire range of adsorption rate constants. Near-perfect separation occurs during the adsorption step and due to the shorter purge time, the overall purity coefficient is far higher; 98.5% and well above the equilibrium concentration. There is no real dependency on the mass-transfer coefficient over the range plotted; both purity and yields remain essentially constant across the domain. Further simulation with smaller κ_A values will have to be done to determine at which point mass-transfer limitations hinder performance.

Yields of around 62% are obtained for these runs (Figure 4.21). Again, the performance is essentially independent of the mass-transfer coefficient.

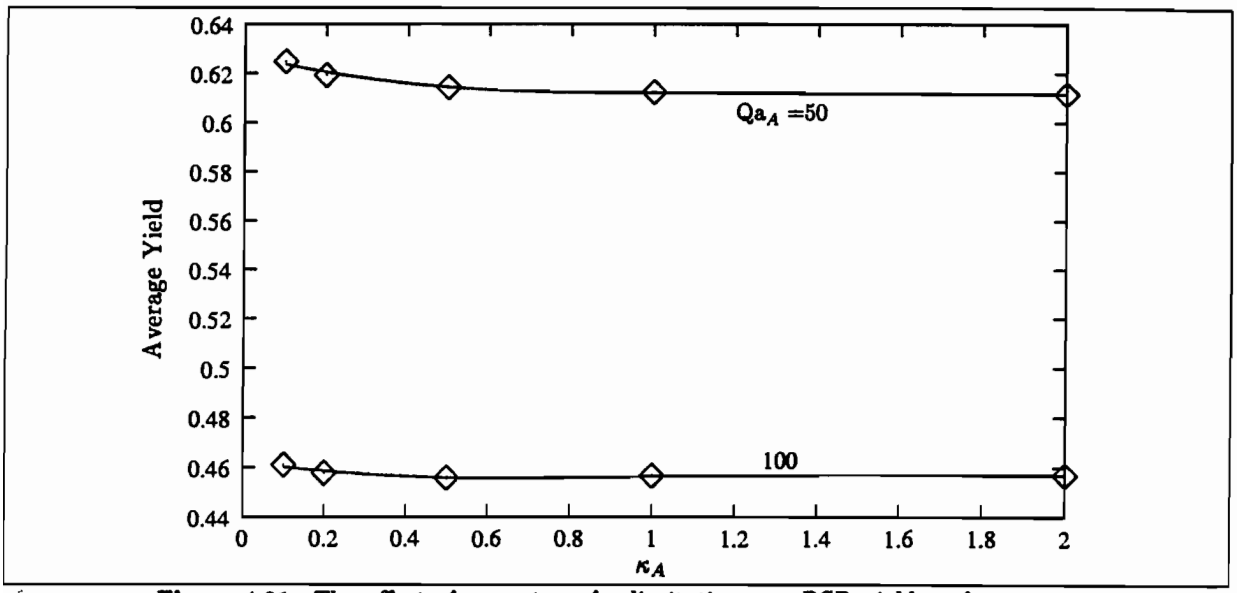

Figure 4.21: *The effect of mass transfer limitations on PSR yield performance.*

4.9.3 Reaction rate and equilibrium

Pressure swing reactor systems were designed primarily with the thought in mind of improving on once-through conversion of equilibrium limited reactions. In this section, the performance of the PSR is examined for a range of reaction equilibrium constants. The equilibrium product mole fraction is varied from 10% to 90%.

The reaction rate was also varied from a steady-state approach to equilibrium of around 20% (for Ke = 9) to one approaching 100% for fast reactions.

The results are presented in Figures 4.22, 4.23 and 4.24. Figure 4.22 shows the average product purity over the whole operation cycle. Overall, the results are fairly disappointing, since the PSR seldom outperformed a fixed-bed reactor. The best results were for reaction with relatively large equilibrium constants (a value of 9 for Ke represents an equilibrium concentration of 90%). For highly reversible reactions (Ke=0.11-0.5), the average purity equalled the steady-state concentration. This was the case over the entire range of reaction rates.

The poor results for the average cycle purity are partly due to low exit concentrations during the blowdown steps, particularly for faster reactions. The purity curves during the adsorption step alone, Figure 4.23 show a more positive picture. In no instance does the PSR perform below the steady-state fixed bed reactor and for the case Ke = 9, significant improvements are made, with several simulations predicting better than equilibrium performance. A optimum reaction number is clearly evident in the simulations for Ke = 9 and less so for Ke = 2, confirming

the trend reported by Vaporciyan and Kadlec (1987) and Alpay et al. (1994). The simulations for smaller equilibrium constants did not exhibit a maximum purity, but tended to track the steady-state line, getting asymptotically closer to it as Ke decreased. In all simulations, very fast reactions (Rn $\gtrsim$ 10) produced exit purities at the equilibrium concentrations. Thus for very fast reactions, pressure swing operation can do little to improve separation.

In all the simulations, a common trend was observed. The approach to equilibrium at the point where PSR operation yielded the greatest improvement over the steady-state conversion was constant at approximately 95%.

The average yields of the simulations are plotted in Figure 4.24. The simulations show a very similar trend as was seen in the purity plots. The yields improve dramatically as the reaction rate increases before reaching a maximum and then levelling off to a constant value. As would be expected, equilibrium favoured reactions produce greater yields.

Very good yields were experienced for high equilibrium constant simulations of up to 72%. The corresponding adsorption step purity for this run was 96% with an average purity of 87% (the equilibrium mole fraction was 0.9). Since the dimensionless equilibrium constant for n-butene and isobutene is typically between 4 and 8, this is a positive sign.

It is unfortunate that reactions with very low equilibrium constants do not perform well under PSR operation. It may be that the poor performances are as a result of a bad set of adsorption parameters. Separation occurs through the adsorption of unused feed at the end of the reactor. It may be possible that the adsorption capacity is too low to accommodate all the unreacted feed because of the low equilibrium conversion. Increasing Qa_A might increase the exit purity during the adsorption step but the may not be worth the resulting drop in the product yield, which is already low (6%). In another simulation, increasing the adsorption number to 500 actually reduced both the yield and purity slightly.

4.10 Conclusions

The numerical analysis of the Pressure Swing Reactor system produced a myriad of results. This is not surprising from a highly nonlinear system with such a large number of parameters. The most important of these results are summarised here.

Two parameters, the Reynolds number and the Euler number produced massive numerical instability in the Navier-Stokes equation. This was overcome by using small values for these parameters.

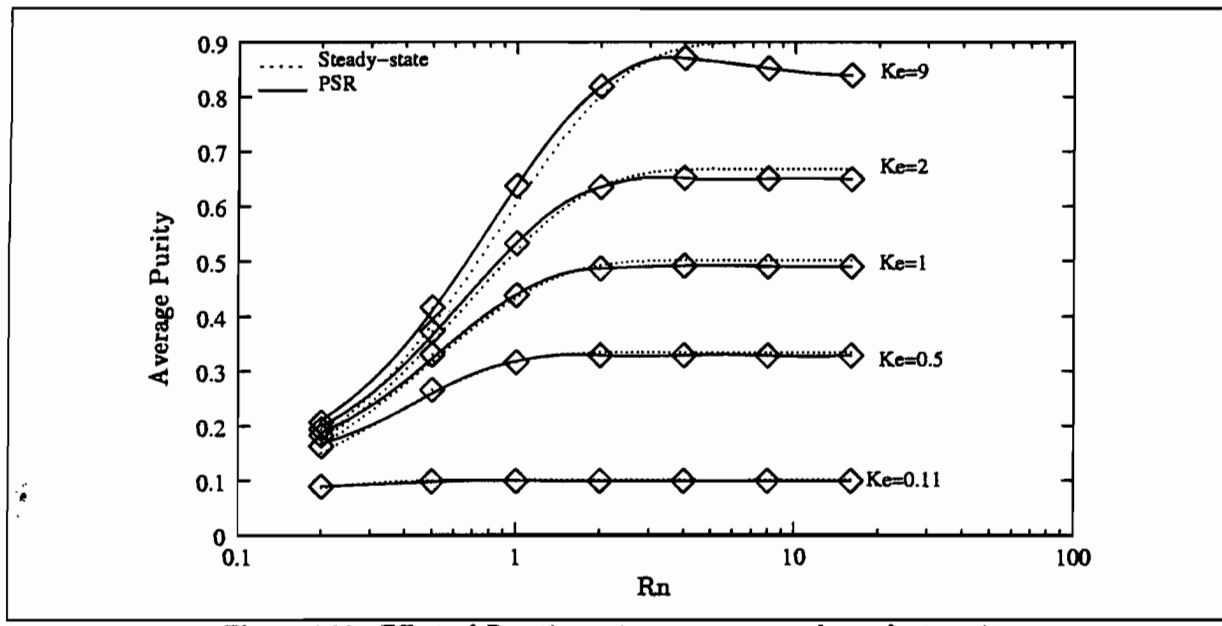

Figure 4.22: *Effect of Reaction rate on average cycle product purity.*

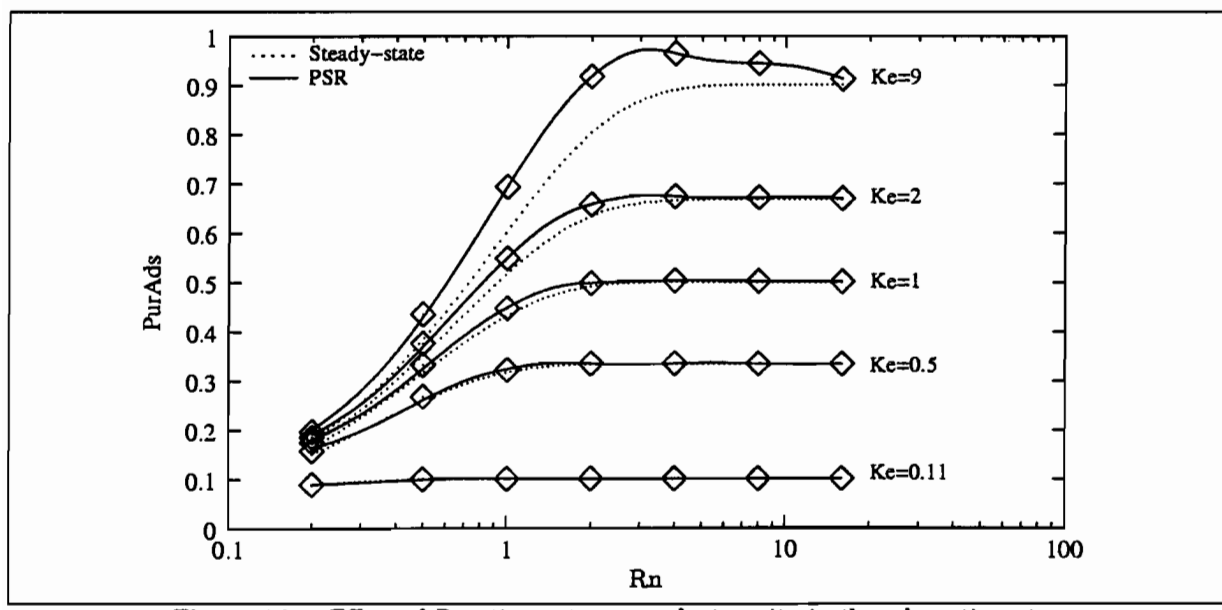

Figure 4.23: *Effect of Reaction rate on product purity in the adsorption step.*

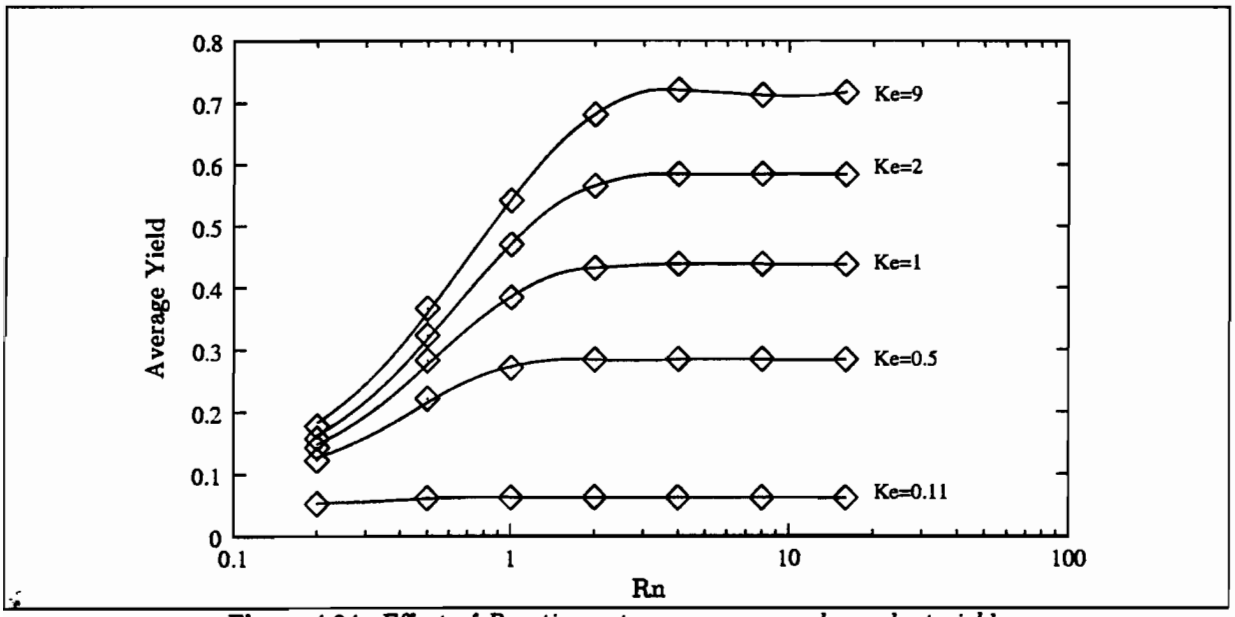

Figure 4.24: *Effect of Reaction rate on average cycle product yield.*

The adiabatic model indicated that temperature effects are significant in the simulations insofar as increasing the amount of time needed to reach cyclic steady state. To facilitate more in-depth analysis of the operating parameters, the isothermal model was used instead.

Two approaches to PSR operation were studied. Only one approach gave any success. This involved using an adsorbent selective to the feed component only. Using this approach, product purities in excess of 99% were obtained, corresponding to overall yields of 62%. Thus the stated objective of achieving simultaneous reaction and separation in one unit was realised.

The isotherm gradient or Henry's constant of adsorption emerged as the most important parameter to successful PSR operation. Larger values for the Henry's constant resulted in better performance.

An optimum reaction rate was found with respect to product purity, reproducing the results of Alpay et al. (1994) and Vaporciyan and Kadlec (1987). Performance also underwent a maximum when the adsorption capacity was varied.

Mass transfer limitations were found to be unimportant in the range investigated.

Longer adsorption steps tended to improve performance. Shorter purge steps tended to improve performance but also increased the time necessary to reach cyclic steady state.

References

Adam, Y. (1985). Nonlinear instability in advection-diffusion numerical models. *Appl. Math. Modelling*, 9.

Alpay, E., Chatsiriwech, D., and Kershenbaum, L. (1994). Combined reaction and separation in pressure swing processes. *Chemical Engineering Science*, 49(24B):5845–5864.

Alpay, E., Kenney, C., and Scott, D. (1993). Simulation of rapid pressure swing adsorption and reactor processes. *Chem. Eng. Science*, 48(18):3173–3186.

Barashenkov, I. (2001a). Method of characteristics and Riemann invariants. Lecture Notes, Advanced Mathematical Methods, University of Cape Town.

Barashenkov, I. (2001b). pers. comm.

Barber, J., Perkins, J., and Sargent, R. (1998). Boundary conditions for flow with dispersion. *Chemical Engineering Science*, 53(7):1463–1464.

Bird, R., Stewart, W., and Lightfoot, E. (1960). *Transport Phenomena.* John Wiley and Sons.

Buzanowski, M. and Yang, R. (1991). Approximations for intraparticle diffusion rates in cyclic adsorption and desorption. *Chemical Engineering Science*, 46(10):2589–2598.

Chan, Y., Hill, F., and Wong, Y. (1981). *Chem. Eng. Sci.*, 36:243.

Chatsiriwech, D., Alpay, E., Kershenbaum, L., Hull, C., and Kirkby, N. (1994). Enhancement of catalytic reaction by pressure swing adsorption. *Catalysis Today*, 20:351–366.

Cheng, Y., Alpay, E., and Kershenbaum, L. (1998). Simulation and optimisation of a rapid pressure swing reactor. *Computers chem. Engng*, 22 Supp:S45–S52.

Cole, J. (1968). *Perturbation Methods in Applied Mathematics.* Blaisdell.

Do, D. D. and Do, H. D. (1997). A new adsorption isotherm for heterogeneous adsorbent based on the isosteric heat as a function of loading. *Chemical Engineering Science*, 52(2):297–310.

Farooq, S. and Ruthven, D. (1991). Dynamics of kinetically controlled binary adsorption in a fixed bed. *AIChE Journal*, 37(2):229–301.

Fogler, H. S. (1992). *Elements of Chemical Reaction Engineering.* Prentice-Hall, 2nd edition.

Furnas, C. C. (1930). *Trans. Am. Inst. Chem. Eng.*, 24:142.

Gildert, G. (1997). Catalytic distillation extends its reach. *Chemical Engineering*, pages 78–84.

Gluekauf, E. (1955). Formulae for diffusion into spheres and their application to chromatography. *J. Chem. Soc.*, 51:1540.

Haberman, R. (1987). *Elementary Applied Partial Differential Equations.* Prentice-Hall, 2nd edition.

Kim, D. (1989). Linear driving force formulas for diffusion and reaction in porous catalysts. *AIChE Journal*, 35(2):343–346.

Klinkenberg, A. (1954). *Industrial Chemical Engineering*, 46:2285.

Kodde, A., Fokma, Y., and Bliek, A. (2000). Selectivity effects on series reactions by reactant storange and PSA operation. *AIChE Journal*, 46(11):2295–2304.

Lapidus, L. and Amundsen, N. R. (1952). *Journal of Physical Chemistry*, 56:984.

Lee, I. and Kadlec, R. (1984). Effects of adsorbent and catalyst distributions in pressure swing reactors. *AIChE Symposium Series*, 84(264):167–176.

Levenspiel, O. and Bischoff, K. (1963). *Advances in Chem. Eng.*, 4:95.

Lu, Z. and Rodrigues, A. (1994). Pressure swing adsorption reactors: Simulation of three-step one-bed process. *AIChE Journal*, 40(7):1118–1137.

Madsen, N. K. and Sincovec, R. F. (1992). PDECOL: General collocation software for partial differential equations. *ACM. Transactions on mathematical software*, 18(3):343–344.

Martinez, G. and Basmadjian, D. (1996). Towards a general gas isotherm. *Chemical Engineering Science*, 51(7):1043–1054.

Mazotti, M., Kruglov, A., Neri, B., Gelosa, D., and Morbidelli, M. (1996). A continuous chromatographic reactor: SMBR. *Chem. Eng. Science*, 51(10):1827–1836.

Migliorini, C., Fillinger, M., Mazotti, M., and Morbidelli, M. (1999). Analysis of simulated moving bed reactors. *Chem. Eng. Science*, 54:2475–2480.

Myers, A. and Prausnitz, J. (1965). *American Institute of Chemical Engineers Journal*, 11(121).

Nayfeh, A. (1981). *Introduction to Perturbation Techniques.* John Wiley and Sons.

Nitta, T. and Shigetomi, T. (1984). An adsorption isotherm of multi-site occupancy model for homogeneous surface. *J. Chem. Eng. Jpn.*, 17:39.

Petzold, L. R. (1982). A description of DDASSL: A differential/algebraic system solver. *Sandia Tech. Rep.*, 82:8637.

Rasmuson, A. (1982). *Chemical Engineering Science*, 37:787.

Rasmuson, A. and Neretnieks, I. (1980). *AIChE Journal*, 26:686.

Ray, A. and Carr, R. (1995). Experimental study of a laboratory-scale simulated countercurrent moving bed chromatographic reactor. *Chemical Engineering Science*, 50:2195–2202.

Rice, R. and Do, D. (1995). *Applied Mathematics and Modelling for Chemical Engineers.* John Wiley and Sons, New York.

Rosen, J. B. (1954). *Ind. Eng. Chem.*, 46:1590.

Ruthven, D. (1984). *Principles of Adsorption and Adsorption Processes.* John Wiley and Sons.

Sandler, S. (1989). *Chemical and Engineering Thermodynamics.* John Wiley and Sons, New York, 2nd edition.

Silva, J. and Rodriques, A. (1998). Separation of n/iso-paraffin mixtures by pressure swing adsorption. *Separation and Purification Technology*, 13:195–208.

Smith, J. M. (1981). *Chemical Engineering Kinetics.* McGraw-Hill, 3rd edition.

Stewart, W., Caracotsios, M., and Sorenson, J. (1996). *PDASAC: Partial-Differential-Algebraic Sensitivity Analysis Code.*

Sun, L. and Meunier, F. (1991). An improved finite difference method for fixed-bed multicomponent sorption. *AIChE Journal*, 37(2):244–254.

Vaporciyan, G. and Kadlec, R. (1987). Equilibrium-limited separating reactors. *AIChE Journal*, 33(8):1334–1343.

Vaporciyan, G. and Kadlec, R. (1989). Periodic separating reactors: Experimients and theory. *AIChE Journal*, 35(5):831–844.

Walter, J. E. (1952). *Journal of Chemical Physics*, 56:984.

Whitham, G. B. (1974). *Linear and Nonlinear waves*. John Wiley and Sons.

Yang, R. T. (1987). *Gas Separation by Adsorption Processes*. Butterworth.

Yongsunthon, I. and Alpay, E. (1999). Design of periodic adsorptive reactors for the optimal integration of reaction, separation and heat exchange. *Chem. Eng. Science*, 54:2647–2657.

Appendix A

Independence Calculation

Denote the set of dimensionless groups by

$$\left\{\mathcal{P} : \mathcal{P} = \Pi_1 \ldots \Pi_n = \left(\mathrm{Pe_m}, \mathrm{Qa}_A, \mathrm{Qa}_B, \mathrm{Cr}, \mathrm{Pe}, \mathrm{Hr}, \mathrm{Ha}, \mathrm{Eu}, \mathrm{Re}, \kappa_A, \kappa_B, \mathrm{Rn}, \beta_A, \beta_B\right)\right\} \quad \text{(A.1)}$$

making $n = 14$.

Furthermore, let the set of variables comprising $\mathcal{P}$ be

$$\left\{\mathcal{X} : \mathcal{X} = x_1 \ldots x_m = \left(v_0, L, D_z, \varepsilon, \rho_s, q_{s,A}, q_{s,B}, C_0, Cp_s, M_r, Cp, k_z, \Delta H_{\mathrm{rxn}}, T_0, \Delta H_{\mathrm{ads}}, P_H, \rho, \mu, k_A, k_B, A_0, B_A, B_B\right)\right\} \quad \text{(A.2)}$$

with $m = 23$.

Constructing the coefficient matrix in (3.41),

$$A_{14\times 23} = \begin{pmatrix}
1 & 0 & 0 & 0 & 1 & 0 & 0 & 1 & 1 & 1 & 1 & 1 & 0 & 0 \\
1 & 0 & 0 & 0 & 1 & 0 & 0 & 0 & 1 & 1 & 1 & 1 & 0 & 0 \\
1 & 0 & 0 & 0 & 0 & 0 & 0 & 0 & 0 & 0 & 0 & 0 & 0 & 0 \\
0 & 1 & 1 & 1 & 0 & 0 & 0 & 0 & 0 & 0 & 0 & 1 & 0 & 0 \\
0 & 1 & 1 & 1 & 0 & 0 & 0 & 0 & 0 & 0 & 0 & 1 & 0 & 0 \\
0 & 1 & 0 & 0 & 0 & 0 & 0 & 0 & 0 & 0 & 0 & 0 & 0 & 0 \\
0 & 0 & 1 & 0 & 0 & 0 & 0 & 0 & 0 & 0 & 0 & 0 & 0 & 0 \\
0 & 1 & 1 & 1 & 1 & 0 & 0 & 0 & 0 & 0 & 0 & 0 & 1 & 1 \\
0 & 0 & 0 & 1 & 0 & 0 & 0 & 0 & 0 & 0 & 0 & 0 & 0 & 0 \\
0 & 0 & 0 & 1 & 1 & 1 & 1 & 0 & 0 & 0 & 0 & 0 & 0 & 0 \\
0 & 0 & 0 & 1 & 1 & 1 & 1 & 0 & 0 & 0 & 0 & 0 & 0 & 0 \\
0 & 0 & 0 & 0 & 1 & 0 & 0 & 0 & 0 & 0 & 0 & 0 & 0 & 0 \\
0 & 0 & 0 & 0 & 0 & 1 & 0 & 0 & 0 & 0 & 0 & 0 & 0 & 0 \\
0 & 0 & 0 & 0 & 0 & 1 & 1 & 0 & 0 & 0 & 0 & 0 & 0 & 0 \\
0 & 0 & 0 & 0 & 0 & 0 & 1 & 0 & 0 & 0 & 0 & 0 & 0 & 0 \\
0 & 0 & 0 & 0 & 0 & 0 & 0 & 1 & 0 & 0 & 0 & 0 & 0 & 0 \\
0 & 0 & 0 & 0 & 0 & 0 & 0 & 1 & 1 & 0 & 0 & 0 & 0 & 0 \\
0 & 0 & 0 & 0 & 0 & 0 & 0 & 0 & 1 & 0 & 0 & 0 & 0 & 0 \\
0 & 0 & 0 & 0 & 0 & 0 & 0 & 0 & 0 & 1 & 0 & 0 & 0 & 0 \\
0 & 0 & 0 & 0 & 0 & 0 & 0 & 0 & 0 & 0 & 1 & 0 & 0 & 0 \\
0 & 0 & 0 & 0 & 0 & 0 & 0 & 0 & 0 & 0 & 0 & 1 & 0 & 0 \\
0 & 0 & 0 & 0 & 0 & 0 & 0 & 0 & 0 & 0 & 0 & 0 & 1 & 0 \\
0 & 0 & 0 & 0 & 0 & 0 & 0 & 0 & 0 & 0 & 0 & 0 & 0 & 1
\end{pmatrix}$$

Using Matlab, Octave or Gauss reduction, Rank(A)=14=n and the groups are independent

Appendix B

PSR solver routines

B.1 Isothermal model using PDASAC

```
      PROGRAM MAIN
      IMPLICIT DOUBLE PRECISION (A-H,O-Z)

      PARAMETER ( NSTVAR = 5 , NPAR = 16 , NSPAR =0 )
      PARAMETER ( LRW = 105000 , LIW = 4100 )
      PARAMETER ( NGRID = 401 )
C
C     ISteps = number of steps in ads/des cycle
C     NTSteps = total number of stesp in the simulation
C
      PARAMETER ( Isteps = 100, NTSTEPS=15000)
C
C     Dimension statements and Externals
C
      DIMENSION Y(NSTVAR,NGRID,NSPAR+1)
      DIMENSION YPRIME(NSTVAR,NGRID,NSPAR+1)
      DIMENSION INFO(18),RWORK(LRW),IWORK(LIW)
      DIMENSION RPAR(NPAR)  1,IPAR(NSPAR)
      DIMENSION XGRID(NGRID)
      DIMENSION tgrid(NTSTEPS),PERFDAT(6,NTSTEPS),PERFOUT(6,NTSTEPS)
      EXTERNAL CDSUB,FSUB,GSUB,ESUB
      LUN=6
      open(1, file="output.dat")
      open(2, file="breakthru.dat")


C
C     IEFORM=0 CORRESPONDS TO Pressurisation Step
C     IEFORM=1 CORRESPONDS TO Adsorption Step
C     IEFORM=2 CORRESPONDS TO Blowdown Step
C     IEFORM=1 CORRESPONDS TO Purge Step
C
      IEFORM=0
```

```
C     Use Rectangular coordinates
      ICORD=0

C     Insert parameter values for reactor model
      call initdimless(RPAR,NPAR,DTPAR)
      dt=dtpar
C
C     Discretization points and initial states
C

      do I=1,NGRID
         XGRID(I)=DBLE(I-1)/DBLE(NGRID-1)
      enddo

      do I=1,NGRID
         Y(1,I,1)=RPAR(12)
         Y(2,I,1)=0.0D0
         Y(3,I,1)=-XGRID(i)+1.0d0
         Y(4,I,1)=0.0d0
         Y(5,I,1)=RPAR(11)*RPAR(12)/(1.0d0+RPAR(11)*RPAR(12))
      enddo

C
C     Insert the default INFO(j) values:
C
      DO 20 J = 1, 18
         INFO(J) = 0
 20   CONTINUE
C
C     Ask PDASAC to initialize yprime, with no
C     t-differencing of F_A functions:
      INFO(11) = 1
      RWORK(44)=0.0D0
C     Request sensitivity analysis for NSPAR parameters:
      INFO(12) = NSPAR

C     Indicate that E is a constant dense matrix at each x:
      INFO(13) = -2
C
C     Provide scalar tolerances in accordance with info(2):
C
      RTOL=1.0D-5
      ATOL=1.0D-4
C
C     Set the bandwidths of the iteration matrix:
C
      IWORK(1)=2*NSTVAR-1
      IWORK(2)=2*NSTVAR-1
C
C     Set tout=t for display of completed initial values:
C
      t=0.0D0
      tout=t
```

```
C     Open valve when exit pressure reached
      if (IEFORM.eq.0)then
         INFO(17)=NSTVAR*(NGRID-1)+1
         RWORK(42)=1.0d0
         RWORK(43)=5.0d-2
         write(2,*)
         write(2,*)
      endif
C
C     Integrator loop. Call the implicit integrator PDASAC
C
      DO 50 IOUT=1,NTSTEPS

 30      CALL PDASAC (t,tout,Ngrid,Xgrid,Icord,Nstvar,Y,Yprime,
     1        RTOL,ATOL,Info,RWORK,LRW,IWORK,LIW,RPAR,IPAR,IDID,LUN,
     2        Ieform,fsub,Esub,CDsub,gsub)
C
C     Write results regardless of the integration status
C
         CALL output(IOUT,t,XGRID,Y,RPAR,NPAR,NSTVAR,NGRID,1,NSPAR)
C
C     Save performance data
C
         TGRID(IOUT)=t
         PERFDAT(1,IOUT)=Y(2,1,1)/Y(1,1,1)
         PERFDAT(2,IOUT)=Y(2,1,1)*Y(3,1,1)
         PERFDAT(3,IOUT)=Y(1,1,1)*Y(3,1,1)
         PERFDAT(4,IOUT)=Y(2,NGRID,1)/Y(1,NGRID,1)
         PERFDAT(5,IOUT)=Y(2,NGRID,1)*Y(3,NGRID,1)
         PERFDAT(6,IOUT)=Y(1,NGRID,1)*Y(3,NGRID,1)
C
C     Change from de-/Pressurisation step to de-/adsorption step
C
         if (idid.eq.4) then
            write(6,100) IWORK(11),IWORK(12),IWORK(13),IWORK(14)
            INFO(1)=0
            INFO(17)=0
            if (IEFORM.eq.0) then
               IEFORM=1
               dt=RPAR(13)/dble(Isteps)
               Icount=0
               write(6,200) "Opening"
            endif
            if (IEFORM.eq.2)then
               IEFORM=3
               dt=RPAR(14)/dble(Isteps)
               Icount=0
               write(6,200) "Closing"
            endif
         endif
C
C     Change from de-/adsorption step to de-/Pressurisation step
```

```
C
          if (Icount.eq.Isteps)then
             Icount=0
             INFO(4)=0
             INFO(1)=0
             IEFORM=MOD(IEFORM+1,4)
             dt=dtpar
             write(6,201)IEFORM
             if (IEFORM.eq.0)then
                INFO(17)=NSTVAR*(NGRID-1)+1
                RWORK(42)=1.0d0
                RWORK(43)=5.0d-2
                write(2,*)
                write(2,*)
             endif
C      Blowdown Step. Stop when exit pressure is within 10% of PiL
             if (IEFORM.eq.2)then
                INFO(17)=NSTVAR*(NGRID-1)+1
                RWORK(42)=RPAR(12)
                RWORK(43)=0.1
             endif
          endif
          if ((IEFORM.eq.1).or.(IEFORM.eq.3))  Icount=Icount+1

          tout=t+dt

C
C      Error capturing
C
          IF(IDID.EQ.-1) THEN
             INFO(1) = 1
             GO TO 30
          ELSE IF(IDID.LT.-1)THEN
             WRITE(6,90) IWORK(11)+1,IDID
             WRITE(6,100) IWORK(11),IWORK(12),IWORK(13),IWORK(14)
             STOP
          END IF
 50    CONTINUE


       WRITE(6,100) IWORK(11),IWORK(12),IWORK(13),IWORK(14)
       close(1)                    !output.dat
       close(2)                    !breakthru.dat
 11       format(20F12.6)
 90    FORMAT(/1X,'Integration failed in step',I6,' with IDID = ',I5)
 100   FORMAT(/1X,'Number of steps taken so far :=',I5/
     1      1X,'Number of function calls   :=',I5/
     2      1X,'Number of Jacobian calls   :=',I5/
     3      1X,'Number of error test fails :=',I5/)
 200   FORMAT(1X,"Exit␣Pressure␣Reached.␣",A,"␣valve.")
 201   FORMAT(1X,"Reversing␣FLow.␣Commening␣step␣",I3,"␣now.")
C
C      Write performance data
```

```
C
      print*, "Simulation completed."
      print*, "Calculating and writing performance data..."
      open(3,file="yields.dat")
      call gensimp(NTSTEPS,6,TGRID,PERFDAT,PERFOUT)
      do i=1,NTSTEPS
      write (3,11) TGRID(i),(PERFOUT(j,i),j=1,6)
      enddo
      close(3)                    !yields.dat
C
C     End of the Main Program
C
      print*,'All done.'
      END
C-----------------------------------------------------------------------
      SUBROUTINE fsub(t,x,Nstvar,U,Ux,dvCDdU,fval,
     1                                Rpar,Ipar,Ieform,Ires)
      implicit real*8(a-h,o-z)
      DOUBLE PRECISION dvCDdU(*), fval(*), U(*), Ux(*),RPAR(*)
      INTEGER Nstvar
C
C     Compute the local elements of the vector  f .
C

C     Multicomponent Langmuir isotherm
      QQ=1.d0+RPAR(10)*U(2)+RPAR(11)*(U(1)-U(2))
      qea=RPAR(10)*U(2)/QQ
      qeb=RPAR(11)*(U(1)-U(2))/QQ
C     Reaction Term
      ra=U(1)/RPAR(7)-U(2)*(RPAR(7)+1.0d0)/RPAR(7)
C     Right hand side of the PDE's
      fval(1)=dvCDdU(1)-U(1)*Ux(3)-U(3)*Ux(1)
      fval(2)=dvCDdU(2)-U(2)*Ux(3)-U(3)*Ux(2)+RPAR(8)*ra
      fval(3)=dvCDdU(3)/U(1)-RPAR(3)*Ux(1)/U(1)-U(3)*Ux(3)
      fval(4)=RPAR(15)*(qea-U(4))
      fval(5)=RPAR(16)*(qeb-U(5))
      RETURN
      END
C-----------------------------------------------------------------------
      SUBROUTINE CDsub(t,x,Nstvar,U,CDval,Rpar,Ipar,Ieform,
     1     Ires)
      implicit real*8(a-h,o-z)
      DOUBLE PRECISION CDVAL(NSTVAR,*),RPAR(*)
C
C     Provide the diffusion coefficient.
C
      CDVAL(1,1)=1.0d0/RPAR(1)
      CDVAL(2,2)=1.0d0/RPAR(1)
      CDVAL(3,3)=2.0d0/RPAR(2)
      CDVAL(4,4)=0.d0
      CDVAL(5,5)=0.d0
      RETURN
      END
```

```
C-----------------------------------------------------------------------
      SUBROUTINE gsub(t,x,Nstvar,U,CDUx,gval,Rpar,Ipar,Ieform,
     1     Ires,Ibnry)
      implicit real*8(a-h,o-z)
      DOUBLE PRECISION U(*),CDUx(*),gval(*),RPAR(*)
      INTEGER IEFORM, IBNRY
C     The adorption BC's never change, so put them here
      QQ=1.d0+RPAR(10)*U(2)+RPAR(11)*(U(1)-U(2))
      qea=RPAR(10)*U(2)/QQ
      qeb=RPAR(11)*(U(1)-U(2))/QQ
      gval(4)=RPAR(15)*(qea-U(4))
      gval(5)=RPAR(16)*(qeb-U(5))
C     Left hand Boundary Conditions
      IF(IBNRY.EQ.1) THEN
         if (IEFORM.eq.0)then
            gval(1)=U(1)-1
            gval(2)=U(2)-U(1)
            gval(3)=U(3)-1
         elseif (IEFORM.eq.1)then
            gval(1)=U(1)-1
            gval(2)=U(2)-U(1)
            gval(3)=U(3)-1
         elseif (IEFORM.eq.2)then
            gval(1)=U(1)-RPAR(12)
            gval(2)=CDUx(2)*U(1)-U(2)*CDUx(1)
            gval(3)=CDUx(3)
         elseif (IEFORM.eq.3)then
            gval(1)=U(1)-RPAR(12)
            gval(2)=CDUx(2)*U(1)-U(2)*CDUx(1)
            gval(3)=CDUx(3)
         endif
      ELSEIF (IBNRY.eq.2)then
C     Right hand Boundary conditions
         IF(IEFORM.EQ.0) THEN
            gval(1)=CDUx(1)
            gval(2)=CDUx(2)
            gval(3)=U(3)
         ELSEIF (IEFORM.eq.1) then
            gval(1)=CDUx(1)
            gval(2)=CDUx(2)
            gval(3)=CDUx(3)
         ELSEIF (IEFORM.eq.2) then
            gval(1)=CDUx(1)
            gval(2)=CDUx(2)
            gval(3)=U(3)
         ELSEIF (IEFORM.eq.3) then
            gval(1)=U(1)-RPAR(12)
            gval(2)=U(2)
            gval(3)=U(3)+1
         END IF
      else
         print*,"UNknown␣Boundary␣value:␣",IBNRY
      END IF
```

```
      RETURN
      END
C-----------------------------------------------------------------------
      SUBROUTINE ESUB(t,x,Nstvar,U,Ework,RPAR,IPAR,IEFORM,
     1     IRES,JLOC)
      implicit real*8(a-h,o-z)
      DOUBLE PRECISION x, EWORK(NSTVAR,*), RPAR(*), IPAR(*),U(*)
      INTEGER JLOC
C
C     JLOC.EQ.1 denotes the left boundary (tube axis: x=0.)
C     JLOC.EQ.2 denotes the right boundary (tube wall: x=1.)
C     JLOC.EQ.0 denotes an intermediate grid point (0.<x<1.)
C
      do i=1,5
         do j=1,5
            EWORK(i,j)=0.0D0
         enddo
      enddo
*     IF(JLOC.EQ.0) THEN
         EWORK(1,1)=1.0D0
         EWORK(1,4)=RPAR(5)
         EWORK(1,5)=RPAR(6)
         EWORK(2,2)=1.0D0
         EWORK(2,4)=RPAR(5)
         EWORK(3,3)=1.0d0
      END IF
      EWORK(4,4)=1.0d0
      EWORK(5,5)=1.0d0
      RETURN
      END

C-----------------------------------------------------------------------
      SUBROUTINE initdimless(RPAR,NPAR,DTPAR)
      implicit real*8(a-h,o-z)
      character*6 var
      real*8 RPAR(NPAR)
C     Read input from stdin
      read (*,*) nlines
      if (nlines.ne.0) open (5,file='input.dat')
      do i=1,nlines
C     RPAR(1) = Pem     Mass Transfer Peclet Number
C     RPAR(2) = Re      Reynolds Number
C     RPAR(3) = Eu      Euler Number
C     RPAR(4) = e       Voidage
C     RPAR(5) = QaA     Adsorption number, A
C     RPAR(6) = QaB     Adsorption number, B
C     RPAR(7) = Ke      Equilibrium constant
C     RPAR(8) = Rn      Reaction Number
C     RPAR(9) = N       Number of Cycles
C     RPAR(10) =Ba      Henry's constant, A
C     RPAR(11) =Bb      Henry's constant, B
C     RPAR(12) = PiL     Desorption Pressure
C     RPAR(13) = tAds    Adsorption period
```

```
C     RPAR(14) = tPrg   Purge Period
C     RPAR(15) = ka     Adsorption constant, A
C     RPAR(16) = kb     Adsorption constant, B
         read(5,*),var,val
          if (var(1:2).eq.'e=') RPAR(4)=val
          if (var(1:4).eq.'Pem=') RPAR(1)=val
          if (var(1:3).eq.'Re=') RPAR(2)=val
          if (var(1:3).eq.'Eu=') RPAR(3)=val
          if (var(1:4).eq.'QaA=') RPAR(5)=val
          if (var(1:4).eq.'QaB=') RPAR(6)=val
          if (var(1:6).eq.'betaA=') RPAR(10)=val
          if (var(1:6).eq.'betaB=') RPAR(11)=val
          if (var(1:5).eq.'xKe0=') RPAR(7)=val
          if (var(1:3).eq.'ka=') RPAR(15)=val
          if (var(1:3).eq.'kb=') RPAR(16)=val
          if (var(1:3).eq.'Rn=') RPAR(8)=val
          if (var(1:5).eq.'tauA=') RPAR(13)=val
          if (var(1:5).eq.'tauD=') RPAR(14)=val
          if (var(1:4).eq.'PiL=') RPAR(12)=val
          if (var(1:4).eq.'cyc=') RPAR(9)=val
          if (var(1:5).eq.'DTPAR') DTPAR=val
      enddo

      if (nlines.ne.0) close(5)
      end
C-----------------------------------------------------------------------
      SUBROUTINE output(IOUT,T,XGRID,Y,RPAR,NPAR,NPDE,NGRID,LUN,NSPAR)
      implicit real*8(a-h,o-z)
      character*20 cdate
      real*8 Y(NPDE,NGRID,NSPAR+1), XGRID(NGRID), RPAR(NPAR)
      data nfirst/1/
      if (nfirst.eq.1)then
         itime=time8()
         cdate=ctime(itime)
10       FORMAT(1X,'#',A6,T9,' - ',A20,':=',T38,D16.4)
         write(LUN,*)"# Pressure Swing Simulation Results"
         write(LUN,*)"# Simulation run ",cdate
         write(LUN,*)"#---------------------------------"
         write(LUN,*)
         write(LUN,*)"#Dimensionless Parameters"
         write(LUN,*)"#----------------------"
         write(LUN,10) "e","Voidage",RPAR(4)
         write(LUN,10) "Re","Reynold number",RPAR(2)
         write(LUN,10) "Eu ","Euler number ",RPAR(3)
         write(LUN,10) "Pem ","Mass transfer Peclet number ",RPAR(1)
         write(LUN,10) "QaA ","Adsorption number, A ",RPAR(5)
         write(LUN,10) "QaB ","Adsorption number,  ",RPAR(6)
         write(LUN,10) "Ke ","Equilibrium constant ",RPAR(7)
         write(LUN,10) "Rn ","Reaction Number ",RPAR(8)
         write(LUN,10) "N ","Number of Cycles ",RPAR(9)
         write(LUN,10) "Ba ","Henry's constant, A ",RPAR(10)
         write(LUN,10) "Bb ","Henry's constant, B",RPAR(11)
         write(LUN,10) "Ka ","Adsorption rate const, A",RPAR(15)
```

```
          write(LUN,10) "Kb␣","Adsorption␣rate␣const,␣B",RPAR(16)
          write(LUN,10) "PiL␣","Desorption␣Pressure␣",RPAR(12)
          write(LUN,10) "Tads␣","Adsorption␣period␣",RPAR(13)
          write(LUN,10) "Tprg␣","Purge␣Period␣",RPAR(14)
          nfirst=2
       endif

C      Write verbose data
       MODAMP=NGRID/50           !intentionally integer
       write (LUN,*) "#", IOUT,".␣t=",t
       write(LUN,11) XGRID(1),(Y(j,1,1),j=1,NPDE)
       do i=1,NGRID-1
          if (MOD(I,MODAMP).eq.0)then
             write(LUN,11) XGRID(i),(Y(j,i,1),j=1,NPDE)
          endif
 11       format(20F12.6)
       enddo
       write(LUN,11) XGRID(NGRID),(Y(j,NGRID,1),j=1,NPDE)
C      write(LUN,*)
       write(LUN,*)
C      Write bounday data
       write(2,11) t,(Y(i,NGRID,1),i=1,3),(Y(j,1,1),j=1,3)
       end
C-----------------------------------------------------------------------
```

B.2 Adiabatic model using PDECOL

```
c-----------------------------------------------------------------------
c      Driver Routine
c-----------------------------------------------------------------------
c      Calls pdeCol to solve the pde system and control output
c-----------------------------------------------------------------------
       implicit real*8(a-h,o-z)
c      First, Set up all the work variables and parameters
       parameter (kord=5,NPDE=7,iquad=0,ncc=2,nint=50)
       parameter (NPTS=51, NDERV=2)
       data     dt/1.0d-12/,    eps/1.0d-6/,    index/1/,   mf/22/
       parameter (ml=NPDE*(kord+iquad-1)-1)
       parameter (NCPTS=kord*nint-ncc*(nint-1))
       parameter (LWORK=KORD+NPDE*(4+9*NPDE)+(KORD+(NINT-1)*(KORD-NCC))*
     *      (3*KORD+2+NPDE*(3*(KORD-1)*NPDE+12)))
       parameter (LIWORK=(NPDE+1)*(KORD+(NINT-1)*(KORD-NCC)))
       data     ndim1/NPDE/,  ndim2/NPTS/
       dimension work(LWORK),      iwork(LIWORK),      xbkpt(NINT+1)
       dimension X(NPTS), USOL(NPDE,NPTS,NDERV+1),SCTCH(KORD*(NDERV+1))

c-----------------------------------------------------------------------
c      Define all the important dimensionless groups
       common /dimvar/ e,xKe0,Ea0,QaA,QaB,Pem,Rn,QrA,QrB,
     $      Hr,Re,Eu,xkappA,xkappB,betaA,betaB,Cr,Pe,phi,Br
       common /periods/ tauC,tauP,tauA,tauB,tauD
       common /opvars/ PiL,ya0,u0,Pad,rem,Ux0
       common /cyc/ cycles
```

```
c-----------------------------------------------------------------------
      iwork(1)=LWORK
      iwork(2)=LIWORK
      do i=1,LWORK
         work(i)=0.0d0
      enddo
      do i=3,LIWORK
         iwork(i)=0
      enddo

c-----------------------------------------------------------------------
      do i=0,NINT
         xbkpt(i+1)=dfloat(i)/dfloat(NINT)
      enddo

c-----------------------------------------------------------------------
c     x-values for which output is desired
      do i=1,NPTS
         X(i)=dfloat(i-1)/dfloat(NPTS-1)
      enddo

c-----------------------------------------------------------------------
c     Nomenclature
c     e    - voidage
c     xKe0- Reference equilibrium constant (dGrxn/RTin)
c     Ea0 - Reference activation energy (Ea/RTin)
c     Qai - Adsorption number
c     Pemi- Mass transfer Peclet number
c     Cr   - Heat capacity ratio
c     Pe   - Peclet number
c     Rn   - Reaction number
c     Qri - Dimensionless heat of adsorption
c     Hri - Dimensionless heat of reaction
c     Re   - Reynolds number
c     Eu   - Euler number
c     xKapp- Dimensionless adsorption rate constant
c     Beta- dimensionless Henry's constant for adsorption
c     phi - Thiele modulus
c     Br   - prop. const in adsorption number calc = dHads/RTin

c     They can be modified/set in the subroutine initdimless
      e=0.4d0
      ! Flow parameters
      Pem=50.0d0
      Re=20.d0
      Eu=0.5d0
      Pe=80.d0
      ! Adsorption parameters
      QaA=11.0d0
      QaB=1.1d0
      QrA=0.01d0
      QrB=0.02d0
      xkappA=10.0d0
```

```
      xkappB=1.d0
      betaA=2.d0
      betaB=1.d0
      Br = 1.0d0
      ! Reaction Parameters
      xKe0=1.d0
      Ea0=1.d0
      Rn=15.0d0
      Hr=0.0d0
      Cr=1.0d5
      phi=1.d0                    !no reaction

      tauP=4.d0
      tauA=100.d0
      tauB=0.d0
      tauD=0.d0

      PiL=0.2d0
*     call initdimless
      tauC=tauP+tauA+tauB+tauD
c-----------------------------------------------------------------------
c     Main Loop
c-----------------------------------------------------------------------
      tfinal=cycles*tauC
      timestep=tauC/200.d0        ! 200 samplings per cycle
      index=1
      nfirst=1
      t0=0.d0
      open (4,file='breakthru.dat')
      open (3,file='perf.dat')
      write(3,*),"Time␣␣␣␣␣Purity␣␣␣␣␣Yield"
      open (2,file='error.dat')
      open (1,file='output.dat')
      print*,''Computing Steady-State Profile...'
      call steady
      print*,'Commencing Simulation...'
      do tout=0.d0,tfinal,timestep
         if (tout .NE. 0)then
            index=0
            nfirst=0
         endif
         call pdecol(t0,tout,dt,xbkpt,eps,Nint,kord,NCC,NPDE,MF,index,
     &        work,iwork)

         call values(X,usol,sctch,ndim1,ndim2,npts,nderv,work)

         call output(nfirst,X,tout,usol,npts,npde,nderv+1)
         call massbal(tout,usol,npts,npde,timestep)
      enddo
      close(1)
      close(2)
      close(3)
      close(4)
```

```
      print*,'Done.'
c-----------------------------------------------------------------------
c     End of Main Loop
c-----------------------------------------------------------------------
      end
c-----------------------------------------------------------------------
c     End of main program
c-----------------------------------------------------------------------

c-----------------------------------------------------------------------
c     User Supplied Subroutines
c-----------------------------------------------------------------------
      SUBROUTINE F( T, X, U, UX, UXX, FVAL, NPDE )
      implicit real*8(a-h,o-z)
      DIMENSION U(NPDE), UX(NPDE), UXX(NPDE), FVAL(NPDE)
      call pdes( T, X, U, UX, UXX, FVAL, NPDE )
      RETURN
      END
c-----------------------------------------------------------------------
      SUBROUTINE BNDRY( T, X, U, UX, DBDU, DBDUX, DZDT, NPDE )
      implicit real*8(a-h,o-z)
      save last
c     Specifies the type of boundary condition that was called last
c     Allows the program to track when the BCs change
      DIMENSION U(NPDE), UX(NPDE), DZDT(NPDE)
      DIMENSION DBDU(NPDE,NPDE), DBDUX(NPDE,NPDE)
      common /periods/ tauC,tauP,tauA,tauB,tauD
      common /opvars/ PiL,ya0,u0,Pad,rem,Ux0
c     Call the correct boundary condition program, depending on the time
      mul=T/tauC                ! Intentionally integer.
      rem=T - dfloat(mul)*TauC  ! Fractional part of period
      if (t.eq.0.d0)then
         last=1
         ya0=0.d0
      endif
      if (rem.lt.tauP)then
         if (last.eq.4)then
            ya0=U(1)
         endif
         if (last.ne.1)print*,'T=',T,' Pressurising...'
         call Pressurisation( T, X, U, UX, DBDU, DBDUX, DZDT, NPDE )
c     print*,'(x,t)=(',x,',',t,') Ya0=',ya0,' U=',U
c     print*,'dZdt=',DZDT
         last=1
      elseif ((rem.ge.tauP).and.(rem.lt.tauP+tauA))then
         if(last.ne.2)print*,'T=',T,' Adsorbing...'
         call Adsorption( T, X, U, UX, DBDU, DBDUX, DZDT, NPDE )
         last=2
      elseif ((rem.ge.tauA+tauP).and.(rem.lt.tauB+tauP+tauA))then
         if(last.ne.3) then
            print*,'T=',T,'Blowdown...'
         endif
```

```
         call Blowdown( T, X, U, UX, DBDU, DBDUX, DZDT, NPDE )
         last=3
      elseif (rem.ge.tauA+tauP+tauB)then
         if (last.eq.3)ya0=U(1)
         if(last.ne.4)print*,'T=',T,'Purging...'
         call Purge( T, X, U, UX, DBDU, DBDUX, DZDT, NPDE )
         last=4
      endif
      RETURN
      END
c-----------------------------------------------------------------------
      SUBROUTINE UINIT( X, U, NPDE )
      implicit real*8(a-h,o-z)
      DIMENSION U(NPDE)
      call newreactor( X,U,NPDE)
      RETURN
      END
c-----------------------------------------------------------------------
c     Dummy procedure
      subroutine derivf(T, X, U, UX, UXX, FVAL, NPDE )
      implicit real*8(a-h,o-z)
      end
c-----------------------------------------------------------------------
      subroutine initdimless
      implicit real*8(a-h,o-z)
      character*6 var
      common /dimvar/ e,xKe0,Ea0,QaA,QaB,Pem,Rn,QrA,QrB,
     $     Hr,Re,Eu,xkappA,xkappB,betaA,betaB,Cr,Pe,phi,Br
      common /periods/ tauC,tauP,tauA,tauB,tauD
      common /opvars/ PiL,ya0,u0,Pad,rem,Ux0
      common /cyc/ cycles

      read (*,*) nlines
      if (nlines.ne.0) open (5,file='input.dat')
      do i=1,nlines
         read(5,*),var,val
         if (var(1:2).eq.'e=') e=val
         if (var(1:4).eq.'Pem=') Pem=val
         if (var(1:3).eq.'Re=') Re=val
         if (var(1:3).eq.'Eu=') Eu=val
         if (var(1:3).eq.'Pe=') Pe=val
         if (var(1:4).eq.'QaA=') QaA=val
         if (var(1:4).eq.'QaB=') QaB=val
         if (var(1:3).eq.'Ha=') Ha=val
         if (var(1:6).eq.'xkappA') xkappA=val
         if (var(1:6).eq.'xkappB') xkappB=val
         if (var(1:6).eq.'betaA=') betaA=val
         if (var(1:6).eq.'betaB=') betaB=val
         if (var(1:3).eq.'Br=') Br=val
         if (var(1:5).eq.'xKe0=') xKe0=val
         if (var(1:4).eq.'Ea0=') Ea0=val
         if (var(1:3).eq.'Rn=') Rn=val
         if (var(1:3).eq.'Hr=') Hr=val
```

```
          if (var(1:3).eq.'Cr=') Cr=val
          if (var(1:5).eq.'tauP=') tauP=val
          if (var(1:5).eq.'tauA=') tauA=val
          if (var(1:5).eq.'tauB=') tauB=val
          if (var(1:5).eq.'tauD=') tauD=val
          if (var(1:4).eq.'PiL=') PiL=val
          if (var(1:4).eq.'cyc=') cycles=val
        enddo

        QrA=Ha*QaA
        QrB=Ha*QaB
        if (nlines.ne.0) close(5)
        end
c-----------------------------------------------------------------------

c-----------------------------------------------------------------------
        SUBROUTINE PDES(t,x,u,ux,uxx,fval,npde)
c       Describes the governing pde's of the PSR system
        implicit real*8(a-h,o-z)
        dimension u(npde),ux(npde),uxx(npde),fval(npde)
        common /dimvar/ e,xKe0,Ea0,QaA,QaB,Pem,Rn,QrA,QrB,
     $      Hr,Re,Eu,xKappA,xKappB,betaA,betaB,Cr,Pe,phi,Br
c       Variable mapping:
c       u(1)=ya, mole fraction species A
c       u(2)=yb, mole fraction species B
c       u(3)=phi, dimensionless concentration
c       u(4)=theta, dimensionless temperature
c       u(5)=u, dimensionless velocity
c       u(6)=qa, dimensionless adsorbed conc species A
c       u(7)=qb, dimensionless adsorbed conc species B

c       VI, VII) rates of adsorption
        call adsrate('LDF',u,ux,uxx,fval,npde)

c       I) Overall Mass Balances (Generalised continuity equation)
        sigQ=QaA*fval(6)+QaB*fval(7)
        fval(3)=uxx(3)/Pem-u(3)*ux(5)-u(5)*ux(3)-sigQ

c       II, III)  Species Balances
        rA=rate('simple',u,ux,uxx,fval,npde)
        rB=-rA
        fval(1)=-u(1)*fval(3) + 2.d0/Pem*ux(1)*ux(3)
     $       + u(1)/Pem*uxx(3) + uxx(1)/Pem
     $       - u(1)*u(5)*ux(3) - u(3)*u(1)*ux(5) - u(5)*ux(1)*u(3)
     $       - QaA*fval(6) + Rn*ra
        fval(1)=fval(1)/u(3)
c       I have checked this:
c       As long as PemA=PemB=Pem then as it stands fval(1)+fval(2)=0
        fval(2)=-fval(1)

c       IV) Energy Balance
        Cre=Cr*(1.d0-e)/e
        sigQr=(QrA*fval(6)+QrB*fval(7))/(Cre+u(3))
        fval(4)=-u(3)/(Cre+u(3))*(u(4)*ux(5)+u(5)*ux(4))+
```

```
     $     uxx(4)/(Pe*(Cre+u(3)))+Hr/(Cre+u(3))*rA-sigQr

c     V) Navier-Stokes Equation (Momentum Balance)
      dPdx=u(4)*ux(3)+u(3)*ux(4)
      ! interstitial velocity
      fval(5)=-u(5)*ux(5)-Eu/u(3)*dPdx +2.d0/Re/u(3)*uxx(5)
      end
c-----------------------------------------------------------------------
      REAL*8 FUNCTION PDROP(type,u,npde)
      implicit real*8(a-h,o-z)
      dimension u(npde)
      character*6 type
      common /dimvar/ e,xKe0,Ea0,QaA,QaB,Pem,Rn,QrA,QrB,
     $     Hr,Re,Eu,xKappA,xKappB,betaA,betaB,Cr,Pe,phi,Br
      if (type(1:5).eq.'Ergun')then
c     Ergun Equation
         Pdrop = 150.d0*(1-e)**2/e**3/(Re*Eu)*u(4)+
     $        1.75d0*(1-e)/e**3*u(3)*u(4)**2
      endif
c     Add other options here...
      return
      end
c-----------------------------------------------------------------------
      REAL*8 FUNCTION EOS(type,u,npde)
      implicit real*8(a-h,o-z)
      dimension u(npde)
      character*6 type
      common /dimvar/ e,xKe0,Ea0,QaA,QaB,Pem,Rn,QrA,QrB,
     $     Hr,Re,Eu,xKappA,xKappB,betaA,betaB,Cr,Pe,phi,Br

      if (type(1:5).eq.'Ideal')then
c     Ideal Gas Law
         EOS=u(3)*u(4)
      endif
      return
      end
c-----------------------------------------------------------------------
      SUBROUTINE ADSRATE(type,u,ux,uxx,fval,npde)
c     Subroutine that calculates the adsorption rate
      implicit real*8(a-h,o-z)
      dimension u(npde),ux(npde),uxx(npde),fval(npde)
      character*6 type
      real*8 qs(2)
      common /dimvar/ e,xKe0,Ea0,QaA,QaB,Pem,Rn,QrA,QrB,
     $     Hr,Re,Eu,xKappA,xKappB,betaA,betaB,Cr,Pe,phi,Br
      if (type(1:3).eq.'LDF')then
c     Linear Driving Force Model
         call qsat('MCLang',u,ux,uxx,qs,npde,2)
         fval(6)=xKappA*(qs(1)-u(6))
         fval(7)=xKappB*(qs(2)-u(7))
      endif
      end
c-----------------------------------------------------------------------
```

```
      SUBROUTINE QSAT(type,u,ux,uxx,qs,npde,nspecies)
c     Subroutine that calculates isotherms
      implicit real*8(a-h,o-z)
      dimension u(npde),qs(nspecies),ux(npde),uxx(npde)
      character*6 type
      common /dimvar/ e,xKe0,Ea0,QaA,QaB,Pem,Rn,QrA,QrB,
     $     Hr,Re,Eu,xKappA,xKappB,betaA,betaB,Cr,Pe,phi,Br

      if (type.eq.'MCLang')then
c     Adsorption coefficient follows Clas-Clap relationship
         ba=betaA*exp(Br*(1.d0/u(4)-1.d0))
         bb=betaB*exp(Br*(1.d0/u(4)-1.d0))

c     Multicomponent Langmuir model
         sigby=ba*u(1)+bb*u(2)
         qs(1)=ba*u(1)*u(3)/(1.d0+u(3)*sigby)
         qs(2)=bb*u(2)*u(3)/(1.d0+u(3)*sigby)
      endif
      end
c-----------------------------------------------------------------------
      REAL*8 FUNCTION RATE(type,u,ux,uxx,fval,npde)
      implicit real*8(a-h,o-z)
      dimension u(npde),ux(npde),uxx(npde),fval(npde)
      character*6 type
      common /dimvar/ e,xKe0,Ea0,QaA,QaB,Pem,Rn,QrA,QrB,
     $     Hr,Re,Eu,xKappA,xKappB,betaA,betaB,Cr,Pe,phi,Br
      a1=exp((xKe0-Ea0)/u(4))
      a2=exp(-xKe0/u(4))
      rate=a1*u(3)*(1.d0-u(1)*(a2+1.d0))
      return
      end
c-----------------------------------------------------------------------
      REAL*8 FUNCTION RXNEQM(u,npde)
      implicit real*8(a-h,o-z)
      dimension u(npde)
      common /dimvar/ e,xKe0,Ea0,QaA,QaB,Pem,Rn,QrA,QrB,
     $     Hr,Re,Eu,xKappA,xKappB,betaA,betaB,Cr,Pe,phi,Br
      rxnEqm=exp(xKe0/u(4))
c     This makes use of the relation dGrxn=-RTlnK
      return
      end
c-----------------------------------------------------------------------

c-----------------------------------------------------------------------
c     Boundary Conditions for the PSR
c-----------------------------------------------------------------------

c     Divided into 4 stages
c     i) Pressurisation
c     ii) Adsorption
c     iii) Blowdown
c     iv) Purge

c     Variable mapping:
```

```
c     u(1)=ya, mole fraction species A
c     u(2)=yb, mole fraction species B
c     u(3)=phi, dimensionless concentration
c     u(4)=theta, dimensionless temperature
c     u(5)=u, dimensionless velocity
c     u(6)=qa, dimensionless adsorbed conc species A
c     u(7)=qb, dimensionless adsorbed conc species B

c     Equation Mapping

c     I) Species A Balance
c     II) Species B Balance
c     III) Overall Mass Balance
c     IV) Energy Balance
c     V) Navier-Stokes Equation
c     VI) Species A Adsorption
c     VII) Species B Adsorption

c-----------------------------------------------------------------------
      SUBROUTINE PRESSURISATION( T, X, U, UX, DBDU, DBDUX, DZDT, NPDE )
      implicit real*8 (a-h,o-z)
      parameter (expfact=5.d0)
      DIMENSION U(NPDE), UX(NPDE), DZDT(NPDE)
      DIMENSION DBDU(NPDE,NPDE), DBDUX(NPDE,NPDE)
      common /dimvar/ e,xKe0,Ea0,QaA,QaB,Pem,Rn,QrA,QrB,
     $     Hr,Re,Eu,xkappA,xkappB,betaA,betaB,Cr,Pe,phi,Br
      common /opvars/ PiL,ya0,u0,Pad,rem
      common /switchvar/ ay0,ay1,ac0,ac1,aT0,aT1,
     $     au0,au1,aqa0,aqa1,aqb0,aqb1,
     $   by0,by1,bc0,bc1,bT0,bT1,bu0,bu1,bqa0,bqa1,bqb0,bqb1

      call Initialise( T, X, U, UX, DBDU, DBDUX, DZDT, NPDE )
      tp=rem
      if (X.eq.0.d0)then
c     For more detailed explanations see BC's MKII in The buk
c     Step change gas composition
c     C=(ConcP-1)*exp(-a.t)+1
         DBDU(3,3)=1.d0
         DZDT(3)=-expfact*(ac0-1.d0)*exp(-expfact*tp)
c     ya=(yaP-1)*exp(-a.t)+1
         DBDU(1,1)=1.d0
         DZDT(1)=-expfact*(ay0-1.d0)*exp(-expfact*tp)
c     Ya+Yb=C
         DBDU(2,2)=1.d0
         DZDT(2)=-DZDT(1)
c     Constant Temperature inlet
c     T=(TempP-1)*exp(-a.t)+1
         DBDU(4,4)=1.d0
         DZDT(4)=-expfact*(aT0-1.d0)*exp(-expfact*tp)
c     Step change inlet velocity
c     u=(uP-1)*exp(-a.t)+1
         DBDU(5,5)=1.d0
         DZDT(5)=-expfact*(au0-1.d0)*exp(-expfact*tp)
```

```
c     dQ/dx=0
         DBDUx(6,6)=1.d0
         DBDUx(7,7)=1.d0
      endif
      if (X.eq.1.d0)then
c     All variables insulated
         DBDUx(1,1)=1.d0
         DBDUx(2,2)=1.d0
         DBDUx(3,3)=1.d0
         DBDUx(4,4)=1.d0
c     except v=0 at x=1
         DBDU(5,5)=1.d0
         DZDT(5)=-expfact*au1*exp(-expfact*tp)
         DBDUx(6,6)=1.d0
         DBDUx(7,7)=1.d0
         by1=Ux(1)
         bc1=Ux(3)
         bT1=Ux(4)
         bu1=Ux(5)
         bqa1=Ux(6)
         bqb1=Ux(7)
      endif
      end
c-----------------------------------------------------------------------
      SUBROUTINE ADSORPTION( T, X, U, UX, DBDU, DBDUX, DZDT, NPDE )
      implicit real*8 (a-h,o-z)
      parameter (expfact=5.d0)
      DIMENSION U(NPDE), UX(NPDE), DZDT(NPDE)
      DIMENSION DBDU(NPDE,NPDE), DBDUX(NPDE,NPDE)
      common /opvars/ PiL,ya0,u0,Pad,rem
      common /periods/ tauC,tauP,tauA,tauB,tauD
      common /switchvar/ ay0,ay1,ac0,ac1,aT0,aT1,
     $     au0,au1,aqa0,aqa1,aqb0,aqb1,
     $   by0,by1,bc0,bc1,bT0,bT1,bu0,bu1,bqa0,bqa1,bqb0,bqb1
      common /dimvar/ e,xKe0,Ea0,QaA,QaB,Pem,Rn,QrA,QrB,
     $     Hr,Re,Eu,xkappA,xkappB,betaA,betaB,Cr,Pe,phi,Br
      call Initialise( T, X, U, UX, DBDU, DBDUX, DZDT, NPDE )
      at=rem-TauP
      if (X.eq.0.d0)then
c     For more detailed explanations see BC's MKII in The buk
         DBDU(1,1)=1.d0          !     Ya=1
         DBDU(2,2)=1.d0          !     Yb=0
         DBDU(3,3)=1.d0          !     C=1
         DBDU(4,4)=1.d0          !     T=1
         DBDU(5,5)=1.d0          !     u=1
         DBDUx(6,6)=1.d0
         DBDUx(7,7)=1.d0
         ay0=Ux(1)
         ac0=U(3)
         aT0=U(4)
         au0=Ux(5)
         aqa0=Ux(6)
         aqb0=Ux(7)
```

```
      endif
      if (X.eq.1.d0)then
c     Unchanged BCs
         DBDUx(1,1)=1.d0
         DZDT(1)=-expfact*by1*exp(-expfact*at)
         DBDUx(2,2)=1.d0
         DZDT(2)=-DZDT(1)
         DBDUx(3,3)=1.d0
         DZDT(3)=-expfact*bC1*exp(-expfact*at)
         DBDUx(4,4)=1.d0
         DZDT(4)=-expfact*bT1*exp(-expfact*at)
c     Slowly convert from 'closed valve' to 'open valve'
         DBDUx(5,5)=1.d0
         DZDT(5)=-expfact*bu1*exp(-expfact*at)
         DBDUx(6,6)=1.d0
         DZDT(6)=-expfact*bqa1*exp(-expfact*at)
         DBDUx(7,7)=1.d0
         DZDT(7)=-expfact*bqb1*exp(-expfact*at)
         ay1=U(1)
         ac1=U(3)
         aT1=U(4)
         au1=U(5)
         aqa1=Ux(6)
         aqb1=Ux(7)
      endif
      end
c-----------------------------------------------------------------------
      SUBROUTINE BLOWDOWN( T, X, U, UX, DBDU, DBDUX, DZDT, NPDE )
      implicit real*8 (a-h,o-z)
      parameter (expfact=5.d0)
      DIMENSION U(NPDE), UX(NPDE), DZDT(NPDE)
      DIMENSION DBDU(NPDE,NPDE), DBDUX(NPDE,NPDE)
      common /dimvar/ e,xKe0,Ea0,QaA,QaB,Pem,Rn,QrA,QrB,
     $     Hr,Re,Eu,xkappA,xkappB,betaA,betaB,Cr,Pe,phi,Br
      common /opvars/ PiL,ya0,u0,Pad,rem
      common /switchvar/ ay0,ay1,ac0,ac1,aT0,aT1,
     $     au0,au1,aqa0,aqa1,aqb0,aqb1,
     $   by0,by1,bc0,bc1,bT0,bT1,bu0,bu1,bqa0,bqa1,bqb0,bqb1
      common /periods/ tauC,tauP,tauA,tauB,tauD
      call Initialise( T, X, U, UX, DBDU, DBDUX, DZDT, NPDE )
      bt=rem-tauP-tauA
      if (X.eq.0.d0)then
c     Drop the inlet pressure to PiL.
         DBDU(3,3)=1.d0
         DZDT(3)=-expfact*(ac0-PiL)*exp(-expfact*bt)
         DBDUx(1,1)=1.d0
         DZDT(1)=-expfact*ay0*exp(-expfact*bt)
         DBDUx(2,2)=1.d0
         DZDT(2)=-DZDT(1)
c     Keep temp at 1
         DBDU(4,4)=1.d0
         DZDT(4)=-expfact*(1.d0-aT0)*exp(-expfact*bt)
         DBDUx(5,5)=1.d0
```

```
         DZDT(5)=-expfact*au0*exp(-expfact*bt)
         DBDUx(6,6)=1.d0
         DZDT(6)=-expfact*aqa0*exp(-expfact*bt)
         DBDUx(7,7)=1.d0
         DZDT(7)=-expfact*aqb0*exp(-expfact*bt)
         by0=Ux(1)
         bc0=Ux(3)
         bT0=Ux(4)
         bu0=Ux(5)
         bqa0=Ux(6)
         bqb0=Ux(7)
       endif

       if (X.eq.1.d0)then
         DBDUx(1,1)=1.d0            ! Ux(1)=0
         DBDUx(2,2)=1.d0            ! Ux(2)=0
         DBDUx(3,3)=1.d0            ! Ux(3)=0
         DBDUx(4,4)=1.d0            ! Ux(4)=0
         DBDU(5,5)=1.d0             ! U(5)=0
         DZDT(5)=-expfact*au1*exp(-expfact*bt)
         DBDUx(6,6)=1.d0            ! Ux(6)=0
         DZDT(6)=-expfact*aqa1*exp(-expfact*bt)
         DBDUx(7,7)=1.d0            ! Ux(7)=0
         DZDT(7)=-expfact*aqb1*exp(-expfact*bt)
         by1=U(1)
         bc1=U(3)
         bT1=U(4)
         bu1=U(5)
         bqa1=Ux(6)
         bqb1=Ux(7)
       endif
       end
c-----------------------------------------------------------------------
       SUBROUTINE PURGE( T, X, U, UX, DBDU, DBDUX, DZDT, NPDE )
       implicit real*8 (a-h,o-z)
       parameter (expfact=5.d0)
       DIMENSION U(NPDE), UX(NPDE), DZDT(NPDE)
       DIMENSION DBDU(NPDE,NPDE), DBDUX(NPDE,NPDE)
       common /dimvar/ e,xKe0,Ea0,QaA,QaB,Pem,Rn,QrA,QrB,
      $     Hr,Re,Eu,xkappA,xkappB,betaA,betaB,Cr,Pe,phi,Br
       common /opvars/ PiL,ya0,u0,Pad,rem
       common /switchvar/ ay0,ay1,ac0,ac1,aT0,aT1,
      $     au0,au1,aqa0,aqa1,aqb0,aqb1,
      $   by0,by1,bc0,bc1,bT0,bT1,bu0,bu1,bqa0,bqa1,bqb0,bqb1
       common /periods/ tauC,tauP,tauA,tauB,tauD
       call Initialise( T, X, U, UX, DBDU, DBDUX, DZDT, NPDE )
       pt=rem-tauP-tauA-tauB
       if (X.eq.0.d0)then
         DBDUx(1,1)=1.d0            ! Ux(1)=0
         DZDT(1)=-expfact*by0*exp(-expfact*pt)
         DBDUx(2,2)=1.d0            ! Ux(1)=0
         DZDT(2)=-DZDT(1)
         DBDUx(3,3)=1.d0            ! Ux(3)=0
```

```
          DZDT(3)=-expfact*bc0*exp(-expfact*pt)
          DBDUx(4,4)=1.d0            ! Ux(4)=0
          DZDT(4)=-expfact*bT0*exp(-expfact*pt)
          DBDUx(5,5)=1.d0            ! Ux(5)=0
          DZDT(5)=-expfact*bu0*exp(-expfact*pt)
          DBDUx(6,6)=1.d0            ! Ux(6)=0
          DZDT(6)=-expfact*bqa0*exp(-expfact*pt)
          DBDUx(7,7)=1.d0            ! Ux(7)=0
          DZDT(7)=-expfact*bqb0*exp(-expfact*pt)
          ay0=U(1)
          ac0=U(3)
          aT0=U(4)
          au0=U(5)
          aqa0=Ux(6)
          aqb0=Ux(7)
        endif

        if (X.eq.1.d0)then
c       C=(Cbl-PiL)exp(-a.t)+PiL
          DBDU(3,3)=1.d0
          DZDT(3)=-expfact*(bC1-PiL)*exp(-expfact*pt)
c       Ya=YaBL*exp(-a.t)
          DBDU(1,1)=1.d0
          DZDT(1)=-expfact*by1*exp(-expfact*pt)
c       Yb=1
          DBDU(2,2)=1.d0
          DZDT(2)=-DZDT(1)
c       T=(Tbl-1)exp(-a.t)+1
          DBDU(4,4)=1.d0
          DZDT(4)=-expfact*(bT1-1.d0)*exp(-expfact*pt)
c       u=(uBL+1)exp(-a.t)-1
          DBDU(5,5)=1.d0
          DZDT(5)=-expfact*(bu1+1.d0)*exp(-expfact*pt)
c       dQ/dx=0
          DBDUx(6,6)=1.d0
          DZDT(6)=-expfact*bqa1*exp(-expfact*at)
          DBDUx(7,7)=1.d0
          DZDT(7)=-expfact*bqb1*exp(-expfact*at)
          ay1=Ux(1)
          ac1=Ux(3)
          aT1=Ux(4)
          au1=U(5)
          aqa1=Ux(6)
          aqb1=Ux(7)
        endif
        end
c-----------------------------------------------------------------------
        subroutine Initialise( T, X, U, UX, DBDU, DBDUX, DZDT, NPDE )
        implicit real*8 (a-h,o-z)
        DIMENSION U(NPDE), UX(NPDE), DZDT(NPDE)
        DIMENSION DBDU(NPDE,NPDE), DBDUX(NPDE,NPDE)
        do i=1,npde
          dzdt(i)=0.d0
```

```
            do j=1,npde
               dbdu(i,j)=0.d0
               dbdux(i,j)=0.d0
            enddo
         enddo
         end
c-----------------------------------------------------------------------

c-----------------------------------------------------------------------
c     Initial conditions for the PSR
c-----------------------------------------------------------------------
c     Variable mapping:
c     u(1)=ya, mole fraction species A
c     u(2)=yb, mole fraction species B
c     u(3)=phi, dimensionless concentration
c     u(4)=theta, dimensionless temperature
c     u(5)=u, dimensionless velocity
c     u(6)=qa, dimensionless adsorbed conc species A
c     u(7)=qb, dimensionless adsorbed conc species B

      subroutine newreactor( X,U,NPDE)
      implicit real*8(a-h,o-z)
      common /opvars/ PiL,ya0,u0,Pad,rem,Ux0
      common /switchvar/ ay0,ay1,ac0,ac1,aT0,aT1,
     $     au0,au1,aqa0,aqa1,aqb0,aqb1,
     $   by0,by1,bc0,bc1,bT0,bT1,bu0,bu1,bqa0,bqa1,bqb0,bqb1
      DIMENSION U(NPDE)
      real*8 qs(2)
c     Initial conditions for t=0. i.e. starting from scratch
c     Everything at reference conditions
c
      U(1)=0.d0
      U(2)=1.d0
      U(3)=PiL
      U(4)=1.d0
c     Create an artificial velocity profile to match bc's
      U(5)=0.d0
c          -X**2+1        !-0.5d0*tanh(50.d0*X-5.d0)+0.5d0
      call qsat('MCLang',U,0.d0,0.d0,Qs,NPDE,2)
      U(6)=Qs(1)
      U(7)=Qs(2)
      ay0=U(1)
      ac0=U(3)
      aT0=U(4)
      au0=U(5)
      aqa0=0.d0
      aqb0=0.d0
      ay1=U(1)
      ac1=U(3)
      aT1=U(4)
      au1=U(5)
      aqa1=0.d0
      aqb1=0.d0
      RETURN
```